INFORMATION TO USERS

This material was produced from a microfilm copy of the original document. While the most advanced technological means to photograph and reproduce this document have been used, the quality is heavily dependent upon the quality of the original submitted.

The following explanation of techniques is provided to help you understand markings or patterns which may appear on this reproduction.

1. The sign or "target" for pages apparently lacking from the document photographed is "Missing Page(s)". If it was possible to obtain the missing page(s) or section, they are spliced into the film along with adjacent pages. This may have necessitated cutting thru an image and duplicating adjacent pages to insure you complete continuity.

2. When an image on the film is obliterated with a large round black mark, it is an indication that the photographer suspected that the copy may have moved during exposure and thus cause a blurred image. You will find a good image of the page in the adjacent frame.

3. When a map, drawing or chart, etc., was part of the material being photographed the photographer followed a definite method in "sectioning" the material. It is customary to begin photoing at the upper left hand corner of a large sheet and to continue photoing from left to right in equal sections with a small overlap. If necessary, sectioning is continued again — beginning below the first row and continuing on until complete.

4. The majority of users indicate that the textual content is of greatest value, however, a somewhat higher quality reproduction could be made from "photographs" if essential to the understanding of the dissertation. Silver prints of "photographs" may be ordered at additional charge by writing the Order Department, giving the catalog number, title, author and specific pages you wish reproduced.

5. PLEASE NOTE: Some pages may have indistinct print. Filmed as received.

Xerox University Microfilms
300 North Zeeb Road
Ann Arbor, Michigan 48106

Reproduced with permission of the copyright owner. Further reproduction prohibited without permission.

75-13,005

REICH, Ricardo, 1942-
ADSORPTION ON ACTIVATED CARBON OF METHANE, ETHANE, AND ETHYLENE GASES AND THEIR MIXTURES AND CARBON DIOXIDE AT 212 K, 260 K, AND 301 K AND UP TO THIRTY-FIVE ATMOSPHERES.

Georgia Institute of Technology, Ph.D., 1974
Engineering, chemical

Xerox University Microfilms, Ann Arbor, Michigan 48106

Reproduced with permission of the copyright owner. Further reproduction prohibited without permission.

ADSORPTION ON ACTIVATED CARBON OF METHANE, ETHANE, AND ETHYLENE GASES AND THEIR MIXTURES AND CARBON DIOXIDE AT 212 K, 260 K, AND 301 K AND UP TO THIRTY-FIVE ATMOSPHERES

A THESIS

Presented to

The Faculty of the Division of Graduate

Studies and Research

By

Ricardo Reich

In Partial Fulfillment

of the Requirements for the Degree

Doctor of Philosophy

in the School of Chemical Engineering

Georgia Institute of Technology

November, 1974

Reproduced with permission of the copyright owner. Further reproduction prohibited without permission.

ADSORPTION ON ACTIVATED CARBON OF METHANE, ETHANE, AND ETHYLENE GASES AND THEIR MIXTURES AND CARBON DIOXIDE AT 212 K, 260 K, AND 301 K AND UP TO THIRTY-FIVE ATMOSPHERES

Approved:

W. T. Ziegler, Chairman

C. Orr, Jr.

R. A. Pierotti

Date approved by Chairman: Nov. 25, 1974

Reproduced with permission of the copyright owner. Further reproduction prohibited without permission.

DEDICATION

To my wife Cecilia

Reproduced with permission of the copyright owner. Further reproduction prohibited without permission.

ACKNOWLEDGMENTS

I wish to express my great admiration and appreciation to my thesis advisor, Dr. W. T. Ziegler, who has throughout these years helped develop my proficiency in experimental techniques as well as improve my understanding of thermodynamics. With deep gratitude, I acknowledge his sharing of vast knowledge and experience with me, and, furthermore, his valuable guidance, advice, and time.

I am very grateful to my reading committee, Dr. C. Orr, Jr. and Dr. R. A. Pierotti, for their time and constructive criticism.

I am indebted to the School of Chemical Engineering and, in particular, to its Director, Dr. G. L. Bridger, who has furnished me with continuous financial support in the form of a teaching assistantship for two years, instructorship for one year, and Georgia Tech Foundation support. I am also grateful to Dr. Bridger for allowing me the privilege of teaching in the School of Chemical Engineering. I thank the Rich Electronic Computer Center for the use of its facilities.

I wish to thank Dr. K. A. Rogers who built the experimental apparatus and who supported me with his experience and friendship. I also wish to thank Dr. Ju-Fu Shiau for his friendship and company.

I thank Mrs. L. Geeslin for her work in typing this dissertation.

Finally, I express my gratitude to my wife Cecilia for her encouragement, patience, help, and love which made this work a reality.

Reproduced with permission of the copyright owner. Further reproduction prohibited without permission.

TABLE OF CONTENTS

Page

ACKNOWLEDGMENTS iii

LIST OF TABLES vii

LIST OF FIGURES ix

NOMENCLATURE xii

SUMMARY xvii

Chapter

I. INTRODUCTION 1

II. EXPERIMENTAL APPARATUS AND PROCEDURE 5

Description of Apparatus
Experimental Procedure

III. EXPERIMENTAL RESULTS AND DISCUSSION 16

Pure Gas Isotherms
Gas Mixture Isotherms
Kinetic Results
Comparison with the Results of Others

IV. THEORY 37

The Polanyi Potential Theory
The Polanyi Theory as Extended by Dubinin and Its Application to Pure Gas Adsorption
Application of the Potential Theory to Gas Mixtures
The Concept of Relative Volatility and Other Correlation Methods for Adsorption Mixtures

V. CORRELATION RESULTS 60

Pure Gas Isotherms
Mixture Gas Isotherms

VI. CONCLUSIONS AND RECOMMENDATIONS 96

Summary of Results
Conclusions
Recommendations for Future Work

Reproduced with permission of the copyright owner. Further reproduction prohibited without permission.

TABLE OF CONTENTS (Continued)

Appendices Page

A. CONVERSION FACTORS TO SI SYSTEM 102

B. SYSTEM MODIFICATIONS AND ADSORPTION CELL DETAILS 104

System Modifications
Adsorption Cell

C. TEMPERATURE SCALE AND CORRECTIONS FOR PRESSURE GAUGES 107

D. PURITY OF GASES AND GAS MIXTURE PREPARATION 109

Purity of Gases
Gas Mixture Preparation

E. CALIBRATION OF GAS CHROMATOGRAPH. 111

Operating Conditions
Calibration Procedure

F. CHARACTERIZATION OF MATERIALS 119

Activated Carbon Adsorbent
Physical Property Data for Pure Components

G. EXPERIMENTAL DATA 127

Pure Gas Isothersm
Binary and Ternary Gas Mixture Isotherms
Kinetic Data

H. ERROR ANALYSIS. 145

Pure Gas Isotherms
Mixture Gas Isotherms

I. SUMMARY OF MODIFICATIONS TO THE POTENTIAL THEORY OF ADSORPTION APPLIED TO PURE GASES. 151

J. INCONSISTENCY IN THE USE OF THE POTENTIAL THEORY APPLIED TO MIXTURES. 155

K. CORRELATION RESULTS 159

Pure Gas Isotherms
Gas Mixture Isotherms

Reproduced with permission of the copyright owner. Further reproduction prohibited without permission.

TABLE OF CONTENTS (Concluded)

Appendices Page

L. FORTRAN PROGRAMS. 172

Common Subroutines
Programs

BIBLIOGRAPHY 177

VITA 182

Reproduced with permission of the copyright owner. Further reproduction prohibited without permission.

LIST OF TABLES

Table		Page
1.	Dubinin-Radushkevich Parameters for Pure Gas Adsorption Data	71
2.	Gas Chromatographic Operating Conditions	112
3.	Comparison of Calibration Curves Analysis with Gas Mixing Burette Analysis	118
4.	Activated Carbon Characteristics	120
5.	BWR Equation of State Parameters	122
6.	Critical Constants and Normal Boiling Point Temperatures for Components	123
7.	Molecular Weights and Saturated Liquid Molar Volumes at Normal Boiling Point for Components	124
8.	Methane Isotherms, Gibbs Definition	129
9.	Ethane Isotherms, Gibbs Definition	130
10.	Ethylene Isotherms, Gibbs Definition	131
11.	Carbon Dioxide Isotherms, Gibbs Definition	132
12.	Methane-Ethane Isotherms, Gibbs Definition	134
13.	Methane-Ethylene Isotherms, Gibbs Definition	136
14.	Ethane-Ethylene Isotherms, Gibbs Definition	138
15.	Methane-Ethane-Ethylene Isotherms, Gibbs Definition	139
16.	Summary of Binary Reproducibility Measurements	140
17.	Error Analysis of Methane Isotherm at 301.4 K	147
18.	Error Analysis of Methane-Ethane (49.9-50.1 mol %) Isotherm at 301.4 K	149

Reproduced with permission of the copyright owner. Further reproduction prohibited without permission.

LIST OF TABLES (Concluded)

Table		Page
19.	Summary of Modifications to the Potential Theory of Adsorption Applied to Pure Gases.	152
20.	Characteristic Curve Ordinates for Pure Gases and Calculated Capacities Using Linear Least Squares Fit	160
21.	Characteristic Curve Ordinates for Gas Mixtures	168

Reproduced with permission of the copyright owner. Further reproduction prohibited without permission.

LIST OF FIGURES

Figure		Page
1.	Schematic Diagram of Pure Gas Adsorption Apparatus	7
2.	Schematic Diagram of Gas Mixture Adsorption Apparatus	9
3.	Pure Gas Isotherms at 301.4 K	18
4.	Pure Gas Isotherms at 260.2 K	19
5.	Pure Gas Isotherms at 212.7 K	20
6.	Methane-Ethylene Isotherms (26.0-74.0 mol %)	25
7.	Methane-Ethylene Isotherms (53.6-46.4 mol %)	26
8.	Methane-Ethylene Isotherms (76.5-23.5 mol %)	27
9.	Ethane-Ethylene Isotherms (24.0-76.0 mol %) Methane-Ethane-Ethylene Isotherms (20.0-19.2-60.8 mol %)	29
10.	Ethane-Ethylene Isotherms (47.2-52.8 mol %) Methane-Ethane-Ethylene Isotherms (62.4-17.4-20.2 mol %)	30
11.	Ethane-Ethylene Isotherms (68.2-31.8 mol %) Methane-Ethane-Ethylene Isotherms (23.0-52.0-25.0 mol %)	31
12.	Kinetic Data for Ethane-Ethylene Mixture (24.0-76.0 mol %) at 212.7 K and 59 psia.	34
13.	Characteristic Curve for Pure Gases, 212.7-301.4 K	66
14.	Characteristic Curve for Pure Gases at 293 K and 363 K	68
15.	Prediction of Pure Gas Isotherms at 301.4 K Using a Linear Fit of the Characteristic Curve.	73

Reproduced with permission of the copyright owner. Further reproduction prohibited without permission.

LIST OF FIGURES (Continued)

Figure		Page
16.	Prediction of Pure Gas Isotherms at 260.2 K Using a Linear Fit of the Characteristic Curve.	74
17.	Prediction of Pure Gas Isotherms at 212.7 K Using a Linear Fit of the Characteristic Curve.	75
18.	Characteristic Curve for Gas Mixtures 212.7 to 301.4 K	80
19.	Methane-Ethylene (26.0-74.0 mol %) Isotherm Prediction.	82
20.	Methane-Ethylene (53.6-46.4 mol %) Isotherm Prediction.	83
21.	Methane-Ethylene (76.5-23.5 mol %) Isotherm Prediction.	84
22.	Ethane-Ethylene (24.0-76.0 mol %) and Methane-Ethane-Ethylene (20.0-19.2-60.8 mol %) Isotherm Prediction.	86
23.	Ethane-Ethylene (47.2-52.8 mol %) and Methane-Ethane-Ethylene (62.4-17.4-20.2 mol %) Isotherm Prediction.	87
24.	Ethane-Ethylene (68.2-31.8 mol %) and Methane-Ethane-Ethylene (23.0-52.0-25.0 mol %) Isotherm Prediction.	88
25.	Relative Volatility for Methane(1)-Ethane(2) System.	94
26.	Relative Volatility for Ethane(2)-Ethylene(3) System.	95
27.	New Adsorption Cell	106
28.	Gas Chromatographic Calibration Curve	114
29.	Schematic Diagram of Gas Chromatographic Calibration Apparatus	115
30.	Kinetic Data for Methane-Ethylene (53.6-46.4 mol %) Mixture at 212.7 K and 140 psia.	142

Reproduced with permission of the copyright owner. Further reproduction prohibited without permission.

LIST OF FIGURES (Concluded)

Figure		Page
31.	Kinetic Data for Methane-Ethane (74.5-25.5 mol %) Mixture at 212.7 K and 65 psia	143
32.	Kinetic Data for Methane-Ethane-Ethylene (52.0-23.0-25.0 mol %) Mixture at 212.7 K and 40 psia	144
33.	Schematic Representation of States. Binary System.	157

Reproduced with permission of the copyright owner. Further reproduction prohibited without permission.

NOMENCLATURE

General Symbols

cal	= calories
cm^3	= cubic centimeter
$f(P,T)$	= fugacity of a pure component at T and P
$\bar{f}_i(P,T,\{y_i\})$	= fugacity of a component i in a solution at P,T and $\{y_i\}$
F	= mathematical function
G	= Gibbs energy
$\tilde{G}$	= Gibbs energy per mole
gC	= gram of activated carbon
h	= constant in Kirchhoff equation (90)
I	= ionization potential
K	= Kelvin
ln	= natural logarithm
M_i	= molecular weight of component i
m	= mass of adsorbent
n_o', n_{oi}'	= number of moles of pure adsorbate i, Gibbs definition
$n_o = n_o'/m$ or n_{oi}	= number of moles of pure adsorbate i per unit mass of adsorbent, Gibbs definition, as defined by equation (2)
n_i'	= number of moles of adsorbate i in an adsorbate solution, Gibbs definition
$n_i = n_i'/m$	= number of moles of adsorbate i per unit mass of adsorbent, as defined by equation (4)

Reproduced with permission of the copyright owner. Further reproduction prohibited without permission.

NOMENCLATURE (Continued)

n_T = total number of moles of adsorbate per unit mass of adsorbent

n_{sv} = number of moles of pure gas in the gas chromatograph sample valve

P = absolute total pressure

P_g = pressure as defined by equation (45)

P_c = critical pressure

$\bar{P}_i = y_i P$ = partial pressure of component i in a solution

$P_R = P/P_c$ = reduced pressure

$p_{si}, p_s(T)$ = vapor pressure of pure liquid component i at T

psia = pounds per square inch absolute

R = universal gas constant

t = temperature

T = absolute temperature

T_c = critical temperature

T_{nbp} = normal boiling point temperature

$T_R = T/T_c$ = reduced temperature

$\tilde{V}$ = molar volume of a gas phase

V_i^o = void or dead space volume

V_a = volume of adsorbed phase

$\hat{V}_a = V_a/m$ = volume of adsorbed phase per unit mass of adsorbent, as defined by equation (5)

$\tilde{V}_a$ = molar volume of adsorbed phase

$\tilde{V}_a''$ = correlating volume

Reproduced with permission of the copyright owner. Further reproduction prohibited without permission.

NOMENCLATURE (Continued)

$\tilde{V}_{ai}$ = molar volume of adsorbate i in the adsorbed phase

$\hat{V}_a^o$ = limiting volume of adsorbed space as defined in equation (22)

$\tilde{V}_{si}$ = saturated molar volume of pure liquid component i at T

V_{sv} = volume of gas chromatograph sample valve

$x_i = n_i/n_T$ = mole fraction of component i in the adsorbed phase, as defined by equation (47)

y_i = mole fraction of component i in the gas phase

$Z = P\tilde{V}/(RT)$ = compressibility factor

z = distance from the adsorbent surface

Greek Alphabet

α = polarizability

α' = relative volatility as defined by equation (52)

β = affinity coefficient in Dubinin theory

γ_i = activity coefficient of component i in a solution

Δ = incremental quantity

ϵ_i, ϵ = Polanyi adsorption potential for pure component i

ϕ = surface potential

π = spreading pressure

μ = chemical potential of a pure component

μ_i = chemical potential of component i in a solution

$\sum$ = summation

Reproduced with permission of the copyright owner. Further reproduction prohibited without permission.

NOMENCLATURE (Continued)

Special Symbols

$A_o, B_o, C_o, a, b, c, \alpha, \gamma$	= parameters of Benedict-Webb-Rubin equation of state
b	= constant in the van der Waals equation of state
k	= constant in equation (22)
BET	= Brunauer-Emmett-Teller
BWR	= Benedict-Webb-Rubin
D-R	= Dubinin-Radushkevich
G-C	= gas chromatograph
{ }	= set of variables

Overlines

~	= molar quantity
—	= partial molar quantity

Superscripts

a	= absolute adsorption

Subscripts

A	= refers to the adsorbent
a	= refers to the adsorbate phase
c	= refers to the critical point
i	= species in multicomponent systems
m	= denotes property for a mixture
g	= refers to the gas phase
oi,o	= refers to pure component i as adsorbate

Reproduced with permission of the copyright owner. Further reproduction prohibited without permission.

NOMENCLATURE (Concluded)

R	= reduced property
r	= reference state
si,s	= pure component i in a saturated state
T	= total

Reproduced with permission of the copyright owner. Further reproduction prohibited without permission.

SUMMARY

The objectives of this study were: (1) to obtain experimental gas adsorption data for methane, ethane, and ethylene gases and several of their binary and ternary mixtures on activated carbon for a wide range of temperatures and pressures, and (2) to test the generality of the Polanyi Potential Theory on physical adsorption, as applied to pure gas and mixture adsorption data, with the experimentally determined results obtained in this work and those of others.

The experimental apparatus was built by Rogers[47] in this laboratory; it uses a volumetric method for both the pure gases and their mixtures.

The adsorbent chosen was a commercially available, microporous, heterogeneous, and high adsorptive capacity activated carbon, type BPL, made by the Pittsburgh Chemical Company, that has been used by several other investigators.[23,24,25,28,35,47]

Adsorptive capacity of this carbon was determined: (1) for pure methane, ethane, ethylene, and carbon dioxide gases at 212.7 K, 260.2 K, and 301.4 K, and at pressures between 0.1 and 550 psia (0.69-3792 kN/m^2), (2) for methane-ethane-ethylene binary gas mixtures at 212.7 K, 260.2 K, and 301.4 K, at mole fractions of the first component in the gas phase of about 0.25, 0.50, and 0.75, and at pressures between 19 and 300 psia (131-2068 kN/m^2), and (3) for methane-ethane-ethylene ternary gas mixtures at 212.7 K and 301.4 K, at mole fractions in the gas phase of about 0.60, 0.20, and 0.20; 0.25, 0.50, and 0.25; and 0.20, 0.20, and 0.60; and at

Reproduced with permission of the copyright owner. Further reproduction prohibited without permission.

pressures between 18 and 430 psia (124-2965 kN/m^2).

The experimental adsorption capacities of pure methane, ethane, ethylene, and carbon dioxide gases, obtained in this study, were essentially correlated in one single characteristic curve, following a modification of the Polanyi-Dubinin Potential theory.[20,40] This same method, when applied to the data of Szepesy and Illes[50,51] on other gases and on a similar adsorbent, yielded a similar correlation with some scatter at low pressures.

The Dubinin-Radushkevich equation[18] was found not to represent well the pure gas adsorption data of this study and to contain temperature dependent parameters which make its use impractical.

A linear least squares fit of the pure gas adsorption correlation developed here permitted the estimation of pure gas adsorption capacities, at the temperature and pressure conditions of this study, with an average deviation of ± 6.1% with respect to the experimental values and with certain limitations in the low pressure region.

The experimental adsorption capacities of methane-ethane-ethylene binary and ternary gas mixtures obtained in this study were essentially correlated in a single characteristic curve superimposable on the pure gas adsorption correlation, following a modification of the method proposed by Grant and Manes.[25] It was found that the equipotential concept, basic to this model, does not hold at 301.4 K. However, a fair estimation of multicomponent adsorption data from the pure gas adsorption correlation was possible.

The Bering *et al.*[7] method for the correlation of binary adsorption

Reproduced with permission of the copyright owner. Further reproduction prohibited without permission.

data was found not to fit satisfactorily the experimental data of this study.

The relative volatility or selectivity of the adsorbent for the more strongly adsorbed component was found, in general, to increase both with decreasing pressure and temperature, and with decreasing concentration of that component in the gas phase at constant temperature and pressure.

Reproduced with permission of the copyright owner. Further reproduction prohibited without permission.

CHAPTER I

INTRODUCTION

In general, most adsorption problems appearing in engineering practice involve mixture adsorption, whether it is in the drying or purification of liquid or gaseous product streams, in the separation of normal paraffins from petroleum hydrocarbon feedstocks, or in heterogeneous catalysis. In all these cases more than one type of molecule (adsorbate) enters a heterogeneous solid surface (adsorbent) and competes for the available adsorption sites. The solution of this problem requires multicomponent adsorption equilibrium data covering a wide range of temperature, pressure, and composition conditions. However, pure component adsorption equilibria are easier to determine experimentally, and a desirable approach would, therefore, be to correlate pure component adsorption data over a wide range of temperature and pressure and utilize these pure component data to predict mixture adsorption equilibria.

The solution of this problem is relatively complicated due to the following facts:

1) The theory of adsorption, especially in the case of heterogeneous adsorbents, is not sufficiently developed at this time. This problem is not well understood and is quite difficult to treat theoretically. In general, present knowledge of physical adsorption together with the different mathematical models developed to describe it, is insufficient to support a solid theoretical foundation of the problem.

Reproduced with permission of the copyright owner. Further reproduction prohibited without permission.

2) These limitations especially apply to gas mixture adsorption where experimental measurements are scarce. Adsorption phenomena are complicated here by mutual adsorbate competition on the adsorbent surface and by mutual interactions which occur under the influence of the adsorbent force field; this last effect is qualitatively and quantitatively difficult to analyze.

3) As experimentally measured mixture adsorption data are scarce in the literature, theoretically evaluated adsorption capacities and experimental data contain important uncertainties.

Of the various theories proposed to describe the physical adsorption properties of gases or vapors on solids, the most successful ones for adsorbent-adsorbate systems of practical significance have been based on the Potential Theory of adsorption as formulated by Polanyi[40,43] and as modified by Dubinin and co-workers[16,17,18] and others to pure gas adsorption, and by Grant and Manes[25] to gas mixture adsorption.

The method of approach and the objectives of this work were:

1) To obtain experimental gas adsorption data for methane, ethane, and ethylene gases and several of their binary and ternary mixtures on activated carbon for a wide range of temperatures and pressures.

2) To test the generality of the Polanyi Potential Theory of physical adsorption, and some of its modifications available today, with the experimentally determined results for pure gases in this work, those obtained by Rogers[47] in this laboratory under similar conditions on methane, carbon dioxide, and hydrogen, and those of others.

3) To test some of the prediction methods available at present

Reproduced with permission of the copyright owner. Further reproduction prohibited without permission.

for the correlation of multicomponent experimental physical adsorption data from pure component adsorption data with experimentally determined results on binary and ternary gas mixtures in this work and those of others.

The experimental apparatus used in this study was built by Rogers[47] in this laboratory. It uses a volumetric method for both the pure gases and their mixtures, and it is described in Chapter II.

The adsorbent used was an heterogeneous microporous activated carbon made from coal. Its commercial description is Type BPL; it is manufactured by the Pittsburgh Chemical Company. This particular type of adsorbent has been used by several other investigators.[23,24,25,28,35,47] The material is characterized in Appendix F.

Pure, binary and ternary gas mixtures for methane, ethane, and ethylene were determined on this adsorbent at 212.7 K, 260.2 K, and 301.4 K along with several composition combinations and pressures up to about 35 atmospheres (3566 kN/m^2). Pure carbon dioxide data, at these same temperatures and similar pressure conditions, were also determined on this carbon. Under these conditions of temperature, methane was above its critical temperature, ethane and carbon dioxide below it, and ethylene below it for the two lowest temperature levels and above for the highest. The pressure limit (about 35 atmospheres), the temperature range (212.7 K to 301.4 K), and the compositions (approximately 0.25, 0.50, and 0.75 in mole fraction of any component in the binary mixtures, and about 0.60, 0.20, and 0.20 in the ternaries) selected were considered to be adequate to test prediction theories and cover the range of common engineering

Reproduced with permission of the copyright owner. Further reproduction prohibited without permission.

interest. The three hydrocarbon gases selected for this study are common gases of industrial interest for which multicomponent adsorption data are scarce or non-existent in the literature. The highly adsorbed components were ethane and ethylene. Methane was included to provide a component of low adsorption capacity and low critical temperature. Carbon dioxide was selected to check the reproducibility of some pure gas adsorption data obtained by Rogers[47] on the same adsorbent material.

Pure gas and mixture adsorption measurements are discussed in detail in Chapter II. The adsorption results of this experimental program are presented and analyzed in Chapter III.

The Polanyi Potential Theory of adsorption and its modifications are presented in Chapter IV. Other correlation methods are also briefly discussed in that chapter.

In Chapter V the pure gas and mixture adsorption data obtained in this study are analyzed and correlated within the context of the Potential Theory and its modifications.

Reproduced with permission of the copyright owner. Further reproduction prohibited without permission.

CHAPTER II

EXPERIMENTAL APPARATUS AND PROCEDURE

Description of Apparatus

Experimental adsorption isotherms are generally obtained by one of three main methods: volumetric, gravimetric, or chromatographic. In this particular investigation the classical volumetric method was used both for the pure gases and for the mixtures. A static equilibrium technique was used for the pure gases. A measured amount of gas is admitted to a vessel of known volume which contains a weighed sample of an adsorbing solid. At equilibrium the amount of non-adsorbed gas can be calculated from the equilibrium pressure, temperature, and volume available to the gas in the adsorption vessel, and an appropriate equation of state for the gas. Using a material balance applied to the adsorption system, the amount of gas adsorbed by the solid at the equilibrium pressure and temperature is determined by subtracting the amount of non-adsorbed gas present in the adsorption vessel from the amount originally injected into it.

An open-system, flow method was used for the gas mixtures; it is based on the static method with necessary modifications. This technique consists of passing a gas mixture of known composition through the adsorbent bed at constant temperature and pressure until the exit stream reaches the same composition as the feed gas. The adsorption cell is isolated when this state of equilibria is achieved. Successive amounts

Reproduced with permission of the copyright owner. Further reproduction prohibited without permission.

of gas mixture are then transferred by desorption from the adsorption space to a calibrated sample reservoir at fixed temperature. The pressure, temperature, volume of the reservoir, the appropriate equation of state for the gas mixture, and its composition determine the total amount of the different components present in the adsorption system. The adsorbed amount of a certain component is evaluated by subtracting its non-adsorbed amount initially present at equilibrium temperature and pressure in the adsorption space from the total amount of component transferred to the sample reservoir.

The same adsorbent bed was used in all experiments. The apparatus for these measurements was built by Rogers[47] and has been described in detail in his dissertation. It is capable of operating in the temperature range from 70 K to 350 K and with pressures up to about 100 atmospheres.

The adsorption cell was redesigned for this experimental work, minor modifications being made on the tubing network. Adsorption cell details and further information on the modifications are given in Appendix B.

Pure Gas Isotherm Apparatus

A schematic diagram of the volumetric apparatus is given in Figure 1. Its significant components, instruments, and valves are numbered and specified below it.

The basic concept of adsorption equilibrium requires that all intensive variables of the system be fixed, i.e., if the adsorbent and adsorbate are specified, the temperature and pressure of the system at equilibrium will define the amount of gas adsorbed.

A cryostat, 2, was used for the purpose of maintaining a constant

Reproduced with permission of the copyright owner. Further reproduction prohibited without permission.

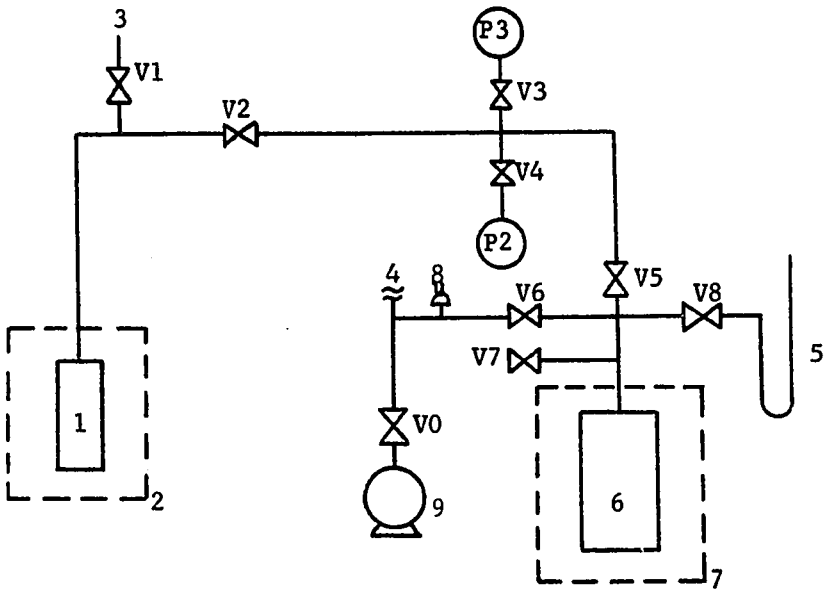

1 - Adsorption cell
2 - Cryostat bath
3 - To vacuum line
4 - To vacuum line
5 - Mercury manometer
6 - Gas reservoir
7 - Water thermostat
8 - Vacuum gauge
9 - Vacuum pump

P2 - 0-1500 psig Martin-Decker gauge
P3 - 0-250 psig Heise gauge

Figure 1. Schematic Diagram of Pure Gas Adsorption Apparatus

Reproduced with permission of the copyright owner. Further reproduction prohibited without permission.

temperature in the adsorption cell. Depending upon the temperature of the experiment, either water or hexane was used as the cryostat fluid. To fix the temperature of the gas to be transferred into the adsorption vessel a water thermostat, 7, was employed. The room conditions determined the temperature of the connecting tubings and instrumentation. Mercury-in-glass thermometers were used to measure the room and water thermostat temperatures. Type E, Chromel-Constantan thermocouples installed in glass wells filled with Nujol, a commercial heavy mineral oil, were used to determine the cryostat temperature. These thermocouples were previously calibrated against a platinum resistance thermometer as a reference standard. Details of this calibration are presented in Appendix C.

A mercury-in-glass manometer was used to determine pressures below two atmospheres and Bourdon-type gauges P2 and P3 for higher pressures. The different equipment void, or dead, spaces required to evaluate the number of moles of gas were determined by helium displacement. Vacuum, when required, was obtained with a mechanical pump. Type BPL activated carbon absorbent (32.19 grams, or millikilograms), as characterized in Appendix F, was placed in the adsorption vessel as described in Appendix B. The same sample of adsorbent was used in the complete set of experiments of this dissertation.

Gas Mixture Isotherm Apparatus

A schematic diagram of the volumetric apparatus used to determine gas mixture isotherms is given in Figure 2. Its components are numbered and specified below it.

As it has been stated before, this equipment is an extension of the

Reproduced with permission of the copyright owner. Further reproduction prohibited without permission.

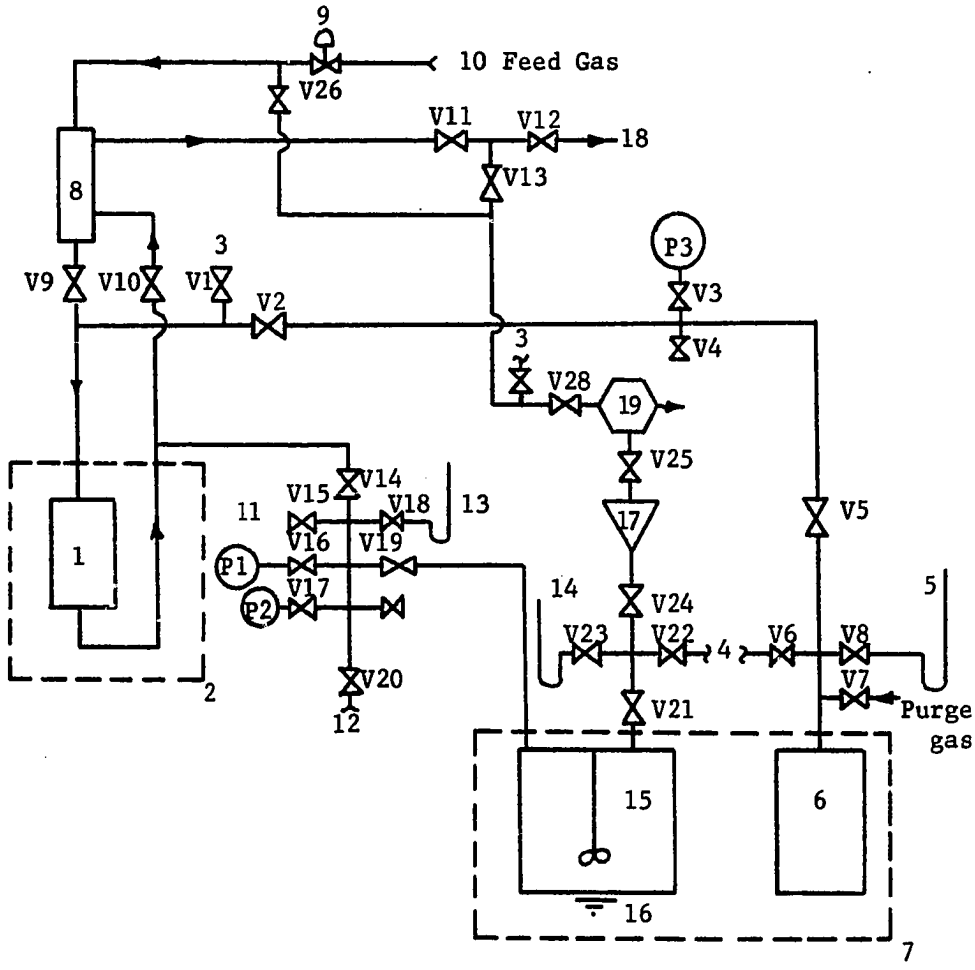

1 - Adsorption cell
2 - Cryostat bath
3 - To vacuum line
4 - To vacuum line
5 - Mercury manometer
6 - Gas reservoir
7 - Water thermostat
8 - Heat exchanger
9 - Control valve
10 - Feed gas mixture
11 - Venting valve
12 - To vacuum line
13 - Mercury manometer
14 - Mercury manometer
15 - Sample reservoir
16 - Magnetic mixer
17 - Sample collector
18 - Flowmeter
19 - Gas chromatographic analyzer

P1 - 0-300 psig Ashcroft gauge
P2 - 0-1500 psig Martin-Decker gauge
P3 - 0-250 psig Heise gauge

Figure 2. Schematic Diagram of Gas Mixture Adsorption Apparatus

Reproduced with permission of the copyright owner. Further reproduction prohibited without permission.

pure gas isotherm apparatus with modifications directed to transform the static conditions of the pure gas to flow conditions of the gas mixture. A gas dome-type pressure regulator (Hoke, Inc.), 9, controlled the gas flow from a mixing steel gas cylinder, 10, into the adsorption system. The different gas mixtures were prepared in this laboratory following a procedure discussed in Appendix D. Heat exchanger 8 served the purpose of bringing the gas mixture temperature closer to that of the adsorption cell effluent stream. The temperature of the adsorption vessel was set as described above in the pure gas isotherm apparatus section. From the heat exchanger, the adsorption vessel exit stream was diverted either to a flowmeter, 18, or to a gas chromatographic analyzer, 19. Details of this latter instrument calibration and its operating conditions are discussed in Appendix E. In the desorption stage of the experiment, cryostat 2 was removed, and electric heaters were placed against the surface of the adsorption vessel. The desorbed gas mixture was then transferred to a calibrated glass sample reservoir, 15, equipped with a magnetic stirrer, 16. A sample collector, 17, connected to both the sample reservoir 15 and to the gas chromatograph 19 was used to analyze the sample reservoir content. Gas reservoir 6, used in determining the pure isotherms, was included in this apparatus as a helium sweep gas container. The helium gas was used to purge the carbon adsorbent and tubing network to insure that all the adsorbate had been transferred to sample reservoir 15. Equilibrium pressure measurements were performed with mercury-in-glass manometers 13 and 14 and Bourdon-type gauges P1 and P3.

Reproduced with permission of the copyright owner. Further reproduction prohibited without permission.

Experimental Procedure

Adsorbent Regeneration

Removal of the adsorbate from the carbon adsorbent prior to any adsorption capacity measurement was required. The regeneration procedure was dependent on the isotherm measurement techniques followed.

Preliminary Regeneration. Once the activated carbon sample was placed in the adsorption vessel (see Appendices B and F), a preliminary conditioning of the adsorbent was followed. The adsorption cell was first degassed at room temperature under vacuum for about twenty hours and then degassed at about 120°C under vacuum for another one and a half hours to remove water vapor. As the evaluation of the dead (void) spaces of the pure gas isotherm apparatus was next accomplished, opening of parts of the system was required. Therefore, once the void space measurements were completed a new regeneration of the adsorbent was performed. The adsorption vessel was degassed at about 130°C for one and a half hours. The cell was now ready for the pure gas isotherm measurements.

Pure Gas Isotherm Experiments. As a general rule degassing at room temperature under vacuum was performed between every isotherm determination. However, in some cases heating to about 130°C under vacuum was accomplished to check the general operating conditions of the apparatus. During those intervals when no experiments were underway, continuous vacuum at room temperature was applied to the system. Generally a vacuum better than ten millitorr (1.3332 N/m^2) was obtained.

Gas Mixture Isotherm Experiments. Since the gas mixture adsorption apparatus set-up required opening parts of the pure gas isotherm equipment, a preliminary regeneration was made of the adsorbent before actual experi-

Reproduced with permission of the copyright owner. Further reproduction prohibited without permission.

mental measurements for gas mixtures were performed. The adsorption cell was heated to about 130°C under vacuum for about one and a half hours.

In the adsorbate desorption heating of the adsorption cell to about 100°C and purging the system with helium gas was used as the regeneration procedure. During those intervals when no experiments were run, continuous vacuum at room temperature was applied to the system.

Pure Gas Isotherm Determination Procedure

The operation procedure for the experimental determination of pure gas adsorption capacities is summarized below. Reference is made to the schematic diagram given in Figure 1. Valves are designated by V's.

Preliminary Steps. With valves V2, V3, V4, V5, and V8 open and V7 closed, vacuum is attained in the system by opening valves V1 and V6. Water thermostat 7 is adjusted to the selected temperature--30°C in this experimental program. Cryostat 2 is adjusted to the temperature level of the experiment, i.e. to 301.4 K, 260.2 K, or 212.7 K.

First Gas Addition. Valves V1, V2, V3, V4, and V6 are closed. Manometer 5 is used to read the pressure in the first transfer of gas to the adsorption space. The selected gas is admitted to gas reservoir 6 by opening V7 and monitoring manometer 5. V7 is closed. When conditions become stable, the thermostat temperature, manometer pressure, and room temperature and pressure are recorded. The gas is admitted now to adsorption vessel 1 by opening V2. When adsorption equilibrium is attained the new reading of manometer 5 is recorded and valve V2 is closed.

Additional Gas Transfers. The procedure is repeated for higher equilibrium pressures. Depending on the pressure level, the appropriate pressure measuring device is selected by opening or closing valves V3, V4,

Reproduced with permission of the copyright owner. Further reproduction prohibited without permission.

and V8. A new amount of gas is admitted to gas reservoir 6 and transferred to the adsorption space after recording the appropriate variables. The preliminary steps stated above are followed once the final equilibrium point in the isotherm determination is reached.

Gas Mixture Isotherm Determination Procedure

The operation procedure for the experimental determination of gas mixture adsorption capacities is summarized below. Reference is made to the schematic diagram given in Figure 2.

Preliminary Steps. Water thermostat 7 is adjusted to the selected temperature, i.e. 30°C. Cryostat 2 is set to the temperature level of the experiment. Gas chromatographic analyzer 19 is placed in operation.

The adsorption section, as characterized by adsorption cell 1 and regenerated as described above in this chapter, is maintained under vacuum conditions by closing valves V2, V6, V9, V10, V15, V18, V19, V22, V27, and V16 or V17, depending on the pressure level of the experiment, and opening valves V1, V14, and V20.

Valves V1 and V20 are now closed. The helium purge gas section, as characterized by gas reservoir 6, is evacuated by closing valves V4, V7, and V8 and opening V3, V5, and V6. Once evacuated, valve V6 is closed and helium sweep gas is admitted to this section by opening V7 and monitoring gauge P3. V7 is closed.

Adsorption Procedure. When all instruments and variables in the system are stabilized the feed gas supply section is evacuated by closing control valve 9, valves V13 and V28, and opening V26 and V27; V26 and V27 are then closed. Valve 9 is opened and the gas supply to the adsorption section is adjusted to the approximate pressure desired with pressure

Reproduced with permission of the copyright owner. Further reproduction prohibited without permission.

regulator 9 and monitoring gauges P1 or P2. V12 is now opened. Valve V11 is slightly opened and serves as a fine flow regulator. Valve V10 is opened allowing the gas mixture to flow through the adsorption cell and out to the flowmeter. The flow rate is adjusted with valve V11 to between 100 and 250 cm^3/min (1.7 to 4.2 cm^3/s), as measured at the outlet with a wet-test meter under approximately one atmosphere pressure and room temperature. Final adjustments of the system pressure are made with pressure regulator 9.

While the flow system proceeds towards equilibrium, sample reservoir 15 is evacuated. Valves V24 and V25 are closed and V21, V22, and V23 are opened. The feed gas is analyzed by opening V26 and V28 and passing the gas mixture to gas chromatographic analyzer 19 sample valve. Valves V26 and V28 are closed. The exit stream is periodically analyzed by closing V12 and opening V13 and V28 to gas analyzer 19. Then V12 is opened, and V13 and V28 are again closed.

When inlet and exit streams reach the same composition, adsorption equilibrium is assumed to exist. The adsorption space is now isolated by closing valves V9 and V10. The main gas supply is closed, and the temperatures of the system and pressure at equilibrium are then recorded. The cryostat is now removed and electric heaters are placed about the adsorption cell. The temperature of the cell is increased gradually to a maximum of about $100^{\circ}C$.

Valve V19 is now closed and the gas mixture contained in the gas reservoir is allowed to mix for about five minutes, the pressure being recorded during this time. Samples are then taken with sample collector 17 by opening V24. After sampling, V24 is closed. The gas sample is now

Reproduced with permission of the copyright owner. Further reproduction prohibited without permission.

analyzed by allowing it to flow to analyzer 19. Analyses are repeated as needed. Before continuing with the next transfer, the reservoir is evacuated by opening V22.

The desorption and transfer procedure is repeated, as described before, until a pressure less than one atmosphere is indicated by manometer 14. When this occurs helium gas is used to purge the adsorption system by opening valve V2. Sufficient gas is admitted to the system so as to increase the pressure in gas reservoir 15 to about one and one half atmospheres. Valve V19 is again closed, the analysis procedure being followed as explained above. The helium purge gas method is continued until analysis of the gas reservoir content shows components present in less than two mole percent. At this point the desorption procedure is terminated, and the equipment prepared for a new adsorption measurement. The electric heaters are disconnected, V2 and V19 are closed, and V20 is opened to allow evacuation of the adsorption space.

Reproduced with permission of the copyright owner. Further reproduction prohibited without permission.

CHAPTER III

EXPERIMENTAL RESULTS AND DISCUSSION

Pure Gas Isotherms

The experimental apparatus and procedure used in the determination of pure gas isotherm data have been described in Chapter II. The experimental adsorption measurements, made for a certain pure gas at constant temperature, supplied experimental raw data which were reduced to a set of equilibrium pressures and adsorbed capacities by solving a material balance on the system. According to the Gibbs definition,[53] the number of moles, n_o', adsorbed by the solid adsorbent at each point on the isotherm is the total number of moles of gas added to the adsorption cell from the gas reservoir (see Figure 1) less the number of moles in the gas phase above the solid, i.e. the dead or void space. That is

$$n_o' = \sum_{j=1}^{k} \left(\frac{PV}{ZRT}\right)_j^{added} - \frac{P}{R} \sum_{i=1}^{r} \left(\frac{V^o}{ZT}\right)_i \qquad (1)$$

where n_o' corresponds to the moles of pure gas adsorbed. The first summation contains the moles or dose added in each increment up to the pressure or equilibrium point of interest, k, where j represents the dose number. P_j, V_j, and T_j are experimentally measured values, and Z_j being evaluated at T_j and P_j from a BWR equation of state for the substance. The second term contains the equilibrium pressure of the adsorption system, the void

Reproduced with permission of the copyright owner. Further reproduction prohibited without permission.

space volumes, V_i^o, determined by helium gas displacement and their corresponding temperatures, T_i, and the compressibility factor of the gas, Z_i, evaluated at T_i and P from the same equation of state; i refers to the different void space volumes and r to their total number. The BWR parameters used in this equation are given in Table 5 in Appendix F.

The moles of gas adsorbed were finally expressed per gram of adsorbent as

$$n_o = n_o'/m \tag{2}$$

The complete calculation, starting with raw experimental data, was performed on a UNIVAC 1108 computer with FORTRAN IV program PISOTH explained briefly in Appendix L.

Pure gas isotherm data for methane, ethane, ethylene, and carbon dioxide at 212.7 K, 260.2 K, and 301.4 K are given in Tables 3, 4, 5, and 6 in Appendix G. Originally, some carbon dioxide measurements were performed in order to check the operation of the apparatus by reproducing some of Rogers's[47] determinations of this gas on his carbon sample. As the experimental results of these tests showed, in general, a significant difference with respect to the values obtained by Rogers[47] (as discussed later in this chapter), it was decided to measure the complete set of carbon dioxide adsorption isotherms so as to provide a consistent set of data that could be used later in the construction of the characteristic curve for pure gases. A graphical representation of these results is given in Figures 3, 4, and 5. For each temperature level the adsorption capacities of the four gases, n_{oi}, appear as ordinates against the equilibrium pressure as abscissas. Adsorption capacities for methane and

Reproduced with permission of the copyright owner. Further reproduction prohibited without permission.

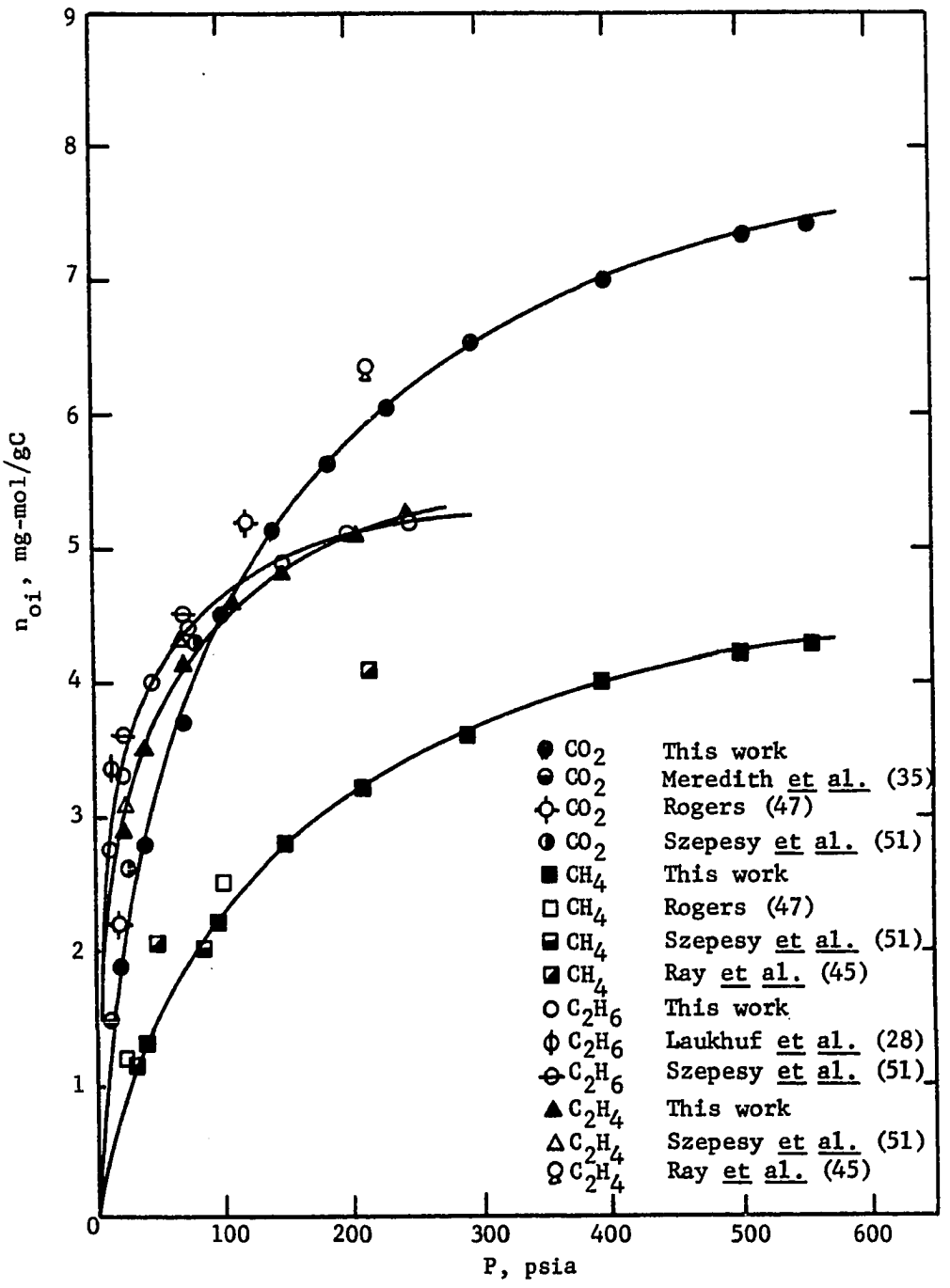

Figure 3. Pure Gas Isotherms at 301.4 K

Reproduced with permission of the copyright owner. Further reproduction prohibited without permission.

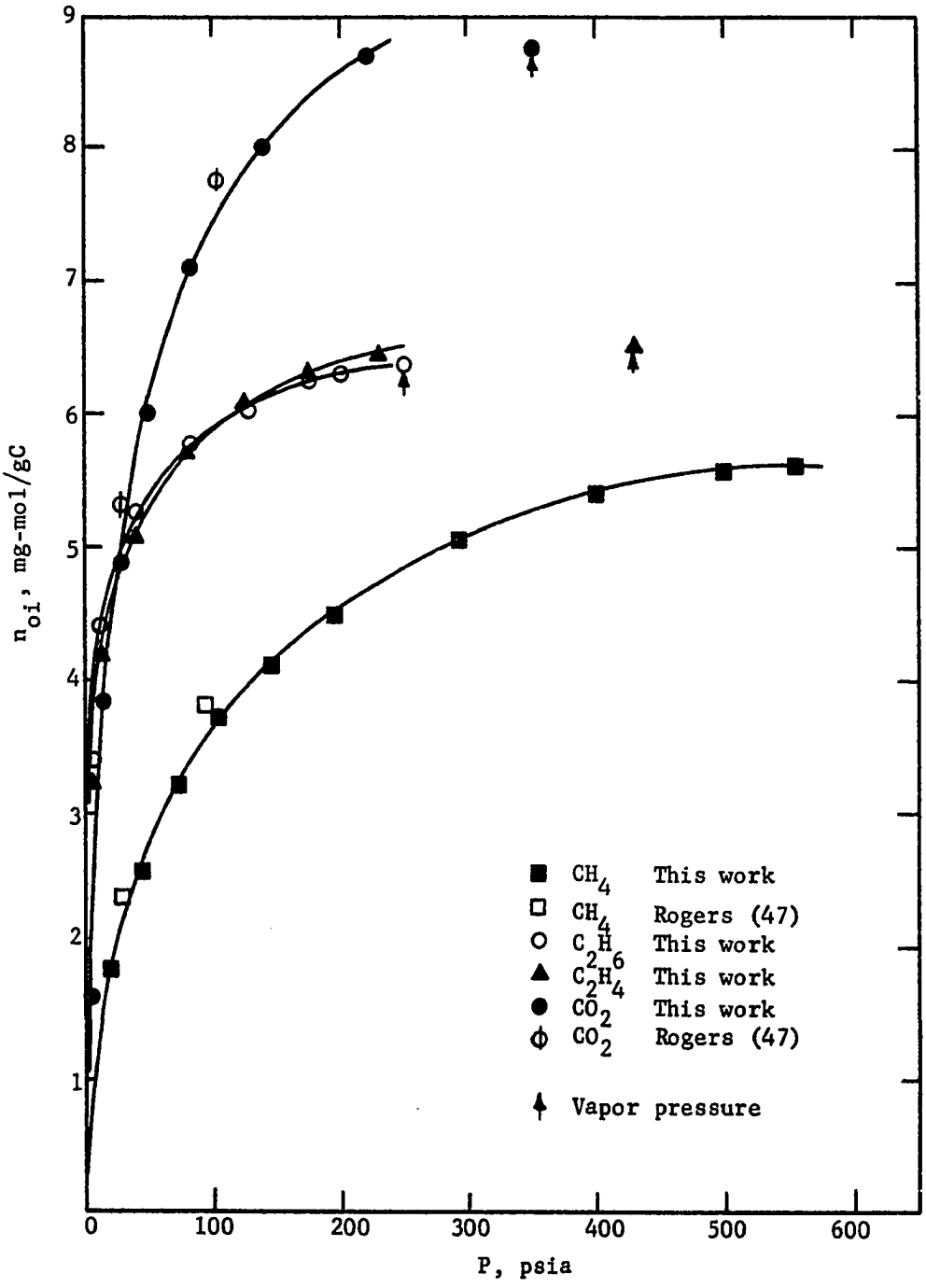

Figure 4. Pure Gas Isotherms at 260.2 K

Reproduced with permission of the copyright owner. Further reproduction prohibited without permission.

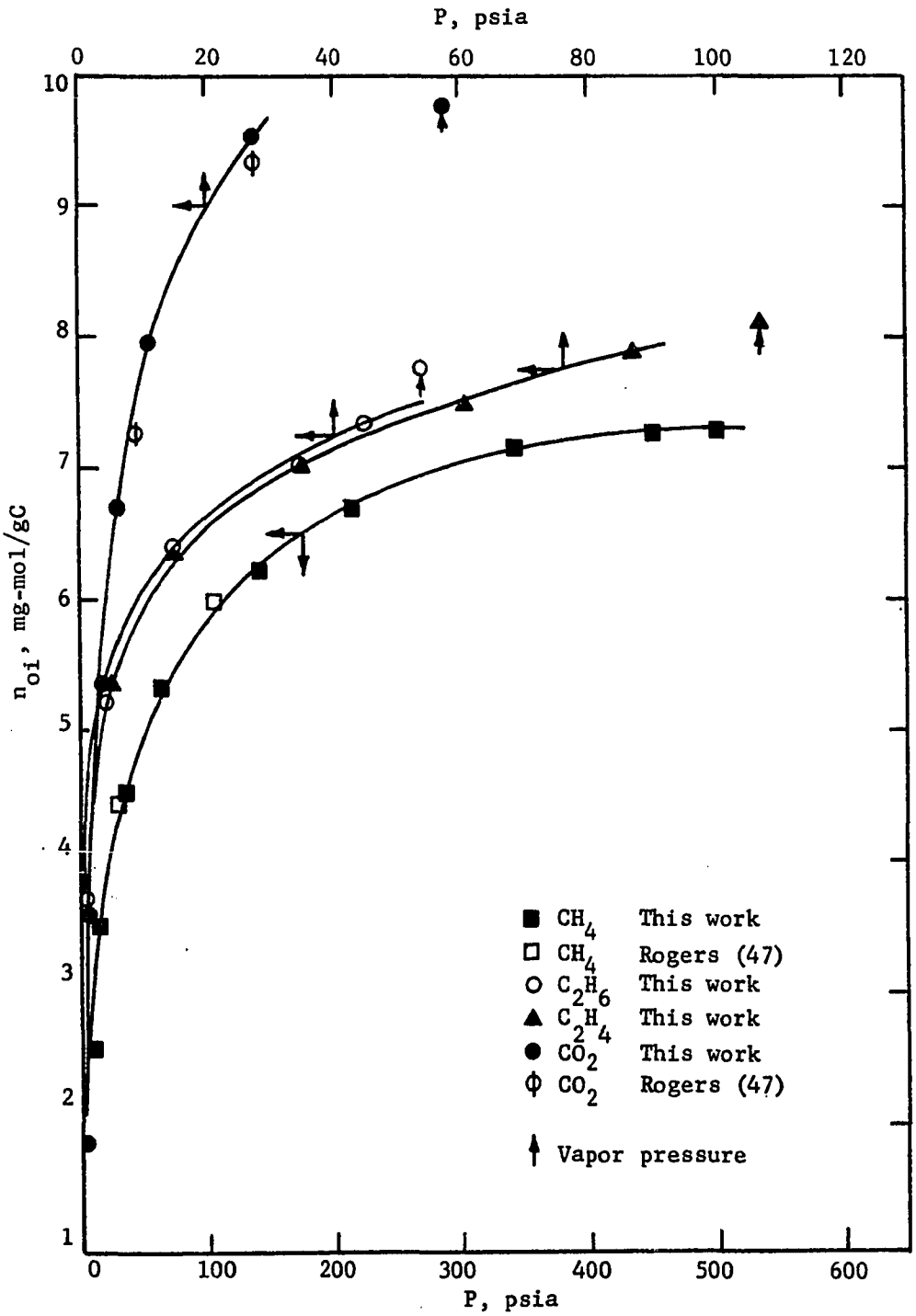

Figure 5. Pure Gas Isotherms at 212.7 K

Reproduced with permission of the copyright owner. Further reproduction prohibited without permission.

carbon dioxide were measured up to about 550 psia and for ethane and ethylene up to about 250 psia. Maximum equilibrium pressures at the lower temperature levels were limited by the substance vapor pressures which are shown in Figures 4 and 5. Some data points are omitted for the sake of clarity.

Figures 3, 4, and 5 show a similar adsorption isotherm shape for methane, ethane, and ethylene; ethane and ethylene having about equal adsorption capacities at all three temperature levels and methane showing a much lower capacity. Carbon dioxide isotherms have, in general, greater slopes and show greater adsorption capacities than the other three gases.

All pure gas isotherms in this work were repeated at least once to check reproducibility and to increase the number of data points. In addition, repetitions were done at several stages of the experimental program. As all pure gas isotherms were measured first and followed by the binary and ternary mixture isotherm determinations, repetitions of pure gas isotherms of carbon dioxide and ethylene were done before starting the mixtures and at the end of the experimental program. These reproducibility checks served the double purpose of verifying pure isotherm reproducibility and adsorbent invariance during the whole experimental work. Thirty-two pure gas adsorption isotherms were determined over a period of two months (see Tables 8 to 11 in Appendix G), and twenty-seven gas mixture isotherms over a subsequent period of three months (see Tables 12 to 15 in Appendix G), a single activated carbon sample being used over the total period of experimentation. Reproducibility of pure gas isotherms is within ± 1%. The final pure ethylene isotherm obtained at the end of this work shows a reproducibility of about ± 2% with respect to isotherms

Reproduced with permission of the copyright owner. Further reproduction prohibited without permission.

measured at the beginning of it.

Since all experimental measurements were directed to obtaining equilibrium data, sufficient time was allowed with each equilibrium measurement to insure attaining this required state. A number of experiments were run in which the adsorption pressure was recorded as a function of time. These tests provided information regarding the time required to approach equilibrium. About 30-40 minutes were required at 301.4 K, and about 30-60 minutes at 212.7 K, the values depending on the pressure level and the particular gas investigated. In general, about 20-30 minutes were allowed before starting to record pressure against time in all equilibrium measurements. The system was considered to be in equilibrium when the pressure became time independent.

An error analysis was attempted for the pure gas isotherm measurements; it is discussed in detail in Appendix H. As a reasonable approximation it is believed that the maximum error involved in these measurements is between 5 and 8%. As the probable error must be smaller than these values due to relative error cancellation, it is thought that the general precision of the pure gas isotherms is within ± 3 to 4%. Actual reproducibilities, as indicated above, were within ± 1 to 2%.

Gas Mixture Isotherms

The experimental apparatus and procedure used in the determination of gas mixture isotherm data have been discussed in Chapter II. The raw data provided by the experimental measurements, made for a gas mixture of fixed composition and at constant temperature, were reduced to a set of equilibrium pressures and amount adsorbed for each component in the ad-

Reproduced with permission of the copyright owner. Further reproduction prohibited without permission.

sorbate solution by solving a material balance on the system. According to the Gibbs definition,[53] the adsorbed amount of a certain component i at each point on the isotherm, n_i', is evaluated as the difference between the total amount of component that is transferred to the sample reservoir by desorption (see Figure 2) and the non-adsorbed amount initially present in the adsorption space, at the equilibrium temperature and pressure of the system:

$$n_i' = (n_i)_{system} - \frac{y_i P}{R} \sum_{j=1}^{r} \left(\frac{V^o}{Z_m T}\right)_j \qquad (3)$$

where $(n_i)_{system}$ is the total number of moles of component i transferred from the adsorption system to the sample reservoir; y_i is the component i composition in the feed gas mixture; P is the equilibrium pressure in the adsorption space; V_j^o is the void space volume of section j of the adsorption space at the corresponding temperature, T_j, and Z_{mj} is the compressibility factor of the gas mixtures at T_j, P, and $\{y_i\}$ as evaluated from the BWR equation of state for the mixture using the pure gas parameters given in Table 5, Appendix F, and the parameter mixing rules of Benedict et al.[3]; r is the number of void spaces.

The moles of component i were finally expressed per gram of adsorbent as

$$n_i = n_i'/m \qquad (4)$$

The complete calculation, starting with raw experimental data, was performed with program MISOTH, explained briefly in Appendix L.

Methane, ethane, and ethylene binary gas isotherms at 212.7 K,

Reproduced with permission of the copyright owner. Further reproduction prohibited without permission.

260.2 K, and 301.4 K are presented in Tables 12, 13, and 14 in Appendix G. Methane, ethane, and ethylene ternary gas isotherms at 212.7 K and 301.4 K are given in Table 15 in the same appendix. Binary adsorption capacity data were measured up to about 300 psia and ternary data up to about 400 psia.

A graphical representation of some mixture data is presented in Figures 6 to 11; for each gas mixture composition the adsorption capacities of the different components in the adsorbate solutions, n_i, appear as ordinates against the gas phase partial pressures of the same components as abscissas. The pure gas isotherms are also included in the same figures for the purpose of comparing adsorption capacities at equal partial pressures. Some data points are omitted for the sake of clarity.

Figures 6, 7, and 8 represent experimental adsorption data for methane-ethylene gas mixtures, the methane content being increased from about 25 mol % to about 75 mol %. For low methane gas concentrations the amount of ethylene adsorbed can be represented approximately, at all values of T, by its adsorption capacity as a pure gas at a fixed partial pressure. The amount of ethylene adsorbed from a known methane-ethylene gas mixture at low methane content may then be estimated at T and P from its pure gas isotherm and its partial pressure. This is not the case for methane, which is greatly affected by the presence of ethylene in the adsorbate mixture. The same result is evident for methane-ethane gas mixtures of low methane content (see Table 12 in Appendix G). However, for higher methane concentrations in the gas phase this behavior is no longer valid as may be seen from Figure 8; interactions between the gases are evident and adsorption capacities for the components cannot be estimated

Reproduced with permission of the copyright owner. Further reproduction prohibited without permission.

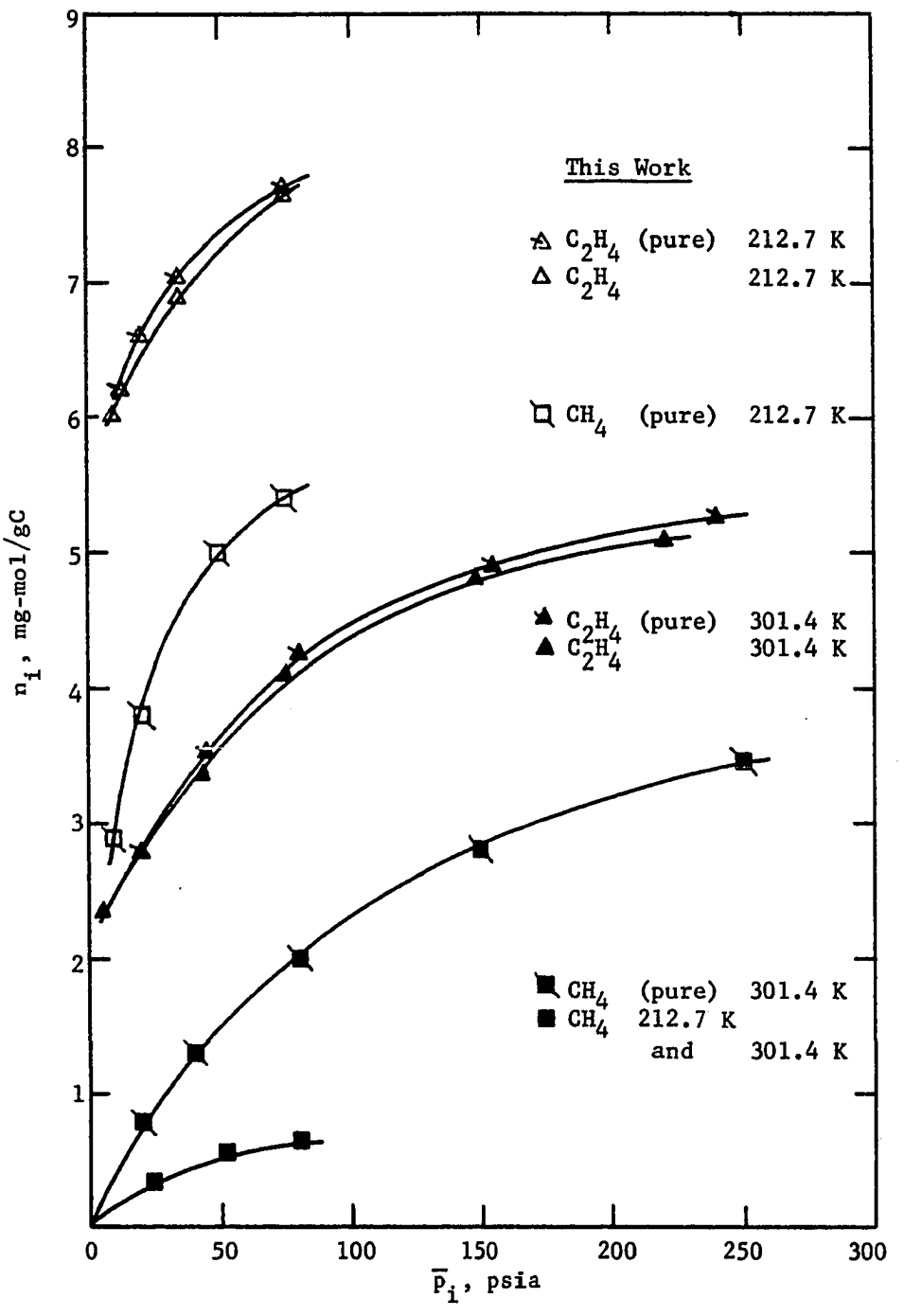

Figure 6. Methane-Ethylene Isotherms (26.0-74.0 mol %)

Reproduced with permission of the copyright owner. Further reproduction prohibited without permission.

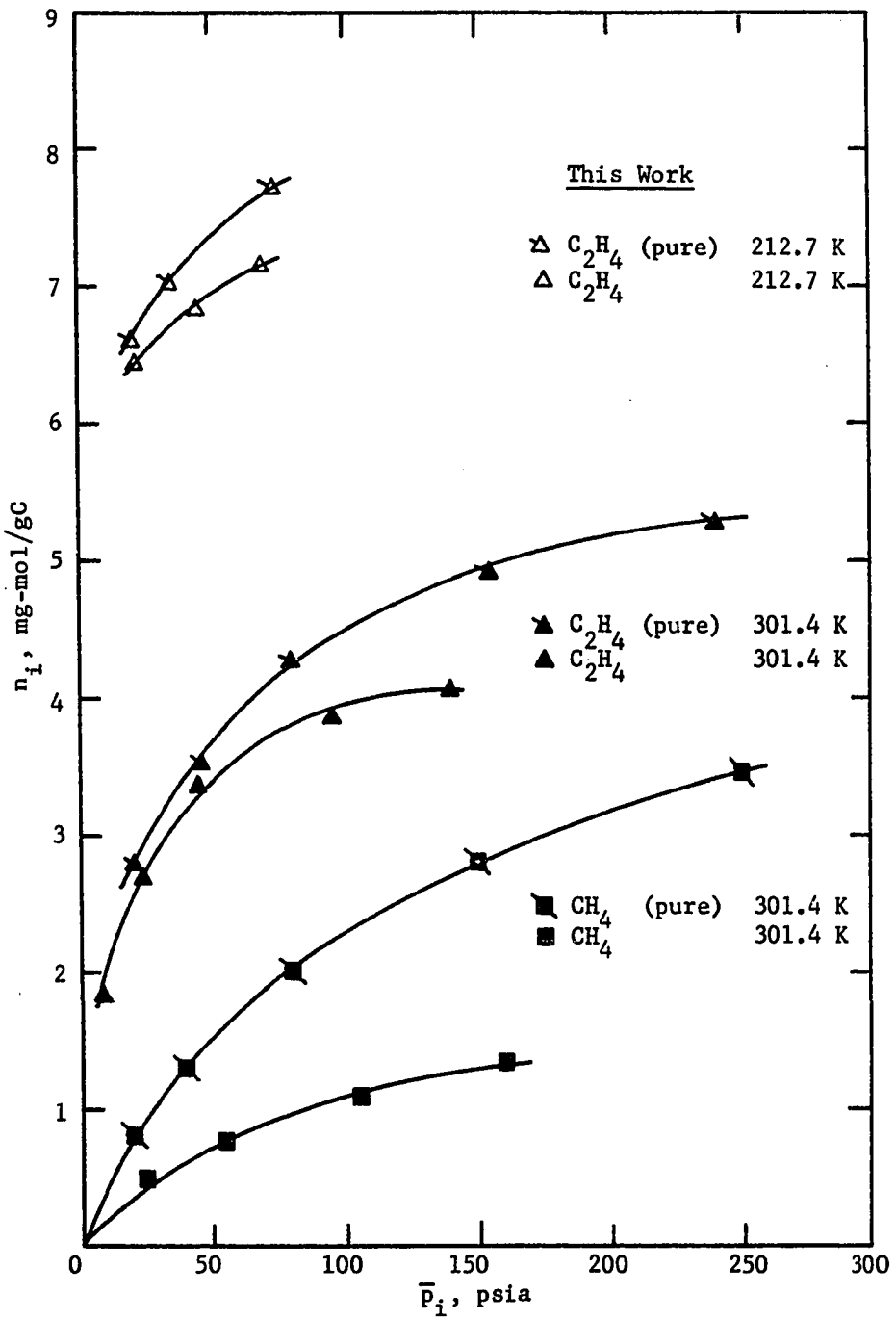

Figure 7. Methane-Ethylene Isotherms (53.6-46.4 mol %)

Reproduced with permission of the copyright owner. Further reproduction prohibited without permission.

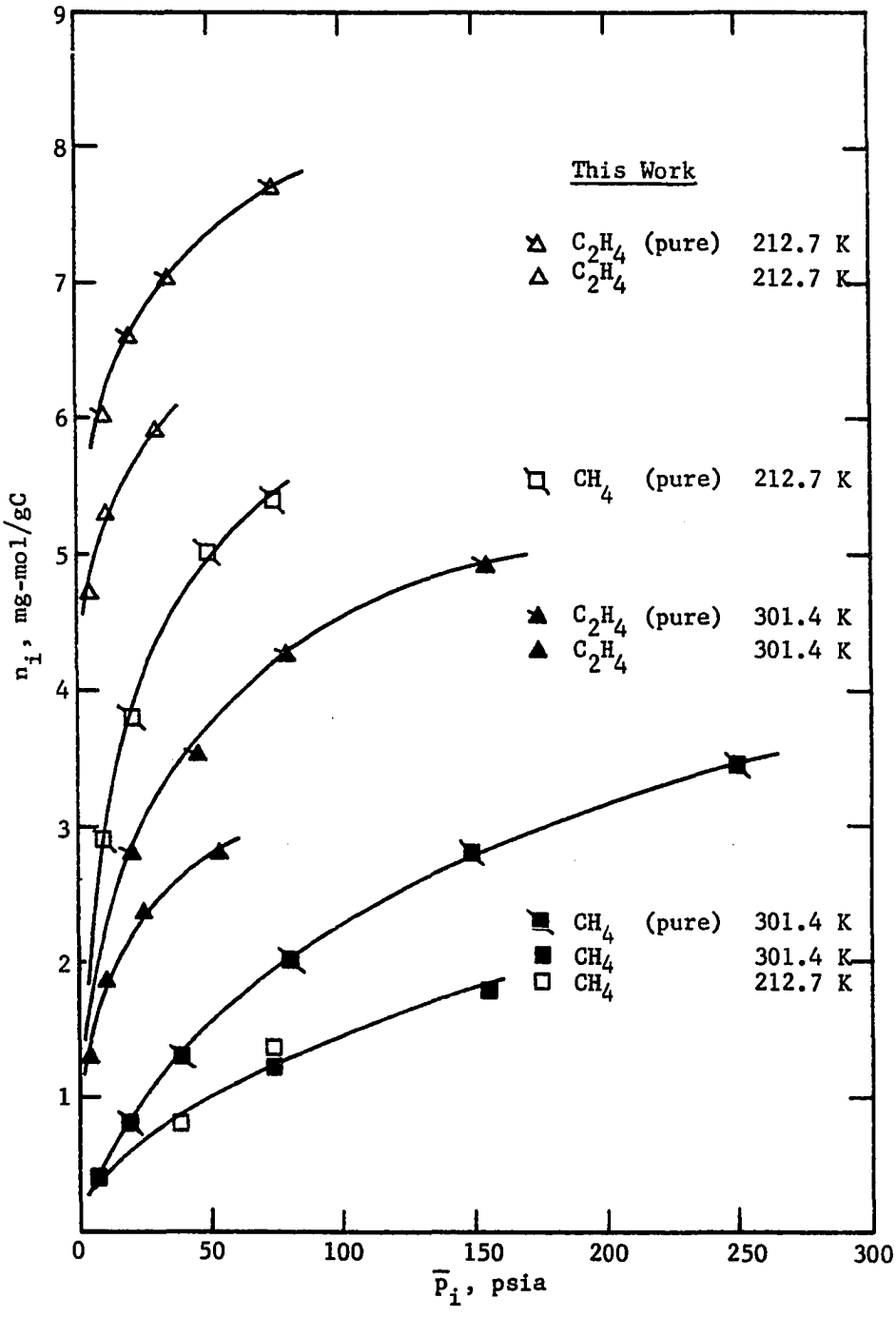

Figure 8. Methane-Ethylene Isotherms (76.5-23.5 mol %)

Reproduced with permission of the copyright owner. Further reproduction prohibited without permission.

directly from pure gas adsorption data and partial pressures at a fixed temperature.

Figures 9, 10, and 11 represent experimental adsorption data for ethane-ethylene and methane-ethane-ethylene gas mixtures, the ternaries having an ethane-ethylene mole ratio approximately equal to its corresponding ethane-ethylene binary. This molar ratio increases from about 0.30 in Figure 9 to about 2.1 in Figure 11. Methane capacities are presented in Figure 9 only in order to simplify the diagrams; low temperature capacities are plotted in Figure 11 only for the same reason.

All three figures show that component interactions are present in the adsorbate phase and that the estimation of component capacities solely from pure adsorption data and the partial pressures of the components at a fixed temperature is not possible. The capacities of the different components are significantly reduced with respect to their adsorption as pure gases at a total pressure equal to the partial pressure of the components in the mixtures. This effect is apparent at all considered temperatures.

These figures show that ternary gas adsorption isotherms behave, in general, in a fashion similar to binary mixtures with the same ethane-ethylene molar ratio at low methane contents. In Figure 10, where the methane content is greater (about 62 mol %) ternary curves depart from the binaries, showing that an increased methane-ethane and methane-ethylene interaction is present.

Figures 10 and 11 reveal that in ethane-ethylene gas mixture adsorption ethane is more strongly adsorbed than ethylene; this is clear in Figure 10 where the ethylene content in the gas phase is larger than

Reproduced with permission of the copyright owner. Further reproduction prohibited without permission.

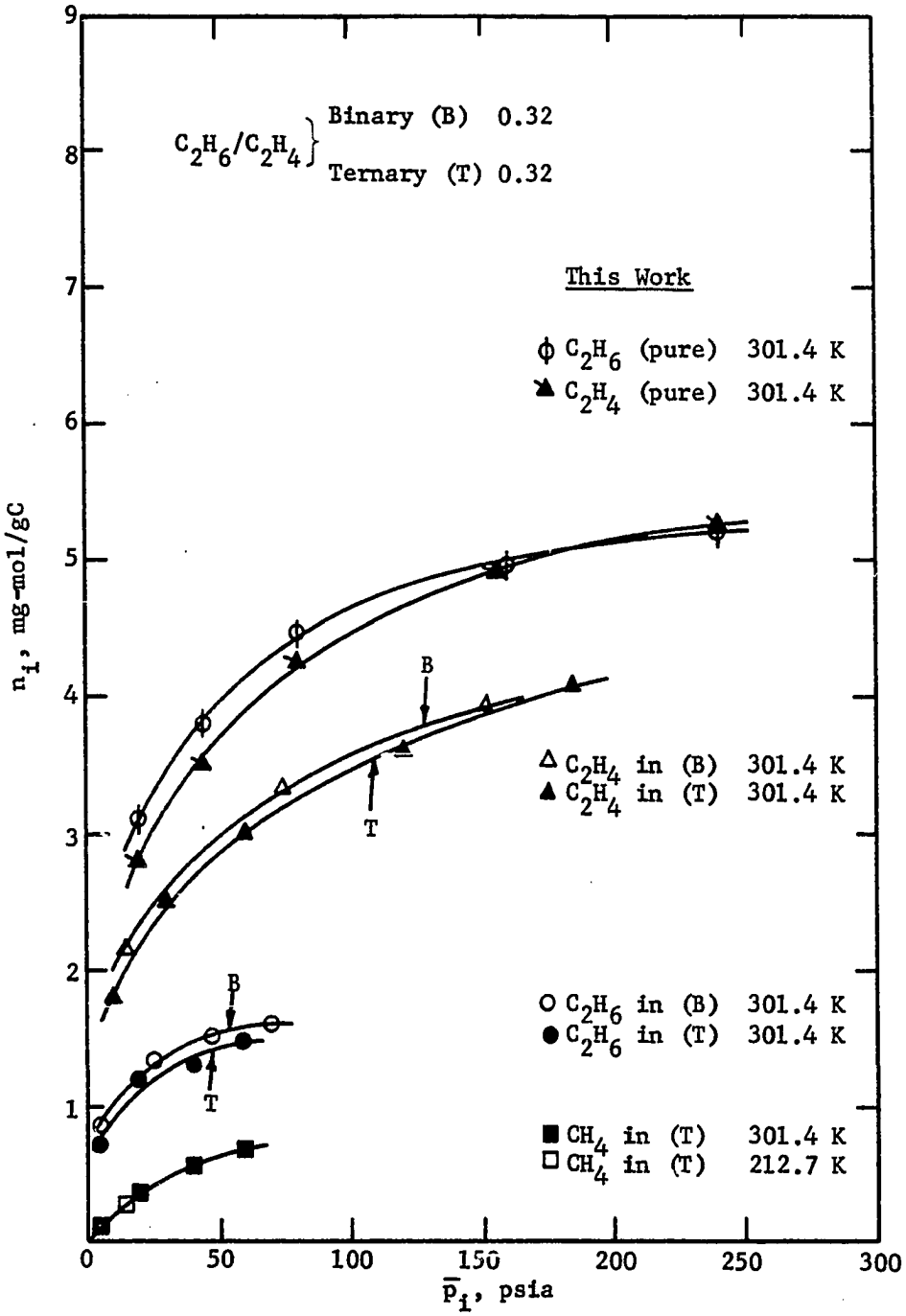

Figure 9. Ethane-Ethylene Isotherms (24.0-76.0 mol %)
Methane-Ethane-Ethylene Isotherms (20.0-19.2-60.8 mol %)

Reproduced with permission of the copyright owner. Further reproduction prohibited without permission.

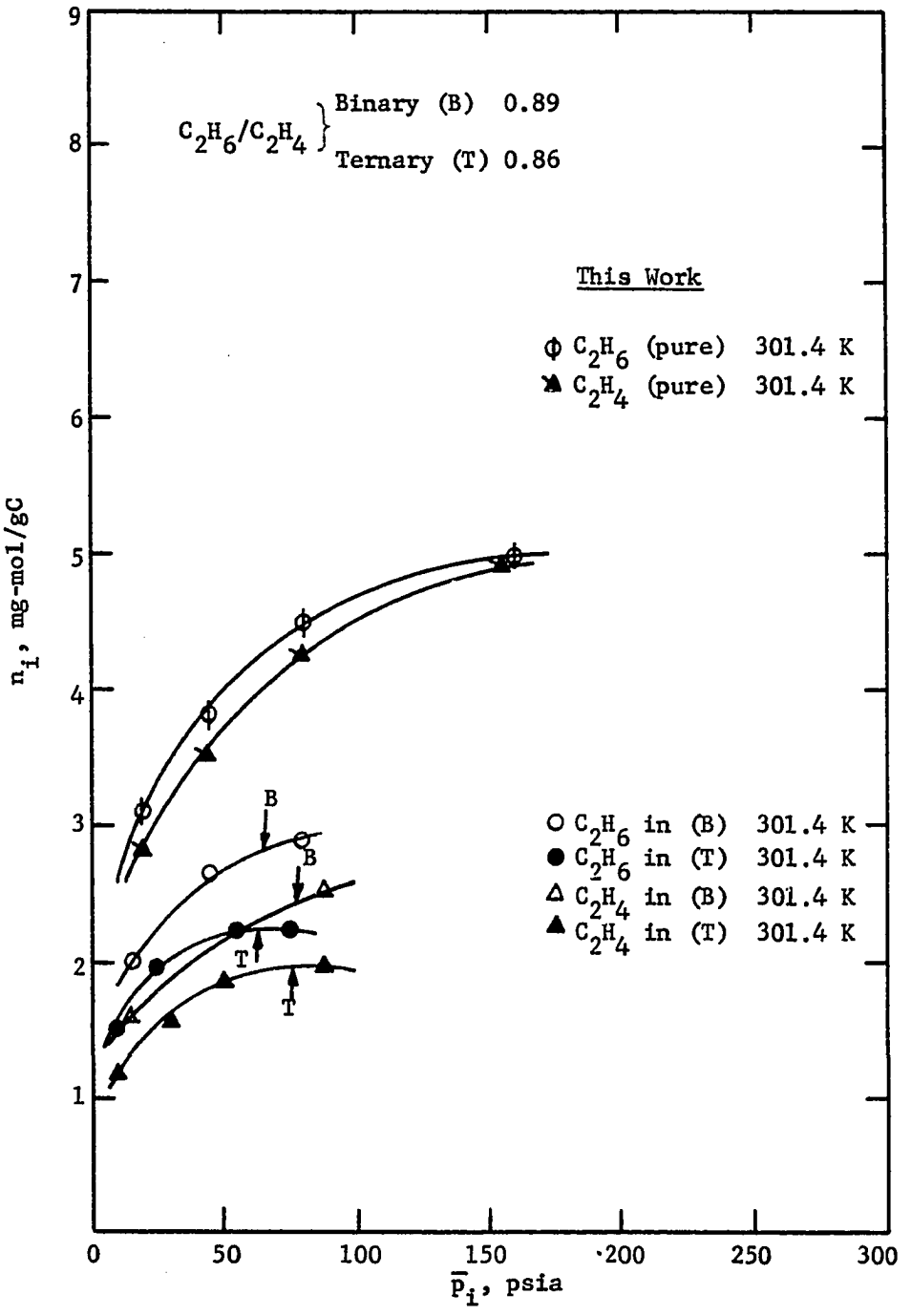

Figure 10. Ethane-Ethylene Isotherms (47.2-52.8 mol %)
Methane-Ethane-Ethylene Isotherms (62.4-17.4-20.2 mol %)

Reproduced with permission of the copyright owner. Further reproduction prohibited without permission.

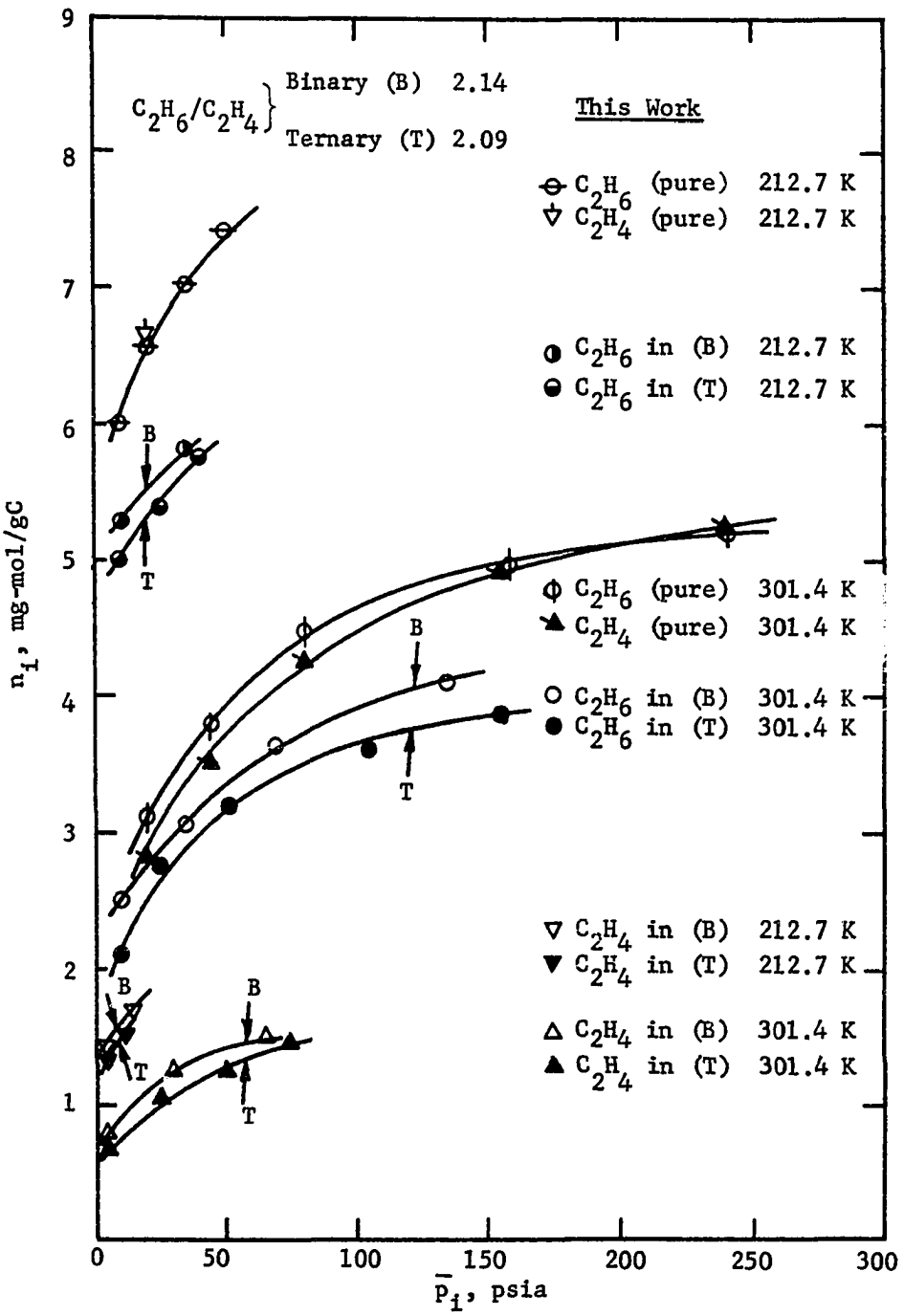

Figure 11. Ethane-Ethylene Isotherms (68.2-31.8 mol %)
Methane-Ethane-Ethylene Isotherms (23.0-52.0-25.0 mol %)

Reproduced with permission of the copyright owner. Further reproduction prohibited without permission.

ethane (molar ratio ethane-ethylene = 0.89).

The conclusion reached from the complete set of gas mixture adsorption data is that the methane adsorption capacities are approximately temperature independent between 212.7 K and 301.4 K. This unexpected behavior may be explained by means of a physical representation where the adsorbent micropore volume is being filled with adsorbate. The kinetic results, to be presented in the next section of this chapter, show a strong initial adsorption of ethane and/or ethylene in the presence of methane. This suggests that the methane is adsorbed only after the pores are essentially filled with ethane or ethylene. As the ethane or ethylene adsorption is enhanced at lower temperatures, the space available for methane would be reduced, this effect being cancelled by its greater adsorption capacity at these temperatures.

Several binary gas mixture adsorption measurements at different equilibrium temperatures and pressures were repeated to check reproducibility. A summary of these data is given in Table 16 in Appendix G. Reproducibility of the measurements was accomplished with a maximum deviation of 5.5% and an average of ± 1.3%.

As all experimental measurements were directed to obtaining true equilibrium data, a check was made of the effect of the gas flow rate through the adsorbent bed on the adsorption cell effluent stream; a too high flow rate could result in an effluent gas stream that was not in equilibrium with the adsorbate mixture. To verify this possible effect the feed gas flow rate was reduced in some experiments, after the system seemed to be at equilibrium, i.e., when feed gas and effluent compositions were essentially the same. The rate was reduced to one half and then to

Reproduced with permission of the copyright owner. Further reproduction prohibited without permission.

one eighth of the normal flow rate; no change was observed in the effluent gas composition.

An error analysis was attempted for the gas mixture isotherm measurements; it is discussed in Appendix H. The maximum random error involved in these determinations is thought to be between 6 and 10% for C_2H_6 and C_2H_4, and between 10 and 20% for CH_4, as a reasonable approximation. A probable error, smaller than these values, is supported by the fact that gas mixture adsorption reproducibilities of about ± 2% were obtained.

Kinetic Results

Some binary and ternary kinetic data were determined in this experimental study. A sample of these results, presented in Figure 12 and in Figures 30, 31, and 32 in Appendix G, is of an approximate nature and only serves for qualitative purposes.

Figure 12 represents a kinetic evaluation of the adsorption of an ethane-ethylene gas mixture high in ethylene content (ethane-ethylene molar ratio = 0.32) at 212.7 K and an equilibrium pressure of 59 psia. The graphical representation shows clearly that initially it is ethane which is adsorbed the faster; this effect levels off later, and then ethylene seems to control the adsorption until equilibrium is attained. This ethane behavior was found at all three ethane-ethylene molar ratios and both in binary and ternary gas mixtures.

Figures 30, 31, and 32 in Appendix G support the conclusion that ethane and ethylene adsorb first when methane is present in binary and ternary gas mixtures.

Reproduced with permission of the copyright owner. Further reproduction prohibited without permission.

Reproduced with permission of the copyright owner. Further reproduction prohibited without permission.

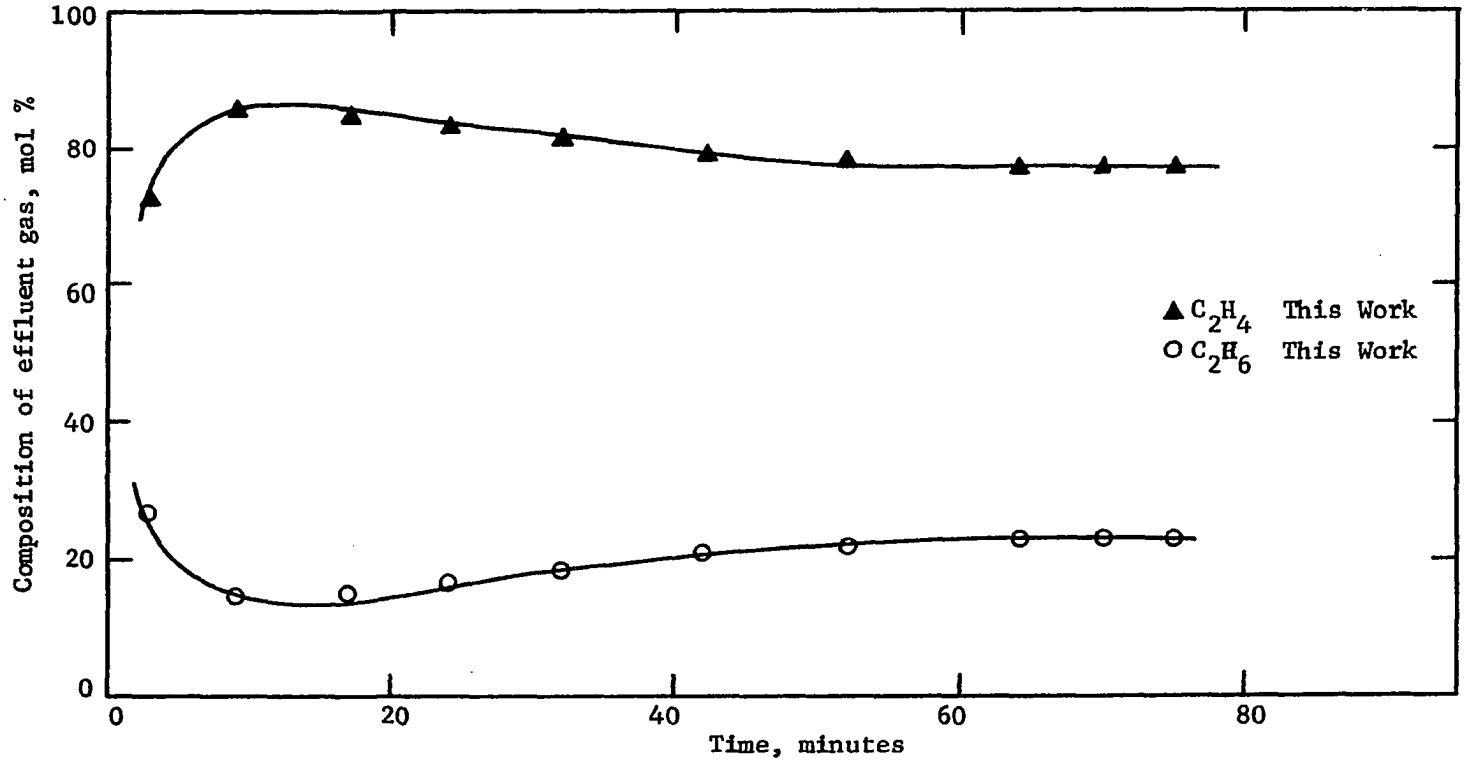

Figure 12. Kinetic Data for Ethane-Ethylene Mixture (24.0-76.0 mol %) at 212.7 K and 59 psia

Comparison with the Results of Others

Pure Gas Isotherms

A comparison with results of others for pure gas isotherm data is attempted in Figures 3, 4, and 5 in this chapter. Methane and carbon dioxide data at 301.4, 260.2, and 212.7 K, determined in this laboratory by Rogers[47] on the same adsorbent, are shown. Agreement with the data obtained in this work exists at 212.7 K within ± 1 to 5%. However, at the other two temperature levels significant differences are observed with average deviations of the order of ± 5 to 15%. In general, the data of Rogers show higher adsorption capacities at these higher temperatures. A reasonable explanation for this disagreement has not been found.

Low pressure adsorption data for ethane and carbon dioxide at 303 K on the same adsorbent are given by Laukhuf and Plank[28] and Meredith and Plank,[35] respectively; good agreement is obtained in this range of equilibrium pressures.

Adsorption data for all gases on a similar adsorbent at 301 K can be interpolated from Szepesy and Illes.[51] Capacities are essentially similar to the results presented here.

Isotherm data for methane and carbon dioxide at 311 K on a similar adsorbent are given by Ray and Box.[45] These latter results show much larger capacities than does this work.

Mixture Gas Isotherms

No published results for the ternary system employed in this work are available for comparison.

Some binary isotherm data on similar adsorbents at 293 K and about one atmosphere pressure are given by Szepesy and Illes.[52] As working

Reproduced with permission of the copyright owner. Further reproduction prohibited without permission.

pressures in this work are greater than one atmosphere and the temperatures are different, no attempt at comparison was made.

Reproduced with permission of the copyright owner. Further reproduction prohibited without permission.

CHAPTER IV

THEORY

For many years it has been the goal of investigators in the field of gas adsorption to be able to collect enough information on adsorbates and adsorbents so that the adsorption of gases and vapors could be predicted from a minimum of data. In pure gas adsorption, the immediate goal of many investigators has been the prediction of gas-phase adsorption isotherms for a number of adsorbates, under a wide range of temperature and pressure conditions, from a single functional relation representing the adsorbent-adsorbates interaction behavior. For gas mixture adsorption the main purpose has been to be able to predict the component adsorption capacities from pure gas adsorption data or correlations for fixed conditions of temperature, pressure, and gas phase compositions. These are the main objectives that motivated this present work; therefore, the theoretical presentation is oriented in that direction.

Of the various theories proposed to predict the adsorption properties of gases or vapors on solids, the most successful for adsorbent-adsorbate systems of practical significance have been based on the potential theory of adsorption as formulated by Polanyi[40,43] and as modified by Dubinin and co-workers[16,17,18] and others for pure gas adsorption, and by Grant and Manes[25] for gas mixture adsorption. Although the theory has been applied to adsorption on homogeneous adsorbents, it has found its most useful application on highly heterogeneous adsorbents such as

Reproduced with permission of the copyright owner. Further reproduction prohibited without permission.

activated carbon and silica gel with large surface areas and pore volumes.

The Polanyi Potential Theory

Although introduced in 1914,[40] the Potential Theory of Michael Polanyi is still regarded as fundamentally sound, in large measure due to its essentially thermodynamic character. The theory does not attempt to describe adsorption on a molecular level and postulates[41,42] energy surfaces surrounding the adsorbent for which the adsorption potentials are equal and temperature invariant. The volumes enclosed by these equipotential surfaces, $\epsilon = \epsilon_1, \epsilon_2, \epsilon_3, \ldots, \epsilon_i \ldots = 0$, might be designated as $V_{a1}, V_{a2}, V_{a3}, \ldots, V_{ai}, \ldots V_{amax}$, where V_{amax} would be the total adsorption space, which in the case of a porous adsorbent like activated carbon, corresponds to its pore volume. The theory is applied by experimentally determining the distribution function

$$\epsilon = F'(V_a) = F(\hat{V}_a) \tag{5}$$

where $\hat{V}_a = V_a/m$.

Polanyi associated the magnitude of the adsorption potential, ϵ, at any particular degree of the pore volume filling, with the work required to attain adsorption at that level. If the gas phase is assumed to be an ideal gas, the liquid-like adsorbate is considered to be incompressible, and negligible work is used in creating the new surface, then the reversible work required to compress the gas from the equilibrium adsorption pressure, P, to the vapor pressure, $p_s(T)$, of the liquid adsorbate at the temperature, T, of the system is given by

Reproduced with permission of the copyright owner. Further reproduction prohibited without permission.

$$\epsilon = RT \ln[p_s(T)/P] \tag{6}$$

The value of the adsorbate volume, V_a, corresponding to ϵ is obtained by multiplying the moles of gas adsorbed at P, n_o', by the adsorbate molar volume, $\tilde{V}_a$,

$$V_a = n_o' \tilde{V}_a \tag{7}$$

or

$$\hat{V}_a = n_o \tilde{V}_a$$

It is therefore possible to construct the distribution function (5) from experimental adsorption data and relations (6) and (7). Polanyi postulated that this distribution function, which is often called the "characteristic curve" for the adsorbent-adsorbate system, is nearly temperature independent for many adsorption systems and can be used to predict adsorption capacities of systems at temperatures other than those measured experimentally.

It is now recognized[20] that the concept of equipotential surfaces is not physically acceptable and that the function ϵ should be interpreted, not as an adsorption potential, but as a change in Gibbs energy, $\Delta\tilde{G}$, or as a difference in the chemical potentials of the adsorbate in a reference state of bulk liquid, μ_r, and in the adsorbed state, μ_a, at one and the same temperature,

$$\epsilon = \mu_r - \mu_a = -\Delta\tilde{G} = RT \ln [p_s(T)/P] \tag{8}$$

or

Reproduced with permission of the copyright owner. Further reproduction prohibited without permission.

$$\mu_a - \mu_r = \Delta\tilde{G} = RT \ln [P/p_s(T)] = -\epsilon \qquad (9)$$

Steele[49] has offered an enlightening interpretation of ϵ based on a theory of the generalized properties of distribution functions of a fluid in an external field, as applied to multilayer adsorption and liquids. It considers, first, a pure liquid adsorbate, and then it couples it to the solid adsorbent. His result for the change in chemical potential upon coupling is given as

$$-\epsilon = \mu_a - \mu_r = \langle U_p(z_n) \rangle_\tau = RT \ln [P/p_s(T)] \qquad (10)$$

where $\langle U_p(z_n) \rangle_\tau$ is the average perturbing energy, at a given value of the adsorbate thickness, z_n, which can be evaluated if the perturbing potential and density distributions over the adsorbate are known. The averaging includes the effect of compression of the film. τ is a surface vector.

It is possible thus to conclude that ϵ is a Gibbs energy and not simply a potential energy. One can anticipate that ϵ will be somewhat temperature dependent, because for ϵ to be temperature invariant the film must be incompressible and the thermal expansion of the adsorbent equal to that of the reference state. These effects, however, are normally unimportant in comparison to experimental uncertainties, and basically the temperature invariance of the characteristic curve can be expected.

If non-idealities in the gas phase are considered, relation (9) may be written as

Reproduced with permission of the copyright owner. Further reproduction prohibited without permission.

$$\mu_a - \mu_r = \Delta\tilde{G} = RT \ln[f(P,T)/f_s(p_s,T)] = -\epsilon \qquad (11)$$

where $f(P,T)$ corresponds to the fugacity of the gas phase evaluated at the adsorption pressure and temperature, and $f_s(p_s,T)$ to the fugacity of the gas at the saturation pressure and temperature.

The Polanyi Theory as Extended by Dubinin and Its Application to Pure Gas Adsorption

The Polanyi Potential Theory, as postulated by Polanyi[22,40,41,42,43] and applied by Berenyi,[4,5] and Lowry and Olmstead,[32] and subject to considerable attacks from the scientific community of that time,[44] was not extensively applied or developed until 1947, when M. M. Dubinin and his collaborators began to make considerable use of it to predict adsorption isotherms for any pure gas, given a single isotherm for one gas on the same adsorbent.

Dubinin and Timofeyev[16] wrote the characteristic curve for all gases on the same adsorbent as*

$$\left(\frac{\epsilon}{\beta}\right)_{\text{all } i} = F(\hat{V}_a) \qquad (12)$$

where

$$\hat{V}_a = n_c \tilde{V}_a \Big|_{\text{all } i} \qquad (13)$$

and β, called the "affinity coefficient" for the adsorbate in question, is a shifting factor causing all the characteristic curves for the indi-

*It is customary to draw the characteristic curve with $\hat{V}_a$ as the ordinate and ϵ/β as the abscissa. As an illustration see Figure 13 in Chapter V.

Reproduced with permission of the copyright owner. Further reproduction prohibited without permission.

vidual gases to fall into a single curve. The prediction of the adsorption isotherms for different gases may be carried out either graphically or analytically, but each method depends on the premise that an experimentally determined characteristic curve defines the adsorption nature of a given adsorbent.

Graphical Analysis

At constant adsorbate volume, $\hat{V}_a$,

$$\left(\frac{\varepsilon}{\beta}\right)_{\text{all } i} = \text{constant} \tag{14}$$

or

$$\frac{\varepsilon_1}{\beta_1} = \frac{\varepsilon_2}{\beta_2} \cdot \cdot \cdot = \frac{\varepsilon_i}{\beta_i} = \text{constant}$$

where

$$\varepsilon_i = RT \ln[f_s(p_s,T)/f(P,T)]\Big|_i \tag{15}$$

It is basically relations (13), (14), and (15) which represent the Polanyi Potential Theory, as extended by Dubinin, when applied graphically to pure adsorbates on the same solid adsorbent.

The characteristic curve for the different adsorbates on the solid adsorbent, equation (12), is constructed from experimental adsorption data given as adsorption capacities, n_{oi}, in mg-mol/g adsorbent, versus equilibrium pressures, P, at a given set of temperatures, T. The ordinate is calculated with relation (13) and the abscissa from (14) and (15); n_{oi}, P, and T are experimental adsorption data; f_s is the fugacity of the pure gas at its vapor pressure, p_s, and T to be evaluated with an appropriate equation of state; f is the fugacity of the pure gas at the equi-

Reproduced with permission of the copyright owner. Further reproduction prohibited without permission.

librium pressure and temperature evaluated as explained before; β is the affinity coefficient which is calculated from physical properties of the substance and $\tilde{V}_a$ is the adsorbate molar volume, normally not known but estimated.

Physically, the affinity coefficient is associated with the strength of the adsorbent-adsorbate interaction. In practice, a value of unity is assigned to β for a reference adsorbate so that β, for any gas for which predictions are desired, has a relative value comparing the gas-solid interaction for that gas to that of the reference adsorbate.

If the adsorbent surface is assumed to be essentially non-polar, the adsorption forces are due mainly to dispersion interactions between the adsorbate and adsorbent which are induced by the fluctuating electrical fields of the molecules. Dubinin,[16] following a development by London[31,43] on applications of the concept of molecular forces to adsorption, assumed that for a molecule at a distance z from a plane surface, the adsorption potential is expressed approximately by the relation

$$\varepsilon = \frac{\pi N \alpha \alpha_A \; II_A}{4z^3 \; (I+I_A)} \tag{16}$$

where A denotes the property for the adsorbent, I is the ionization potential for the gas molecule, α is the polarizability, and N is the number of atoms in the adsorbate per cm^3. Temperature is assumed not to affect the adsorption forces.

For equal values of z or adsorbate volume, V_a, according to (12)

Reproduced with permission of the copyright owner. Further reproduction prohibited without permission.

$$\beta = \frac{\varepsilon}{\varepsilon_r} = \frac{\alpha}{\alpha_r} \frac{\frac{II_A}{I+I_A}}{\left\{\frac{II_A}{I+i_A}\right\}_r} \tag{17}$$

This relation can be approximated by

$$\beta \simeq \frac{\alpha}{\alpha_r} \tag{18}$$

since the ionization potentials of most substances do not differ very much from one another.

Based on qualitative arguments of general validity, Dubinin finally postulated that as an approximation the polarizability of the molecules is proportional to its volume or to the molar volume of the liquid adsorbate, leaving (14) and (18) as

$$\beta = \tilde{V}_a / (\tilde{V}_a)_r \tag{19}$$

$$\left.\frac{\varepsilon}{\tilde{V}_a}\right|_{\text{all } i} = \text{constant} \tag{20}$$

As the affinity coefficient, as stated before, implied temperature independence, Dubinin assumed the liquid adsorbate volume to be temperature invariant[17]; however, it is not clear what numerical values were selected.

A similar method for estimating the affinity coefficients was reported by Dubinin and Zhukovskaia.[19] The affinity coefficients are ex-

Reproduced with permission of the copyright owner. Further reproduction prohibited without permission.

pressed by the ratio of parachors of the substances. By this means, molar volumes are determined under conditions of equal molecular compression, thus representing the molecular volume ratios more closely. Temperature independence is also exhibited.

Following a similar line of reasoning Grant and Manes[24] thought it best to compare molar volumes at corresponding states; the normal boiling point being selected for convenience. This is expressed by

$$\left.\frac{\varepsilon}{\tilde{V}_s(T_{nbp})}\right|_{\text{all } i} = \text{constant} \qquad (21)$$

It is basically the estimation of the adsorbate molar volume, $\tilde{V}_a$, and the affinity coefficient, β, that have led to the several modifications of the adsorption Potential Theory, as applied to pure gases and vapors, available today in the literature. A summary of different modifications is presented in Appendix I.

In general, the adsorbate is assumed to behave as a liquid-like material. Most modifications center around assigning numerical values to $\tilde{V}_a$ which tend to improve the overall correlation; β is normally associated with a molar volume of the liquid adsorbate, as proposed by Dubinin and co-workers.[16]

Analytical Method

Dubinin and Radushkevich[18] proposed an analytical expression which allows the prediction of adsorption data for pure substances on heterogeneous adsorbents like activated carbon.

Based on the empirical fact that the shape of the characteristic

Reproduced with permission of the copyright owner. Further reproduction prohibited without permission.

curves for different specimens of microporous active carbons showed a Gaussian form, they represented this function by an equation involving the Gaussian distribution

$$\hat{V}_a = n_o \tilde{V}_a = \hat{V}_a^o \exp\left[-k \frac{\epsilon^2}{\beta^2}\right] \tag{22}$$

where $\hat{V}_a^o$ is the volume of adsorbate at $\epsilon = 0$ interpreted as the limiting volume of the adsorption space expressing the volume of micropores of the activated carbon, $\hat{V}_a$ is the adsorbate volume at the adsorption potential ϵ (given by equation (15)) and k is a constant which is thought to express the distribution function of pore volumes with respect to their size. The linear form of this equation is then given by

$$\ln \hat{V}_a = \ln \hat{V}_a^o - k \left(\frac{\epsilon}{\beta}\right)^2 \tag{23}$$

Inserting equation (15) into (23) gives

$$\ln \hat{V}_a = \ln \hat{V}_a^o - k \left\{\frac{RT}{\beta} \ln[f_s(p_s,T)/f(P,T)]\right\}^2 \tag{24}$$

The parameters $\hat{V}_a^o$ and k are evaluated from experimental adsorption data for a reference adsorbate on the same adsorbent ($\beta_r = 1.0$) and equations (24) and (25), provided a suitable value for $\tilde{V}_a$ is chosen.

Given a specific adsorbate, at fixed equilibrium temperature and pressure, the amount adsorbed can be predicted from equation (24) and

Reproduced with permission of the copyright owner. Further reproduction prohibited without permission.

$$n_o = \hat{V}_a / \tilde{V}_a \tag{25}$$

provided a value for $\tilde{V}_a$ is chosen.

Nikolaev and Dubinin[37] proposed a functional scheme which describes the dependence of the adsorbate molar volume, $\tilde{V}_a$, on the system temperature.

For temperatures below the normal boiling point of the substance, saturated liquid molar volumes at the system temperature were used

$$\tilde{V}_a = \tilde{V}_s(T) \qquad T < T_{nbp} \tag{26}$$

For temperatures between the normal boiling point and the critical point, a linear relation was used

$$\tilde{V}_a = A + BT \tag{27}$$

A and B being constants to be evaluated with the following boundary conditions:

$$\tilde{V}_a(T=T_{nbp}) = \tilde{V}_s(T_{nbp}) \tag{28}$$

$$\tilde{V}_a(T=T_c) = b = RT_c/(8P_c)$$

b is one of the constants in the van der Waals equation of state; it is evaluated from critical properties of the substance.

The final form of equation (27) is

Reproduced with permission of the copyright owner. Further reproduction prohibited without permission.

$$\tilde{V}_a = b - [b-\tilde{V}_s(T_{nbp})]\left[\frac{T_c-T}{T_c - T_{nbp}}\right] \qquad T_{nbp} \leq T \leq T_c \tag{29}$$

For temperatures above the critical point the adsorbate molar volume was assumed to be constant and equal to the van der Waals b of the substance

$$\tilde{V}_a = b \qquad T > T_c \tag{30}$$

The complete scheme is justified, according to the authors, by considering that the adsorbed phase, under conditions of temperature close to the critical and above it, exists in a greatly compressed state in the field of the adsorption forces. Under these conditions the use of normal saturated liquid densities is no longer justified.

The same authors have modified equation (24), for temperatures above the critical, to

$$\ln \hat{V}_a = \ln \hat{V}_a^o - k\left[\frac{RT}{\beta} \ln \frac{T^2P_c}{T_c^2P}\right]^2 \tag{31}$$

Relation (24), often called the Dubinin-Radushkevich equation (D-R) for very fine microporous active carbons, has been found reasonably successful in describing characteristic curves for a number of experimental systems,[11,15,17,18,21,37,54] and its general use is justified on empirical grounds.

Insight into the theoretical basis of this equation has been provided by Steele[49] who has observed that, when a modified Gaussian site-

Reproduced with permission of the copyright owner. Further reproduction prohibited without permission.

distribution function is used in the Frenkel-Halsey-Hill theory of multilayer adsorption instead of the exponential distribution function, the D-R equation is obtained. The basis of this theory[39,53] is that the adsorption potential varies simply as the inverse cube of the distance from the surface; patchwise heterogeneity of the adsorbent surface is also assumed.

One difficulty with equation (22) arises from the fact that it does not reduce to a linear isotherm in the limit of very low coverages, i.e., it does not follow Henry's law at low pressures.

Application of the Potential Theory to Gas Mixtures

In the adsorption of a pure gas on a solid adsorbent three intensive variables are required to specify the system, namely the temperature, pressure, and the amount adsorbed per unit mass of adsorbent. In the adsorption of a binary gas mixture there are five variables to be designated before the system is fully specified. These are frequently chosen to be the temperature, the partial pressures of the components in the gas phase, and the amount adsorbed of both components. A ternary adsorption system is similarly defined with seven variables.

The prediction of a binary adsorption isotherm reduces then to the evaluation of the amounts adsorbed of both components, given the pure component isotherm functions or a characteristic curve for the adsorbates-adsorbent system

$$n_o = F'(\varepsilon)/\tilde{V}_a\Big|_{\text{all } i} \tag{34}$$

Reproduced with permission of the copyright owner. Further reproduction prohibited without permission.

Grant and Manes[25] extended the Polanyi Potential Theory to gas mixture adsorption by considering the liquid-like adsorbate as a mixture in which the adsorption potential of each pure adsorbed component was determined by the adsorbate volume of the mixture, i.e.

$$\epsilon = F(\hat{V}_{am})\Big|_{\text{all } i} \tag{35}$$

or

$$\epsilon = RT \ln [f_s(p_s,T)/f(\tilde{V}_{am},T)] = F(\hat{V}_{am})\Big|_{\text{all } i} \tag{36}$$

By using equations (21) and (36)

$$\frac{\epsilon_1}{\tilde{V}_{s1}(T_{nbp})} = \frac{\epsilon_2}{\tilde{V}_{s2}(T_{nbp})} = \cdots \text{ etc.} \tag{37}$$

$$\frac{RT}{\tilde{V}_{s1}(T_{nbp})} \ln[f_{s1}(p_{s1},T)/f_1(\tilde{V}_{am},T)] \tag{38}$$

$$= \frac{RT}{\tilde{V}_{s2}(T_{nbp})} \ln[f_{s2}(p_{s2},T)/f_2(\tilde{V}_{am},T)] = \cdots \text{ etc.}$$

and assuming ideal adsorbed solution

$$\bar{f}_i(P,T,\{y\}) = x_i\, f_i(\tilde{V}_{am},T) \tag{39}$$

$$\frac{RT}{\tilde{V}_{s1}(T_{nbp})} \ln\left[\frac{x_1 f_{s1}(p_{s1},T)}{\bar{f}_1(P,T,\{y\})}\right] = \frac{RT}{\tilde{V}_{s2}(T_{nbp})} \ln\left[\frac{x_2 f_{s2}(p_{s2},T)}{\bar{f}_2(P,T,\{y\})}\right] = \ldots \text{ etc.} \tag{40}$$

or

$$\frac{RT}{\tilde{V}_s(T_{nbp})} \ln\left[\frac{x f_s(p_s,T)}{\bar{f}(P,T,\{y\})}\right] = F(n_T\tilde{V}_{am})\Big|_{\text{all } i} \tag{41}$$

Reproduced with permission of the copyright owner. Further reproduction prohibited without permission.

Relation (41) represents the characteristic curve for the gas mixtures and should be superimposable on the pure isotherm characteristic curve

$$\frac{RT}{\tilde{V}_s(T_{nbp})} \ln [f_s(p_s,T)/f(P,T)] = F(n_o\tilde{V}_a)\Big|_{\text{all } i} \qquad (42)$$

In Grant and Manes's model, the assumption of determining the adsorption potential of each pure adsorbed component by the adsorbate volume of the mixture is equivalent to defining a standard state where the pure adsorbate is at the same volume as that of the adsorbed mixture. Sircar and Myers[48] have recently pointed out that the selection of this particular standard state leads to the incorrect conclusion of equality of surface potentials of the adsorbed phase at saturation, which can be true only if the composition of the adsorbed phase is equal to the composition of the bulk liquid phase. A discussion of this argument is given in Appendix J.

From a prediction point of view this model is used as follows:

given P, T, $\{y\}$ and the characteristic curve for the pure gases on the adsorbent,

1) Equation (40) and the relation between the adsorbate mole fractions

$$\sum_{i=1}^{\text{all } i} x_i = 1 \qquad (43)$$

are solved iteratively for all x_i.

2) The abscissa of the characteristic curve

Reproduced with permission of the copyright owner. Further reproduction prohibited without permission.

$$\frac{\epsilon}{\tilde{V}_s(T_{nbp})} = \frac{RT}{\tilde{V}_s(T_{nbp})} \ln\left[\frac{xf_s(p_s,T)}{\bar{f}(P,T,\{y\})}\right] \tag{44}$$

is determined with any of the x_i's.

3) $(n_T\tilde{V}_{am})$ is obtained from the characteristic curve (41) or (42) and the calculated abscissa

$$\frac{\epsilon}{\tilde{V}_s(T_{nbp})}$$

4) The molar volume of the adsorbate mixture is estimated assuming additivity of pure component volumes

$$\tilde{V}_{am} = \sum_{i=1}^{all\ i} x_i \tilde{V}_{si}(P_g = Py/x)_i \tag{45}$$

5) The total amount adsorbed is evaluated as

$$n_T = (n_T\tilde{V}_{am})/\tilde{V}_{am} \tag{46}$$

and the individual components as

$$n_i = x_i n_T \tag{47}$$

Bering et al.[6,7] extended the application of the Dubinin-Radushkevich equation (24) to the adsorption of binary gas mixtures. If the pure gas isotherms, represented by equation (33), satisfy the D-R equation for very fine micropore adsorbents, equation (24), then

Reproduced with permission of the copyright owner. Further reproduction prohibited without permission.

$$n_o = \frac{\hat{V}_a^o}{\bar{V}_a} \exp\left\{-\frac{k}{\beta^2}\left[RT \ln \frac{f_s(p_s,T)}{f(P,T)}\right]^2\right\}_{\text{pure } i} \tag{48}$$

this relation being generalized for the case of a gas mixture adsorption to

$$n_T = \sum_{i=1}^{\text{all } i} n_i = \frac{\hat{V}_a^o}{\sum_{i=1}^{\text{all } i} x_i \bar{V}_{ai}} \tag{49}$$

$$\exp\left\{\frac{-k}{\left[\sum_i x_i \bar{\beta}_i\right]^2}\left[\sum_{i=1}^{\text{all } i} x_i \ln \frac{f_{si}(p_{si},T)}{f_i(P,T,\{y\})}\right]^2\right\}$$

where $\{x_i\}$ are the adsorbate mole fractions, $\bar{V}_{ai}$ is the adsorbate partial molar volume of component i, and $\bar{\beta}_i$ is the component i affinity coefficient.

Given P,T,{y} and the characteristic curve for the pure gases, (48) and (49) can be solved for the amount adsorbed of the components in a binary mixture if an additional independent relation between n_o and n_i is available.

Bering et al.[6,7] selected for their purposes a relation proposed by Lewis et al.[29] which applies only to an ideal adsorbed solution

$$\left.\sum_{i=1}^{\text{all } i} \frac{n_i(\bar{p}_i,T)}{n_{oi}(P,T)}\right|_{P=\bar{p}_1+\bar{p}_2 = \text{constant}} = 1.0 \tag{50}$$

Reproduced with permission of the copyright owner. Further reproduction prohibited without permission.

at pure component equilibrium pressures equal to the mixture total pressure, P.

Unfortunately, the use of equation (50) does not satisfy the well known mole fraction relation

$$\sum_{i=1}^{\text{all } i} \frac{n_i(\bar{p}_i,T)}{n_T(P,\{y_i\},T)} = \sum_{i=1}^{\text{all } i} x_i = 1.0 \qquad (51)$$

for many systems as reported by others.[12,25,47]

The Concept of Relative Volatility and Other Correlation Methods for Adsorption Mixtures

Relative Volatility

During the adsorption of a gas mixture there is a competition among the components for the adsorbent surface. Such a competition produces a separation phenomenon similar to that experienced in many of the well known separation processes such as distillation or extraction. The adsorbent is said to adsorb selectively one gas over another. In general, the pure gas for which the adsorbent exhibits the higher capacity is that preferentially adsorbed from a mixture. This preferential action of the adsorbent is normally dependent on the adsorbent and adsorbate physical properties, and the temperature, pressure, and composition of the system. Regardless of which properties cause the components in a mixture to be adsorbed preferentially, there will be less of a given component adsorbed from a mixture as such than as a pure gas at the same partial pressure in the mixture. This is the result of each component interfering with the adsorption of the others, thus decreasing the individual adsorption capa-

Reproduced with permission of the copyright owner. Further reproduction prohibited without permission.

cities.

Lewis et al.[29] introduced into adsorption work the relative volatility or separation factor, α', a variable which measures the selectivity or preferential adsorption of the adsorbent for one component over the other in a binary gas mixture. It is defined as

$$\alpha'_{12} = \frac{x_2 y_1}{x_1 y_2} = \frac{x_2 \bar{P}_1}{x_1 \bar{P}_2} \tag{52}$$

where component 2 is the more strongly adsorbed, i.e., $\alpha' > 1$.

The dependence of the relative volatility on the system variables can be obtained from adsorption thermodynamics.[8,36] The chemical potential of component i in the gas and adsorbed phases may be written as

$$\mu_{gi}(P,T,\{y_i\}) = \mu_{gi}(1,T) + RT \ln \bar{f}_i(P,T,\{y_i\}) \tag{53}$$

$$\mu_{ai}(\emptyset,T,\{x_i\} = \mu_{ai}(\emptyset,T) + RT \ln \gamma_{ai} x_i \tag{54}$$

where

$$\mu_{ai}(\emptyset,T) = \mu_{gi}(1,T) + RT \ln f_i(\emptyset,T) \tag{55}$$

and $\emptyset$ is the surface potential of the adsorbate mixture, as defined by Bering, et al.[8]

$$\emptyset = \frac{\pi A}{n_A} - (\mu_A - \mu_A^o) \tag{56}$$

π being the spreading pressure of the adsorbate mixture, A the adsorbent surface, n_A the moles of adsorbent, and $(\mu_A - \mu_A^o)$ the difference in chemi-

Reproduced with permission of the copyright owner. Further reproduction prohibited without permission.

cal potential of the adsorbent when in the presence of adsorbate and when pure, i.e., for an inert adsorbent $(\mu_A - \mu_A^o) = 0$.

At equilibrium

$$\mu_{gi} = \mu_{ai} \tag{57}$$

and therefore

$$\bar{f}_i(P,T,\{y_i\}) = \gamma_{ai} x_i f_i(\emptyset,T) \tag{58}$$

$$\alpha'_{12} = \frac{\bar{f}_2(P,T,\{y_i\}) f_1(\emptyset,T)\ \gamma_{a1}(\emptyset,T,\{x_i\})\ y_1}{\bar{f}_1(P,T,\{y_i\}) f_2(\emptyset,T)\ \gamma_{a2}(\emptyset,T,\{x_i\})\ y_2} \tag{59}$$

$$\alpha'_{12} = F(P,T,\emptyset,\{y_i\},\{x_i\}) \tag{60}$$

If ideal solution is assumed in both phases

$$\alpha'_{12} = \frac{f_2(P,T)\ f_1(\emptyset,T)}{f_1(P,T)\ f_2(\emptyset,T)} = F(P,T,\emptyset) \tag{61}$$

which reduces to

$$\alpha'_{12} = \frac{P_1(\emptyset,T)}{P_2(\emptyset,T)} = F(\emptyset,T) \tag{62}$$

at low pressures, $P_i(\emptyset,T)$ being the equilibrium gas pressure corresponding to the solution temperature and to the mixture surface potential, $\emptyset$, (i.e., spreading pressure) for the adsorption of pure component i.[36] $\emptyset$ can be evaluated from the Gibbs isotherm[9]

$$\emptyset = RT \int_o^P \sum_{i=1}^{all\ i} \frac{n_i}{n_A}\, d\ln P \tag{63}$$

Reproduced with permission of the copyright owner. Further reproduction prohibited without permission.

In general, the relative volatility or selectivity of the adsorbent for the more strongly adsorbed component is found to decrease both with increasing pressure and temperature, and with concentration of that component at constant T and P.[29,47]

Other Correlation Methods for Adsorption Mixtures

Myers and Prausnitz[36] developed a method based on solution thermodynamics and an ideal adsorbed solution model. Basically, equation (58), applied to the case of an ideal gas phase and an ideal solution in the adsorbed phase, is used, leading to the expression

$$\bar{p}_i = y_i P = P_i(\phi,T)x_i \tag{64}$$

This together with the fact that the ideal solution assumption ($\gamma_{ai} = 1$) is thermodynamically consistent when the temperature, T, and surface potential of the mixture, ϕ, are both held constant gives

$$\sum_{i=1}^{\text{all } i} x_i \, d\ln\gamma_{ai} = 0 \qquad (T \text{ and } \phi = \text{constant}) \tag{65}$$

This is the Gibbs-Duhem equation applied to an adsorbed phase at constant T and ϕ.

The method, as applied to a binary adsorption mixture at fixed T, is summarized below:

Given the pure gas isotherms

$$n_{o1} = F(P) \tag{66}$$
$$n_{o2} = F(P)$$

Reproduced with permission of the copyright owner. Further reproduction prohibited without permission.

the total pressure, P, and y_1.

1) The surface potentials for the pure components are calculated from equation (63)

$$\phi_{o1} = RT \int_o^P n_{o1}\, d\ln P \tag{67}$$

$$\phi_{o2} = RT \int_o^P n_{o2}\, d\ln P$$

2) Since the mixing process indicated by equation (65) is carried out at constant T and ϕ of the mixture

$$\phi = \phi_{o1} = \phi_{o2} \tag{68}$$

For a set of fixed $\phi = \phi_{o1} = \phi_{o2}$:

3) $P_1(\phi,T)$ and $P_2(\phi,T)$ are determined from (67)

4) x_1 and x_2 are evaluated from equation (64) applied to both components

$$x_1 = Py_1/(P_1(\phi,T)) \tag{69}$$

$$x_2 = P(1-y_1)/(P_2(\phi,T))$$

5) The total amount adsorbed, n_T, is determined from

$$1/n_T = x_1/n_{o1} + x_2/n_{o2} \qquad (T,\phi = \text{constant}) \tag{70}$$

6) The individual amounts adsorbed are then given by

$$n_i = x_i n_T \tag{71}$$

Reproduced with permission of the copyright owner. Further reproduction prohibited without permission.

The most important limitation of this method lies in the evaluation of the Gibbs isotherm integrals given by equation (67), which are very sensitive in the low coverage region (low pressures) for microporous adsorbents. This implies the availability of very precise low pressure adsorption data.[9,36]

The semi-empirical method of Cook and Basmadjian[13] is based on an equation derived by Basmadjian[12] on the assumption of small and constant relative volatility. Like the Myers and Prausnitz method, it requires integration of adsorption pressures to zero coverage. Along with other difficulties this makes the method difficult to apply to multicomponent systems.[25]

A review on other methods applied with some success to the adsorption of gas mixtures can be found elsewhere.[9,13,48]

Reproduced with permission of the copyright owner. Further reproduction prohibited without permission.

CHAPTER V

CORRELATION RESULTS

Pure Gas Isotherms

Graphical Correlation

With respect to pure gas adsorption, the main goal of this work was to obtain a single correlation for all four gases (methane, ethane, ethylene, and carbon dioxide) under a wide range of temperature (212.7 K, 260.2 K, and 301.4 K) and pressure (0.1 - 550 psia/0.69 - 3792 kN/m^2) conditions, within the framework of the Potential Theory of adsorption discussed in Chapter IV. This theory is represented by relations (13), (14), and (15) in the chapter describing the characteristic curve for the adsorbent-adsorbates system. Repeated here they are

$$(\epsilon/\beta)_{\text{all } i} = \text{constant} \tag{14}$$

$$\epsilon_i = RT \ln \left[f_s(p_s,T)/f(P,T) \right]_i \tag{15}$$

$$\hat{V}_a = n_o \tilde{V}_a \Big|_{\text{all } i} \tag{13}$$

When data are plotted, the ordinate is the adsorbate volume per gram of adsorbent, $\hat{V}_a$, and the abscissa is the ratio of the adsorption potential to the affinity coefficient, ϵ/β. As discussed before, the affinity coefficient may be represented as proportional to a molar volume of the sub-

Reproduced with permission of the copyright owner. Further reproduction prohibited without permission.

stance and therefore

$$\left(\frac{\varepsilon}{\tilde{V}_a}\right)_{\text{all i}} = \text{constant} \qquad (20)$$

The adsorbate molar volume, $\tilde{V}_a$, in equations (13) and (20) is normally not known and a value has to be assigned to it, generally the saturated liquid molar volume for the substance. The fugacity at the saturation pressure and T imply a system temperature below the critical temperature of the substances. Since the working temperatures in this work are higher than the critical for methane at all T and for ethylene at 301.4 K, f_s becomes a fictitious number under those conditions and an arbitrary number has to be assigned to it, in this case an extrapolation of a ln p_s versus 1/T correlation of experimental data at $T \leq T_c$ (see Appendix F). A summary of different modifications to the theory found in the literature, arising from assigning different values to $\tilde{V}_a$ and β, is given in Appendix I.

Different schemes were tried for the adsorbate volume, $\hat{V}_a$, in order to determine whether or not a single characteristic curve could be obtained for the present adsorbent-adsorbates system. Among these was included the one proposed by Rogers[47] in which $\tilde{V}_a$ is assumed to be constant and equal to the molar volume of the saturated liquid at its normal boiling point. None of these schemes gave as satisfactory a correlation as the one to be described next.

In this work, a modification of the original Dubinin et al.[20] method (see Chapter IV and Appendix I) was used to test the experimental data. Absolute, instead of Gibbs adsorption capacities (see discussion later in

Reproduced with permission of the copyright owner. Further reproduction prohibited without permission.

this chapter) were used in the ordinate together with the same scheme for the adsorbate molar volume. Pressures were substituted for fugacities in equation (15) in the abscissa and the Kirchhoff equation (see Appendix F) was used to represent vapor pressures for the substances at all temperatures. The characteristic curve was described by the following relations:

$$\epsilon/\tilde{V}_s(T_{nbp})\Big|_{\text{all } i} = \text{constant} \tag{21}$$

$$\epsilon_i = RT \ln[f_s(p_s,T)/f(P,T)] \tag{15}$$

$$\hat{V}_a = n_o^a \tilde{V}_s(T) \tag{72}$$

where $\tilde{V}_s(T_{nbp})$ is the saturated molar volume of the liquid substance at its normal boiling point, $f_s(p_s,T)$ the fugacity of the gas at the saturation pressure and T, $f(P,T)$ the fugacity of the gas at the equilibrium pressure and temperature, R the gas constant, $\tilde{V}_s(T)$ the saturated molar volume of the liquid at T, $\hat{V}_a$ the adsorbate volume per gram of adsorbent at P and T, and n_o^a the absolute adsorption capacity at P and T, as defined later in this chapter by equation (76). The correlation obtained for all the experimental data of this work is presented in Table 20 in Appendix K, the different variables being defined below:

1) Basically, the Nikolaev and Dubinin[37] scheme for the temperature dependence of the liquid saturated volume, $\tilde{V}_s(T)$, was followed (see equations (26) to (30) in Chapter IV), i.e.

$$\tilde{V}_s(T) = b - [b-\tilde{V}_s(T_{nbp})] \left\{\frac{T_c - T}{T_c - T_{nbp}}\right\} \qquad T_{nbp} \le T \le T_c \tag{29}$$

Reproduced with permission of the copyright owner. Further reproduction prohibited without permission.

$$\tilde{V}_s(T) = b = RT_c/(8P_c) \qquad T > T_c \tag{30}$$

where b is a constant in the van der Waals equation of state.

2) The absolute amount adsorbed, n_o^a, as defined by Young and Crowell[53] and discussed next, was used to calculate the adsorbate volume from relation (72).

The Gibbs amount adsorbed,[53] n_o, as used in representing the experimental adsorption capacities in this work (see Chapter III and Appendix G), is derived by subtracting the moles of non-adsorbed gas taken up by the so-called dead space from the moles of gas admitted during the adsorption measurements at the same temperature and pressure. This method of computing the amount adsorbed assumes constant dead spaces, i.e. it neglects the volume of the adsorbate, V_a. The dead space is defined here as

$$\sum_{i=1}^{r} V_i^o = V_{system} - V_{solid} \tag{73}$$

where r is the number of void spaces in the adsorption system.
It is a constant; it yields the amount adsorbed in excess of the non-adsorbed gas occupying the same volume; and it is used commonly in the course of the usual helium dead space determination. It is well known that this definition yields isotherms which go through a maximum at sufficiently high equilibrium pressures.[34]

In the absolute adsorption definition[53] all of the gas molecules in the range of the interaction forces are included, i.e., the adsorbate volume is considered in the analysis. This is the proper expression to

Reproduced with permission of the copyright owner. Further reproduction prohibited without permission.

use in any application of the Polanyi theory, since the potential forces are visualized as acting on the total amount of gas present within the effective adsorption space. The dead space is then defined as

$$\sum_{i=1}^{r} V_i^{oa} = V_{system} - V_{solid} - V_{adsorbate} \tag{74}$$

or

$$\sum_{i=1}^{r} V_i^{oa} = \sum_{i=1}^{r} V_i^{o} - mn_o^a \tilde{V}_a \tag{75}$$

If equation (75) is used in relation (1), representing the amount adsorbed of a pure gas, and solved for n_o^a, the following relation between the Gibbs and the absolute adsorption capacities is obtained:

$$n_o^a = \frac{n_o}{1 - \tilde{V}_a P/(ZRT)} \tag{76}$$

In the low pressure region the two definitions lead to almost identical isotherms. (See Table 20 in Appendix K. $\tilde{V}_a$ was determined by equations (29) and (30).)

3) The saturated liquid molar volume at the normal boiling point, as proposed by Grant and Manes,[25] $\tilde{V}_s(T_{nbp})$, was used as the correlating parameter in the abscissa.

4) The fugacities in the abscissa, f_s and f, were evaluated at the corresponding temperature and pressure with a BWR equation of state for the substances. The vapor pressure, p_s, was determined at T using the reduced Kirchhoff equation[46] (see Appendix F), which is basically an approximated integration of the Clausius-Clapeyron equation and which

Reproduced with permission of the copyright owner. Further reproduction prohibited without permission.

requires only a knowledge of the critical properties and the normal boiling point temperature for the gases.

A graphical representation of the characteristic curve data, reported in Table 20 of Appendix K, is given in Figure 13. Some points have been omitted for the sake of clarity. The data of Table 20 were produced with program DUBIN1 described briefly in Appendix L.

From this figure it is seen that the adsorption capacities of methane, ethane, ethylene, and carbon dioxide on activated carbon, type BPL, in the range of temperatures between 212.7 K and 301.4 K and of pressures between 1 psia and 550 psia essentially correlate in one single characteristic curve defined by equations (15), (21), (29), (30), (72), and (76).

It is important to emphasize that the scheme selected for the saturated liquid molar volumes, $\tilde{V}_s(T)$, (equations (29) and (30)) is arbitrary and that some other reasonable procedure might have been used instead. However, the major advantage of this scheme, besides giving a reasonable correlation for the data in this work, is that it provides a consistent procedure for the evaluation of the ordinates of the characteristic curve based on well known physical properties of the substances which can be found easily in the literature, i.e., the critical temperature and pressure, the normal boiling point temperature, and the saturated liquid molar volume at the normal boiling point. The other thermodynamic variables, $f_i(P,T)$ and $Z(P,T)$, were determined from the BWR equation of state for the substances. The use of the saturated liquid molar volume of the substances at their normal boiling point temperatures as the correlating parameter in the abscissa is justified on the grounds of the

Reproduced with permission of the copyright owner. Further reproduction prohibited without permission.

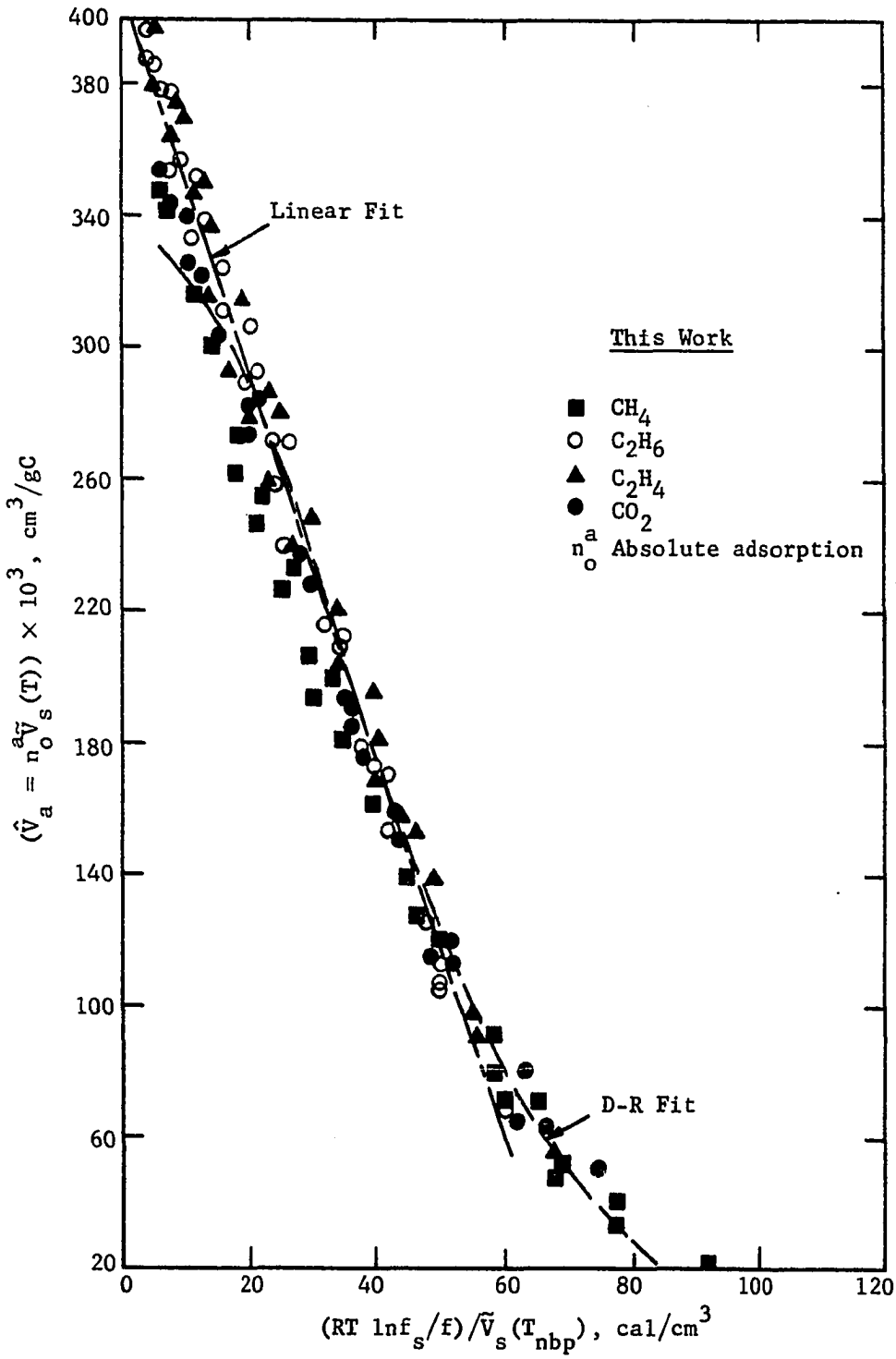

Figure 13. Characteristic Curve for Pure Gases, 212.7 - 301.4 K

Reproduced with permission of the copyright owner. Further reproduction prohibited without permission.

basic origin of the affinity coefficient, β, in the Polanyi-Dubinin theory (see equations (16) to (21) in Chapter IV) which considers it to be a temperature independent physical property of the substances.

This same characteristic curve method was used to analyze the adsorption data of Szepesy and Illes[50,51] for methane, ethane, ethylene, carbon dioxide, propane, propene, and butane on a similar adsorbent at 293.2 K and 363.2 K and for pressures between 0.001 and 7 atmospheres (101.3 - 709.3 kN/m^2). The correlation obtained is given in Figure 14. It is essentially similar to the one in this work, with the exception of the low pressure region of the characteristic curve (abscissas greater than 60 cal/cm^3) which shows branching for the different gases according to their saturated liquid molar volumes at the normal boiling point (or to their critical temperatures if carbon dioxide is not considered) and of the carbon dioxide data which are larger in adsorption capacity.

This suggests that the characteristic curve, represented by Figure 13, could be used in the prediction of adsorption capacities for gases other than the ones used in constructing it, like propane, propene, butane, and possibly others, if caution is observed at pressures below approximately one atmosphere.

Analytical Correlation

Dubinin-Radushkevich Equation. All the experimental adsorption data of this study were least square fitted by the linear form of the D-R equation, given by equation (24) in Chapter IV, i.e., by

$$Y = \ln \hat{V}_a^o - k X \qquad (77)$$

where

Reproduced with permission of the copyright owner. Further reproduction prohibited without permission.

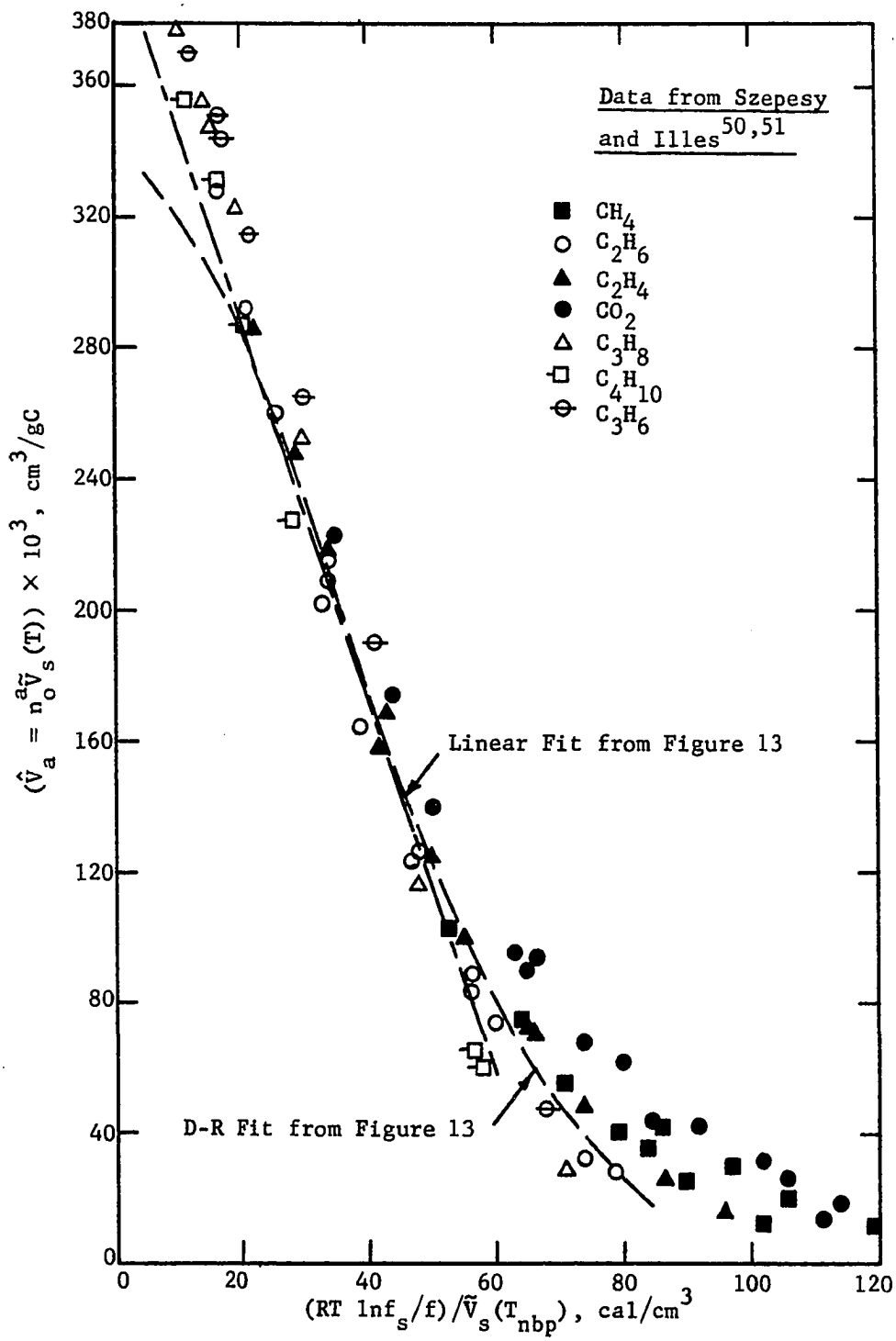

Figure 14. Characteristic Curve for Pure Gases at 293 K and 363 K

Reproduced with permission of the copyright owner. Further reproduction prohibited without permission.

$$Y = \ln \hat{V}_a \tag{78}$$

$$X = \left\{\frac{RT}{\beta} \ln[f_s(p_s,T)/f(P,T)]\right\}^2$$

and $\hat{V}_a$ and β were determined by equations (21), (72), (29), and (30). The least squares fit of Y versus X, according to relation (77), gave the following constants:

$$\hat{V}_a^o = 0.3341 \text{ cm}^3/\text{gC} \tag{79}$$

$$k = 0.3898 \times 10^{-3} \text{ [cm}^3/\text{cal]}^2$$

The calculation of the adsorption capacities of the gases with this equation, at the same conditions of pressure and temperature of the present experimental program, gave a maximum deviation of 40% and an average deviation of ± 8% with respect to the experimental values.

This empirical equation is plotted in Figure 13 for comparison with the characteristic curve that represents the experimental adsorption data of this work. This graph shows that the D-R equation, with the constants given by relation (79), represents the experimental data well in the region of abscissas of the correlation between 20 and 80 cal/cm^3. However, it does not represent the data at abscissas less than 20 cal/cm^3.

The Dubinin-Radushkevich method (see Chapter IV) postulated that $\hat{V}_a^o$, the volume of micropores of the activated carbon, and k, a constant which is thought to represent the distribution function of pore volumes with respect to their size, are constants that are temperature independent.

Reproduced with permission of the copyright owner. Further reproduction prohibited without permission.

To test this assertion, the experimental adsorption data for the individual gases at the three different temperature levels were least square fitted, according to equation (77), yielding $\hat{V}_a^o$ and k at different temperatures. These constants, given in Table 1, show that $\hat{V}_a^o$ and k are not temperature independent for the set of adsorption data of this study. The same effect has been reported by Rogers.[47] The computations were handled with program DUBIN3, discussed briefly in Appendix L. This suggests that the D-R equation does not represent well the data of this work over the whole range of temperature and pressure conditions and that it contains temperature dependent parameters which make its use impractical.

Linear Fit. As the characteristic curve data in Figure 13 suggested a linear relation between the adsorbate volume, V_a, and the abscissa, $\epsilon/\tilde{V}_s(T_{nbp})$, between abscissas of 5 and 60 cal/cm^3, a least squares fit of all the adsorption data having abscissas between these values was done using a linear relation given as

$$Y' = A + B\,X' \tag{80}$$

where

$$Y' = \hat{V}_a \tag{81}$$

$$X' = \frac{RT}{\beta} \ln[f_s(p_s,T)/f(P,T)]$$

$\hat{V}_a$ and β being determined by equations (21), (72), (29), and (30).

The least squares fit of Y' versus X', according to relation (80), gave the following constants:

$$A = 0.398855 \text{ cm}^3/\text{gC} \tag{82}$$
$$B = -0.57061 \times 10^{-2} \text{ cm}^3/\text{cal}$$

Reproduced with permission of the copyright owner. Further reproduction prohibited without permission.

Table 1. Dubinin-Radushkevich Parameters for Pure Gas Adsorption Data

Gas	Temperature, K	$\hat{V}_a^o$, cm^3/gC	$k \times 10^3$, cm^3/cal
Methane	212.7	0.3134	0.4093
	260.2	0.2758	0.3566
	301.4	0.2547	0.2998
Ethane	212.7	0.3947	0.5065
	260.2	0.3771	0.4896
	301.4	0.3508	0.4780
Ethylene	212.7	0.3870	0.4527
	260.2	0.3606	0.4131
	301.4	0.3260	0.3959
Carbon Dioxide	212.7	0.3412	0.4409
	260.2	0.3379	0.4181
	301.4	0.3081	0.3682

NOTE: To convert from cal to J, multiply by 4.148.

Reproduced with permission of the copyright owner. Further reproduction prohibited without permission.

This correlation is plotted in Figure 13 for comparison with the characteristic curve representing the experimental data of this work, and the D-R equation. The equation seems to fit weel the data within the range of abscissas selected (5 to 60 cal/cm^3). The adsorption capacities of the four gases were then calculated with this correlation, at the same conditions of pressure and temperature of this experimental program and within abscissas of the characteristic curve between 5 and 60 cal/cm^3, giving a maximum deviation of 42% (the second highest being 29%) and an average of ± 6.1% with respect to the experimental values.

Tabular values of the adsorption capacities calculated using the linear correlations (80) and (82) are presented in Table 20 in Appendix K. The computations were carried out with program LINFIT, described briefly in Appendix L.

A graphical comparison of these calculated adsorption values with the experimental data of this study is given in Figures 15 to 17. It can be concluded from these figures and Table 20 in Appendix K that the linear fit correlation represents best the experimental data for ethane, ethylene, and carbon dioxide in the temperature range of 212.7 K to 301.4 K for all of which the temperature is approximately less than the critical, suggesting that the adsorbed phase is more liquid-like. This finding, together with the results of the correlation developed for other gases in Figure 14 for which $T < T_c$ (propane, butane, and propylene), suggests that the linear fit correlation be used for gases for which $T \leq T_c$ for best results. The correlation should not be used for any gas at pressures below one atmosphere.

Reproduced with permission of the copyright owner. Further reproduction prohibited without permission.

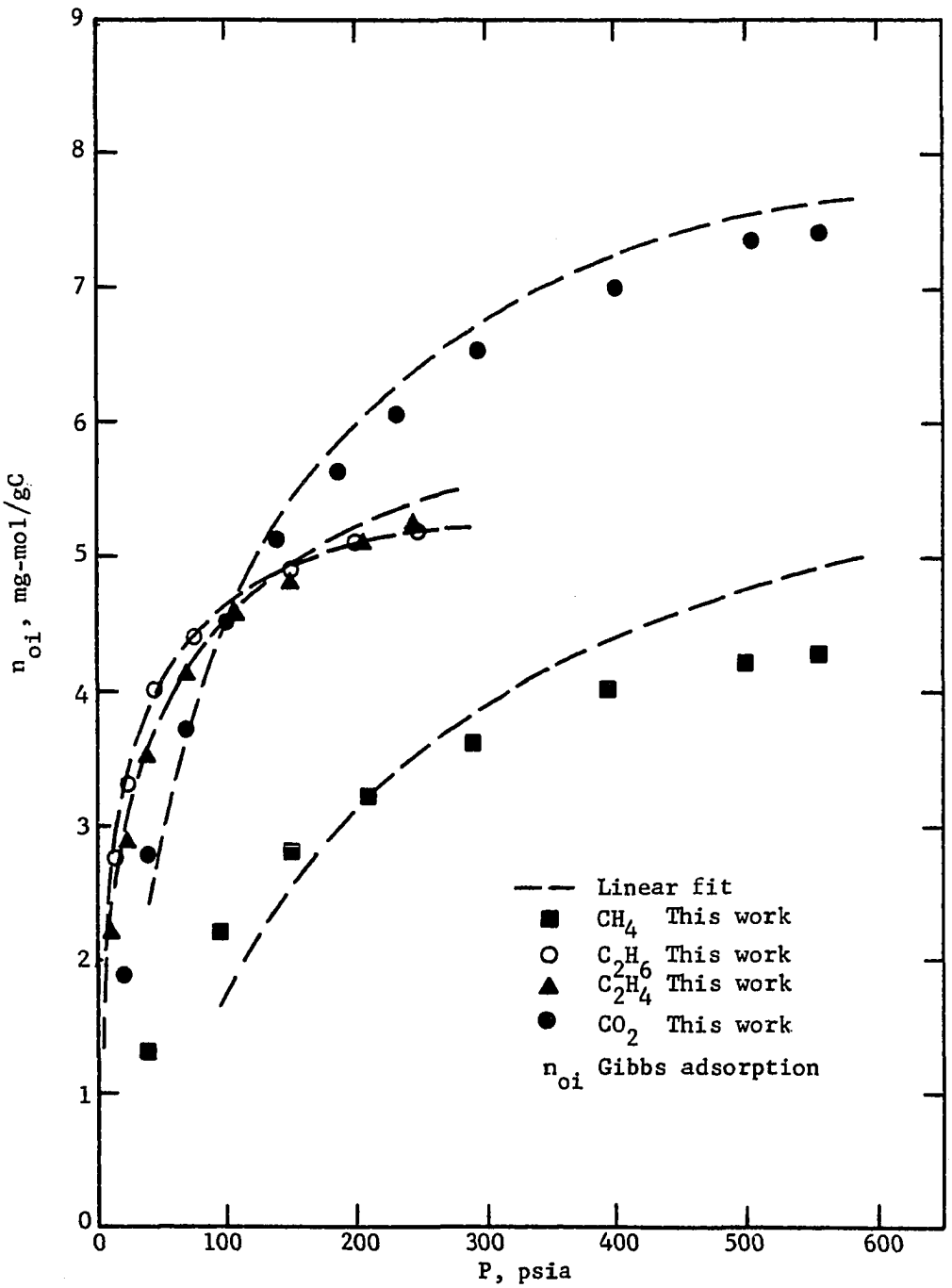

Figure 15. Prediction of Pure Gas Isotherms at 301.4 K Using a Linear Fit of the Characteristic Curve

Reproduced with permission of the copyright owner. Further reproduction prohibited without permission.

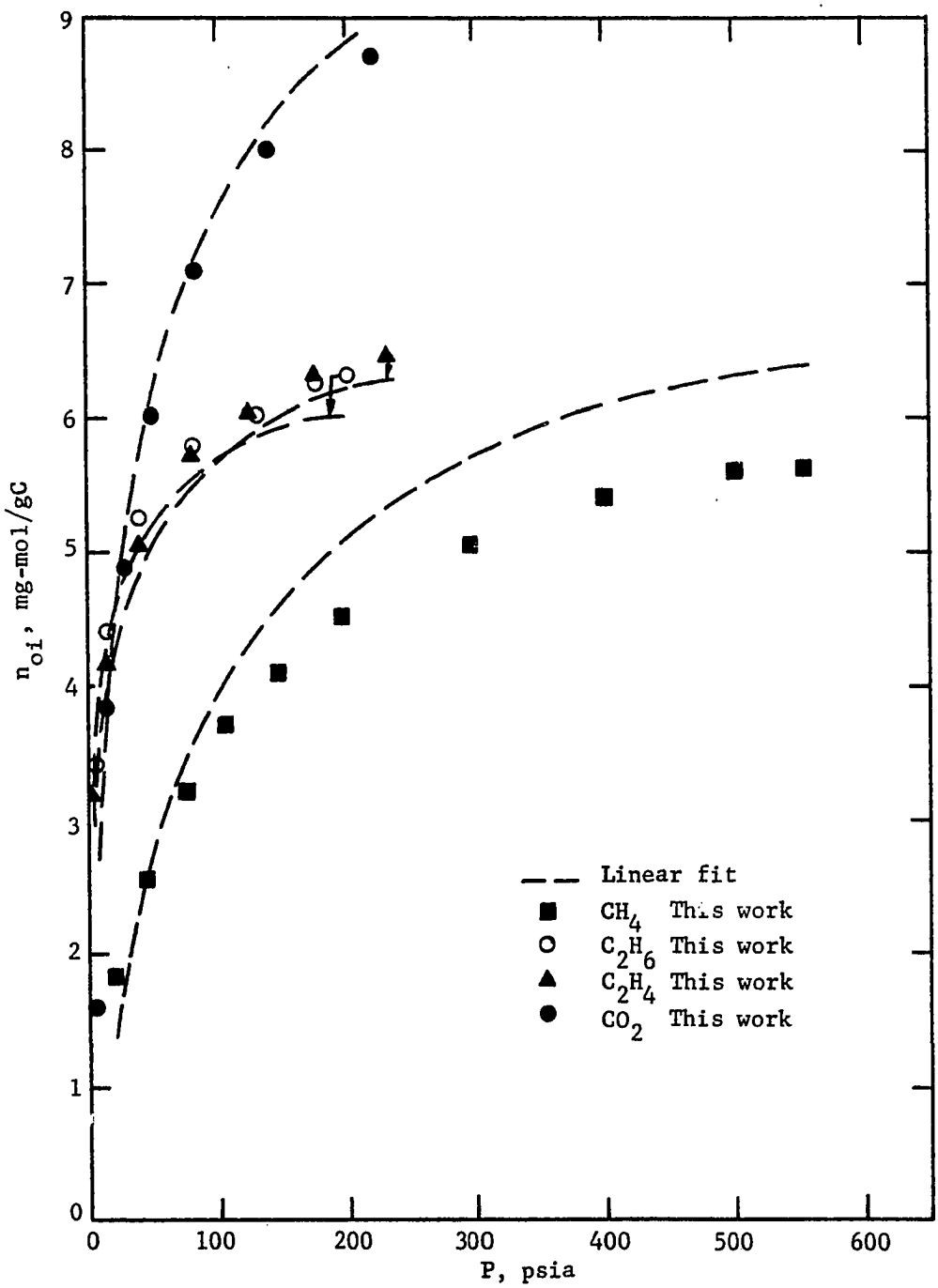

Figure 16. Prediction of Pure Gas Isotherms at 260.2 K Using a Linear Fit of the Characteristic Curve

Reproduced with permission of the copyright owner. Further reproduction prohibited without permission.

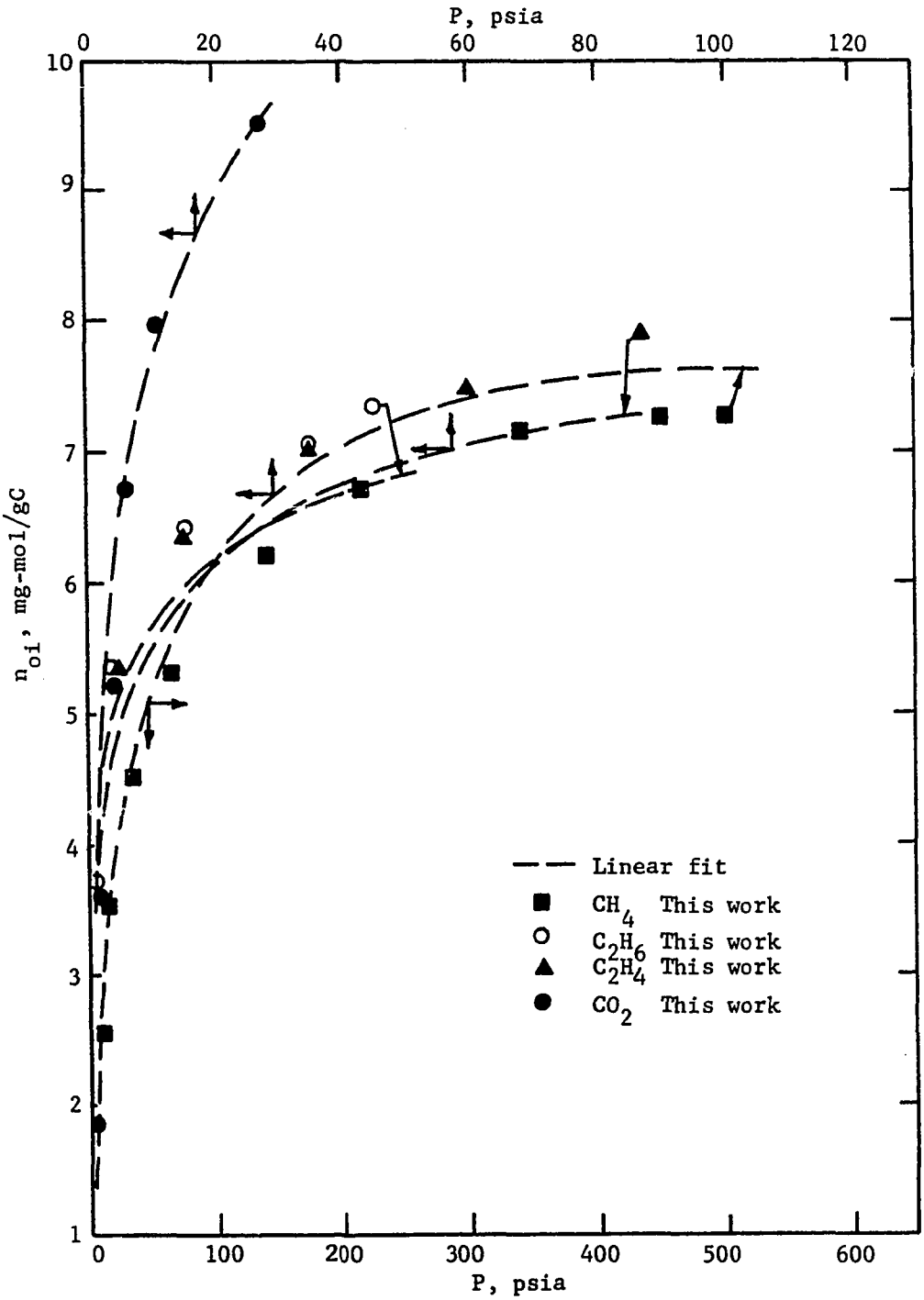

Figure 17. Prediction of Pure Gas Isotherms at 212.7 K Using a Linear Fit of the Characteristic Curve

Reproduced with permission of the copyright owner. Further reproduction prohibited without permission.

Prediction of Adsorption of Pure Gases from Characteristic Curve (Figure 13)

A method is presented next for the prediction of pure gas adsorption data on activated carbon, type BPL, for gases for which $T \leq T_c$, using the characteristic curve represented in Figure 13.

Data Required for the Substance.

1. Critical temperature and pressure, T_c and P_c
2. Normal boiling point temperature, T_{nbp}
3. Saturated liquid molar volume at the normal boiling point, $\tilde{V}_s(T_{nbp})$
4. BWR equation of state parameters

Given the equilibrium temperature and pressure, T and P, the adsorption capacity is predicted from Figure 13 as follows:

Abscissa (equations (15) and (21)).

5. The saturation pressure, p_s, at T is evaluated with the Kirchhoff equation (see equation (90) in Appendix F)
6. The fugacity at p_s and T, $f_s(p_s,T)$, is evaluated from the BWR equation of state for the substance
7. The fugacity at P and T, $f(P,T)$, is evaluated from the BWR equation of state for the substance
8. The abscissa of the characteristic curve is determined as

$$\frac{RT}{\tilde{V}_s(T_{nbp})} \ln[f_s(p_s,T)/f(P,T)] \qquad (83)$$

Ordinate (equation (72)).

9. The ordinate corresponding to P and T is determined graphically from Figure 13 or analytically from equations (77) to (79)

Reproduced with permission of the copyright owner. Further reproduction prohibited without permission.

(D-R equation least squares fit) or (80) to (82) (linear least squares fit). This value corresponds to

$$\hat{V}_a = n_o^a \tilde{V}_s(T) \tag{72}$$

Adsorption Capacity.

10. The saturated liquid volume of the substance at T, $\tilde{V}_s(T)$, is evaluated from equation (29) or (30)
11. The absolute adsorption capacity, n_o^a, is determined from relation (72)
12. The Gibbs adsorption capacity, n_o, is evaluated with equations (76), (29), and (30).

Mixture Gas Isotherms

Grant and Manes[25] proposed a correlation method, based on the Potential Theory of adsorption, in which gas mixture adsorption data were computed from a characteristic curve for pure components only (see Chapter IV). This method implies that a characteristic curve for the gas mixtures can be constructed and that it is essentially identical to the one constructed for the pure gases. A superimposable correlation of this kind was developed with success for the first time on the system methane-carbon dioxide-activated carbon by Rogers.[47]

The main purpose in this dissertation regarding mixture gas adsorption was to obtain a single characteristic curve for all the binary and ternary mixture combinations studied (methane, ethane, and ethylene), under a wide range of temperature (212.7 K to 301.4 K) and pressure (20 to 450 psia/138 to 3100 kN/m^2) conditions that was superimposable on the pure

Reproduced with permission of the copyright owner. Further reproduction prohibited without permission.

gas adsorption correlation, so that adsorption capacities for mixtures could be predicted from pure gas adsorption data only. The correlation was to follow the Grant and Manes[25] method represented by equation (41),

$$\frac{RT}{\tilde{V}_s(T_{nbp})} \ln\left[\frac{x f_s(p_s,T)}{\bar{f}(P,T,\{y_i\})}\right] = F(n_T\tilde{V}_{am})\Big|_{\text{all } i} \tag{41}$$

its ordinate being the mixture adsorbate volume per gram of adsorbent, $\hat{V}_{am}$, and the abscissa the ratio of the adsorption potential to the affinity coefficient (evaluated as $\tilde{V}_s(T_{nbp})$), assuming an ideal adsorbed solution.

The mixture adsorbate molar volume, $\tilde{V}_{am}$, was estimated by Grant and Manes[25] by additivity of pure liquid component saturated molar volumes at an arbitrary pseudo-pressure defined by equation (45). The total amount adsorbed, n_T, corresponds to the summation of the individual component adsorbed, the mole fraction of a component in the adsorbed phase, x_i, being the ratio of n_i to n_T. The fugacity of the pure components at the saturation pressure and T, $f_s(p_s,T)$, and the fugacity of the components at P, T, and $\{y_i\}$ are determined from an appropriate equation of state.

In this work, a modification of the Grant and Manes[25] method was used to test the experimental data. The characteristic curve was described by equation (41) where

$$\hat{V}_{am} = n_T \tilde{V}_{am} \tag{84}$$

$$\tilde{V}_{am} = \sum_{i=1}^{\text{all } i} x_i \tilde{V}_s(T) \tag{85}$$

and $\tilde{V}_s(T)$ follows the same scheme given for pure gas adsorption data by

Reproduced with permission of the copyright owner. Further reproduction prohibited without permission.

equations (29) and (30). Gibbs adsorption capacities were used instead of absolute values to simplify the use of the correlation; the use of either of these definitions did not affect the correlation substantially. The correlation obtained for all mixture adsorption data in this work is given in Table 21 in Appendix K; it was produced with program GRANTB, described briefly in Appendix L. A graphical representation of these data is given in Figure 18. Some data points have been omitted for the sake of clarity. From this figure it is concluded that the adsorption capacities of the components (methane, ethane, or ethylene) in binary and ternary mixtures on activated carbon, type BPL, at temperatures between 212.7 K and 301.4 K, pressures between 20 and 450 psia, and gas phase compositions defined in Tables 12-15, Appendix G, do not correlate well in one single characteristic curve defined by equations (41), (29), (30), and (85). From Table 21 in Appendix K it can be shown that it is methane at 301.4 K, both in binary and ternary gas mixtures, that does not satisfy the equi-potential concept at constant $\hat{V}_{am}$ in equation (41). That is, for a fixed ordinate, $\hat{V}_{am}$, more than one abscissa is obtained for a certain adsorption mixture. A similar effect for hydrogen, in hydrogen-methane-carbon dioxide binary and ternary systems, has been reported by Rogers.[47] This effect can be seen in Figure 18 where the methane data points at 301.4 K are scattered to the extreme right (see continuous line labeled R) of the linear fit of the pure gas correlation (in segmented line) which has been included in the figure for comparison. If these methane points are not considered in the correlation, a characteristic curve for the mixtures that is essentially superimposable on the characteristic curve of the pure gases given in Figure 13 is obtained. This conclusion is the

Reproduced with permission of the copyright owner. Further reproduction prohibited without permission.

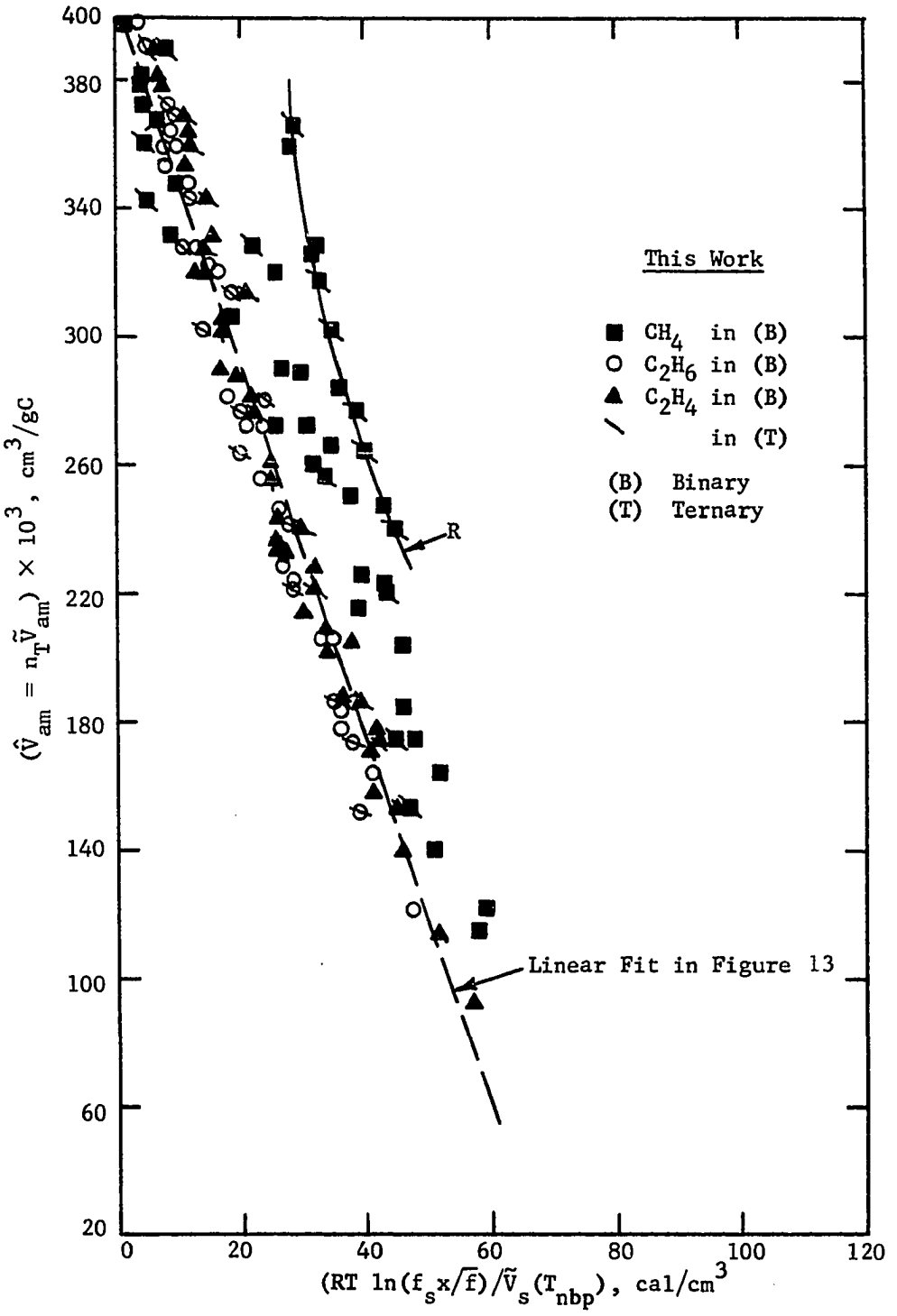

Figure 18. Characteristic Curve for Gas Mixtures 212.7 to 301.4 K

Reproduced with permission of the copyright owner. Further reproduction prohibited without permission.

basic requirement of the Grant and Manes's[25] method that permits the prediction of mixture adsorption capacities from pure gas adsorption data.

It is necessary to emphasize at this point that the selection of the saturated liquid molar volumes scheme for the pure components in this correlation (see equations (29) and (30)) is arbitrary and that some other reasonable procedure, like equation (45), could have been used instead. However, the major advantage of this scheme is that it is consistent with the pure gas characteristic curve developed in Figure 13; it is simple to use; and it requires information that is readily available in the literature. Equation (45), on the other hand, is arbitrary too, cannot be used normally for methane ($P_g > P_c$ under some conditions), and requires density data for the pure liquid components as functions of the temperature.

Having basically met the Grant and Manes[25] requirement of superimposability of the mixture and pure gas characteristic curves, the calculation of adsorption capacities for gas mixtures from pure gas adsorption data, at the same experimental conditions of this study, was attempted. The calculation procedure followed equations (43) to (47) in Chapter IV, equation (45) being replaced by (85), and equations (80) to (82) in this chapter being used as pure gas adsorption correlations. The calculations were performed with program GRANTF described briefly in Appendix L. A representative sample of calculation results is given graphically in Figures 19 to 24. In Figures 19 to 21 predicted adsorption capacities for methane-ethylene gas mixtures (the methane content increasing from 26% to 76.5 mol %, respectively) at 212.7 K and 301.4 K, and pressures from about 20 to 300 psia, are presented. Predictions for ethylene were reasonably good and improved with increasing ethylene content in the gas phase and

Reproduced with permission of the copyright owner. Further reproduction prohibited without permission.

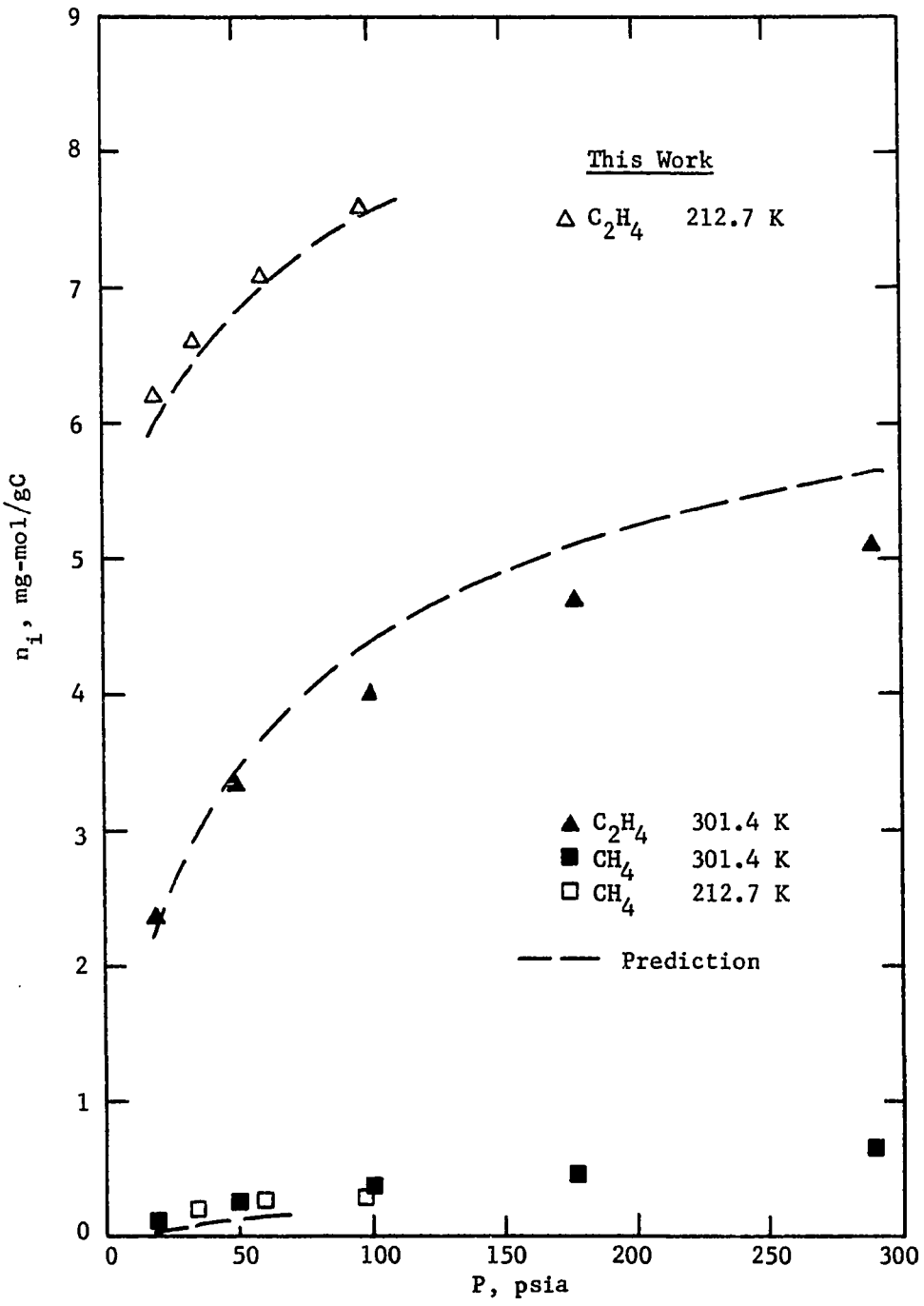

Figure 19. Methane-Ethylene (26.0-74.0 mol %) Isotherm Prediction

Reproduced with permission of the copyright owner. Further reproduction prohibited without permission.

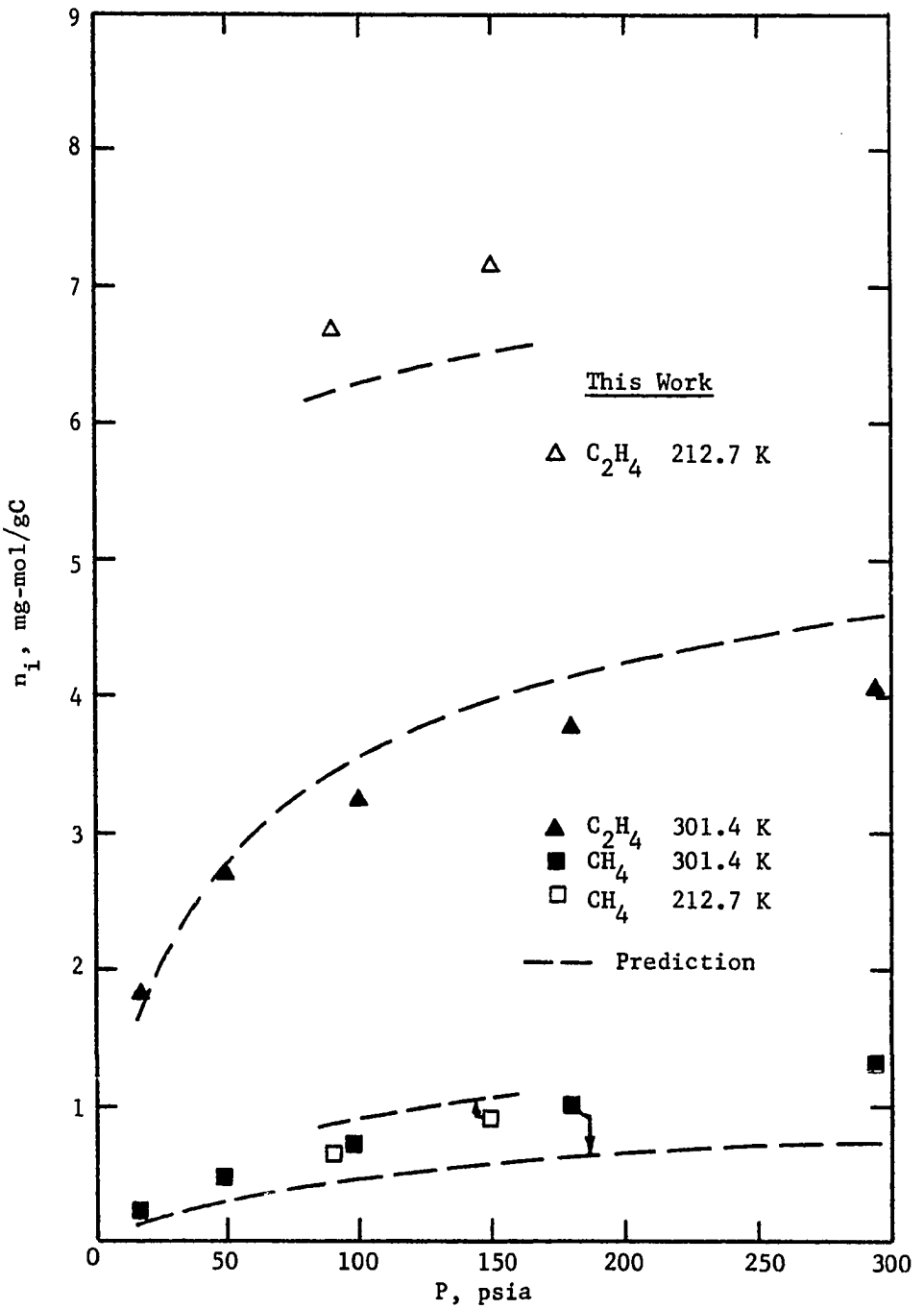

Figure 20. Methane-Ethylene (53.6-46.4 mol %) Isotherm Prediction

Reproduced with permission of the copyright owner. Further reproduction prohibited without permission.

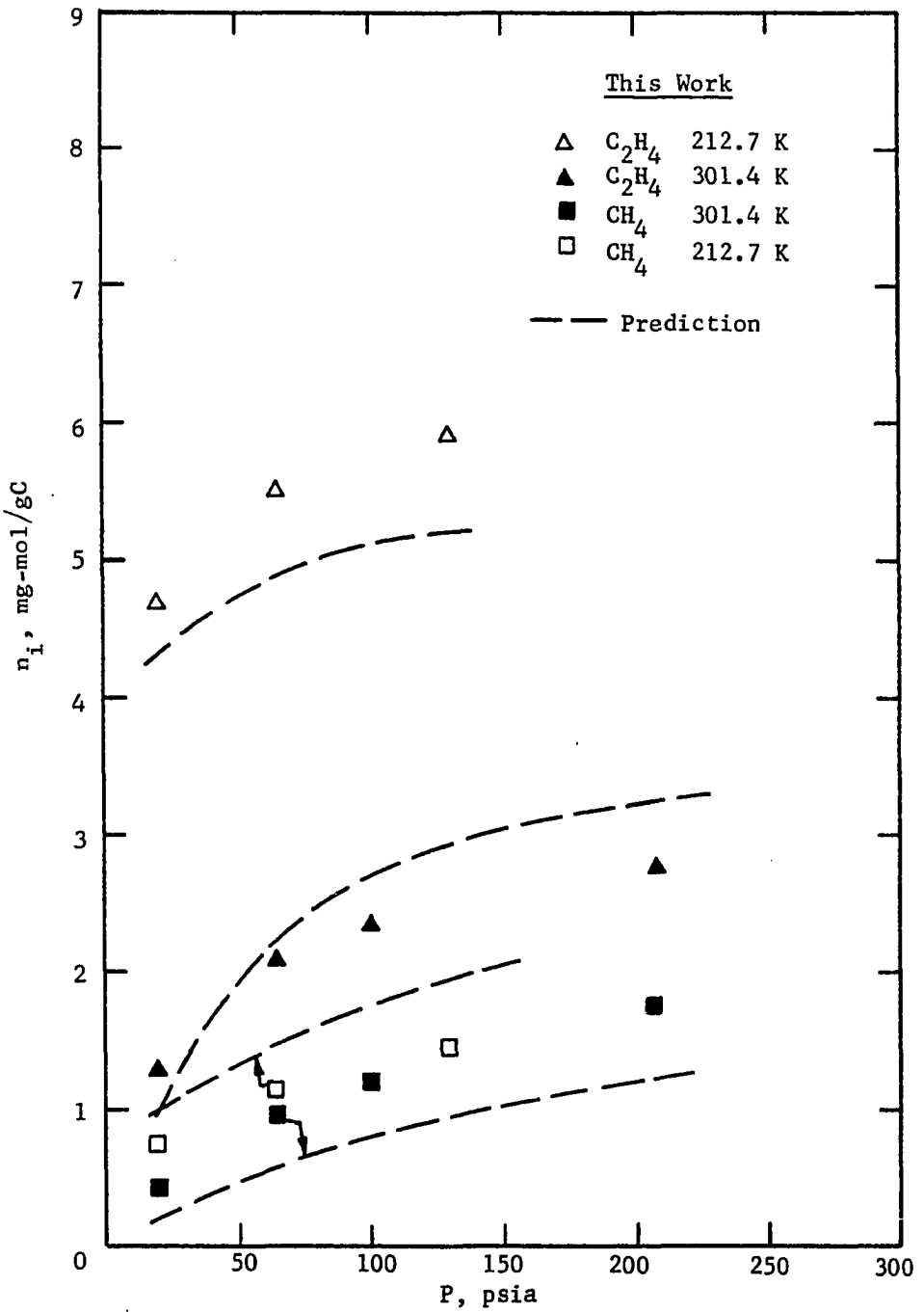

Figure 21. Methane-Ethylene (76.5-23.5 mol %) Isotherm Prediction

Reproduced with permission of the copyright owner. Further reproduction prohibited without permission.

decreasing equilibrium pressure. The maximum deviation for ethylene, with respect to the experimental adsorption data of this study, was 24%, the average deviation being ± 7.7%.

The methane capacity predictions instead were poor, showing deviations as large as 54.4% with respect to experimental data. The average deviation for methane in methane-ethylene mixtures was ± 28.8%. In addition, in some instances it was not possible to obtain predictions at low methane compositions (see Figure 19) as the iteration procedure involved in solving equations (41) and (43) in Chapter IV did not converge.

Similar results were obtained with methane-ethane gas mixtures. The maximum deviation in the prediction for ethane was 12.3% and the average ± 5.6%. For methane, the maximum deviation was 71% and the average ± 38.5%.

In Figures 22 to 24, predicted adsorption capacities for ethane-ethylene gas mixtures (the ethane-ethylene mole ratio increasing from 0.32 to 2.14, respectively) under similar conditions of temperature, pressure and gas phase compositions are presented. Again, the prediction of adsorption capacities for ethane and ethylene was reasonably good considering the overall scatter in Figures 13 and 18. Maximum deviations with respect to the present experimental data for ethane and ethylene were 38.4% and 25.8%, respectively; average deviations being ± 11.2% and ± 17.8%.

In summary, it was possible to predict with reasonable success ethane and ethylene adsorption capacities in methane-ethane-ethylene binary mixtures, under the temperature, pressure, and gas phase composition conditions of this experimental study from a linear fit of the

Reproduced with permission of the copyright owner. Further reproduction prohibited without permission.

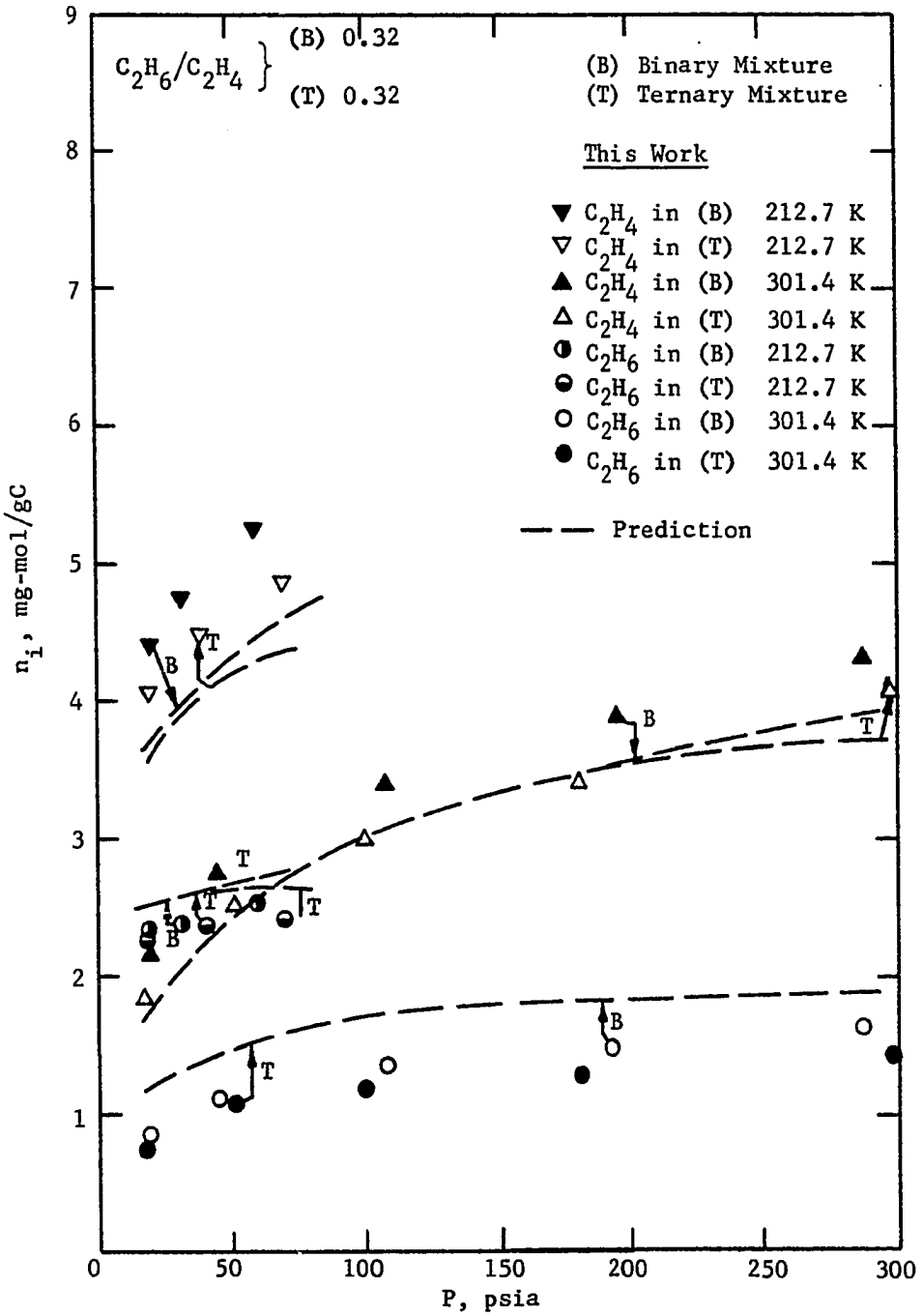

Figure 22. Ethane-Ethylene (24.0-76.0 mol %) and Methane-Ethane-Ethylene (20.0-19.2-60.8 mol %) Isotherm Prediction

Reproduced with permission of the copyright owner. Further reproduction prohibited without permission.

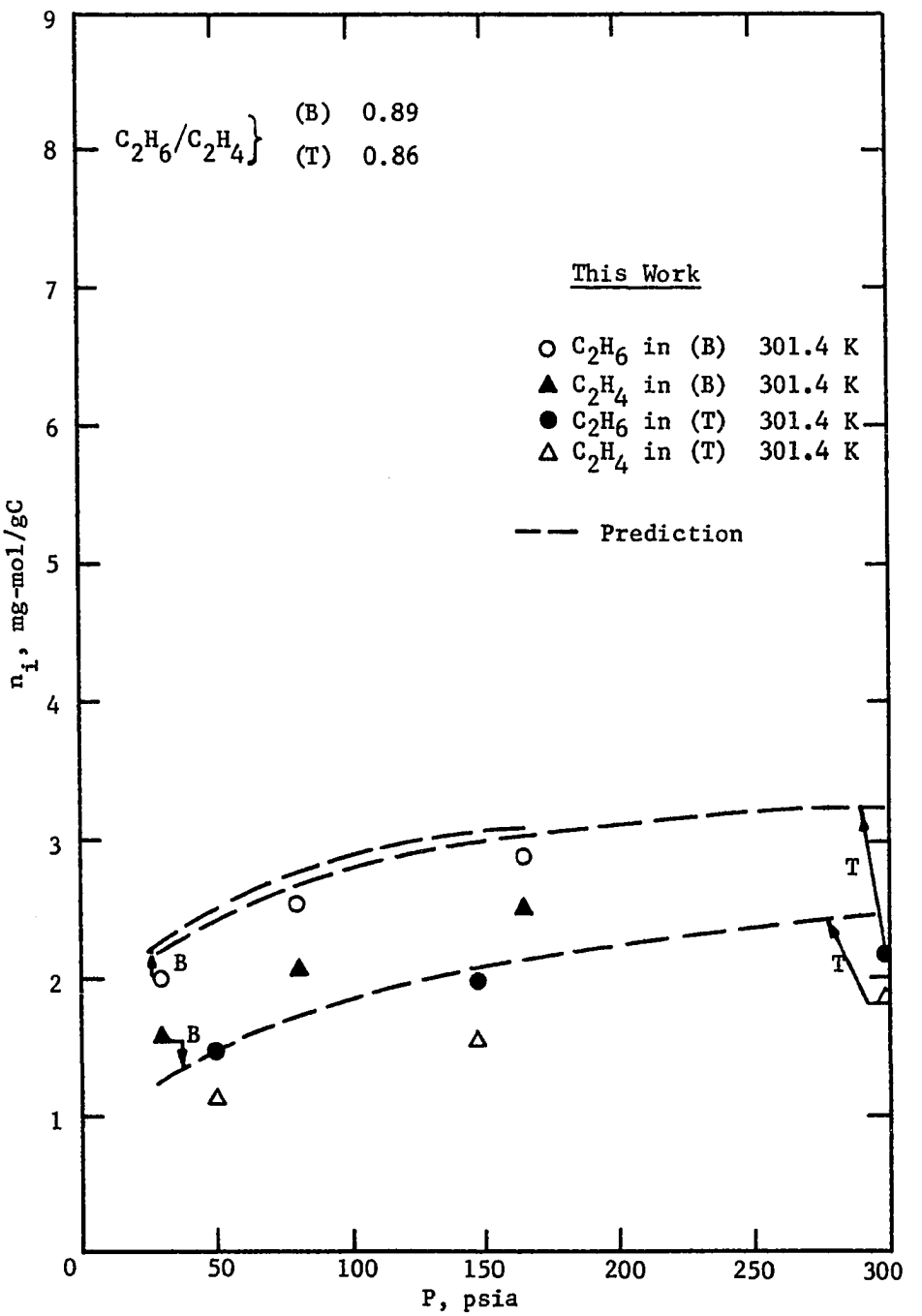

Figure 23. Ethane-Ethylene (47.2-52.8 mol %) and Methane-Ethane-Ethylene (62.4-17.4-20.2 mol %) Isotherm Prediction

Reproduced with permission of the copyright owner. Further reproduction prohibited without permission.

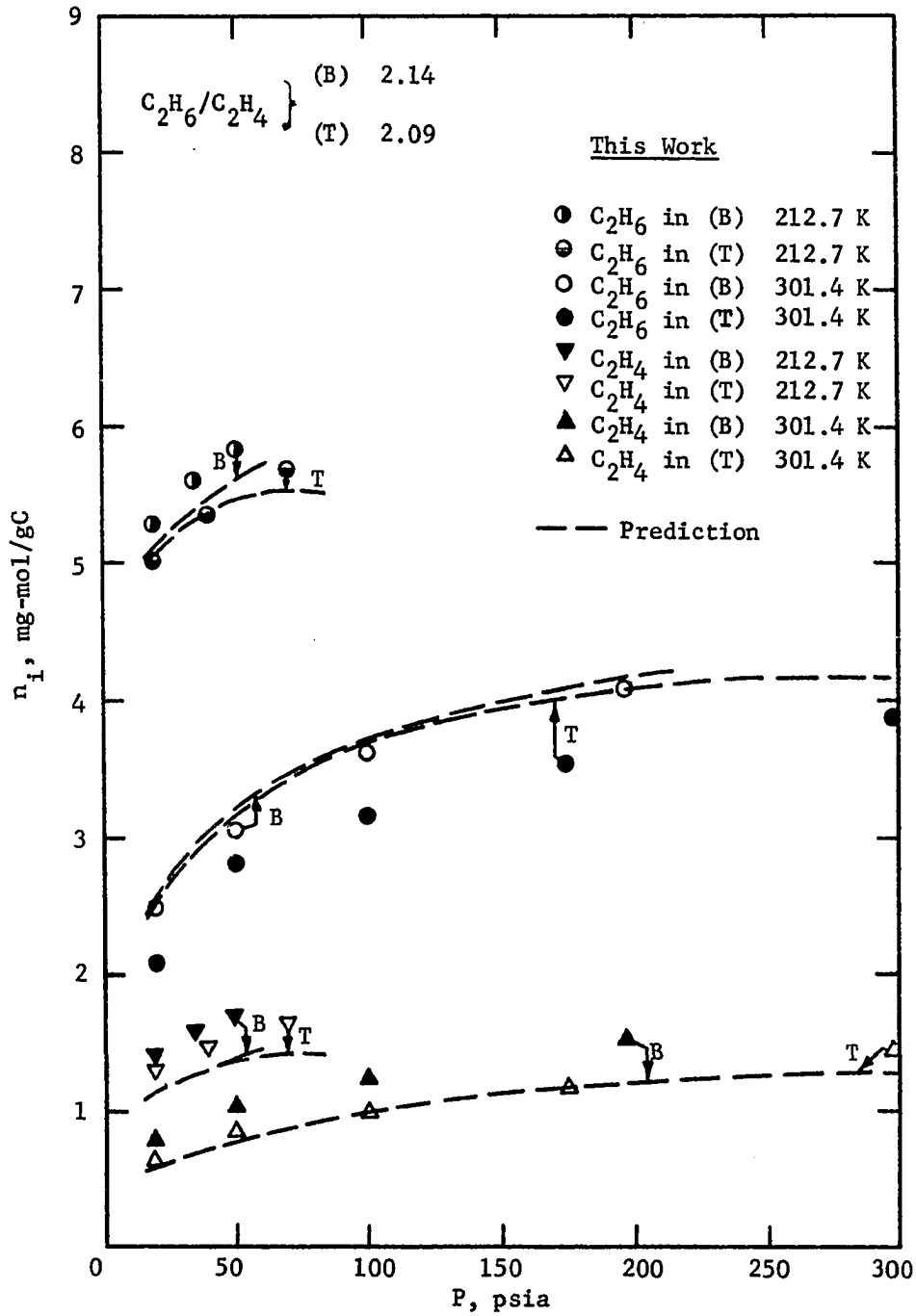

Figure 24. Ethane-Ethylene (68.2-31.8 mol %) and Methane-Ethane-Ethylene (23.0-52.0-25.0 mol %) Isotherm Prediction

Reproduced with permission of the copyright owner. Further reproduction prohibited without permission.

characteristic curve for pure gas adsorption with average deviations better than ± 15%. Methane adsorption capacity predictions with this method were poor; however, values could be estimated with average deviations better than ± 40%.

In principle, the same correlation procedure could have been used to calculate the ternary adsorption capacities, the only variation being an iterative solution of equations (41) and (43) in two variables, i.e., two mole fractions in the adsorbate phase. As the methane content in the ternary adsorbate mixtures was generally small, difficulties were expected to occur in this calculation scheme. An alternative approach was used in which the adsorption capacities for ethane and ethylene in the adsorbate were estimated by considering the ternary mixture as a pseudo-binary mixture of a composition calculated on a methane-free basis and equilibrium pressures equal to the sum of the ethane and ethylene partial pressures in the ternary mixture. The results of this method are shown together with the binary mixtures, of approximately the same ethane-ethylene mole ratio, in Figures 22 to 24. These results are similar to the respective binary adsorption mixtures discussed before in this chapter. Estimation of the methane content in the ternary adsorbates may be obtained by considering a binary mixture of methane-ethane or methane-ethylene with a methane content equal to that of the ternary. It is concluded that a fair estimation of ternary adsorption capacities can be made for methane-ethane-ethylene gas mixtures from a linear correlation of the pure gas adsorption data, treating the ternary mixture as a pseudo-binary.

From the over analysis of the binary and ternary gas adsorption

Reproduced with permission of the copyright owner. Further reproduction prohibited without permission.

data of this study it is reasonable to conclude that a fair estimation of methane-ethane-ethylene binary and ternary gas capacities from a pure gas characteristic curve, like Figure 13, is possible. Furthermore, it is believed that the estimation of other binary and ternary systems can be attempted under the same scheme of calculations even though the Grant and Manes[25] method appears to be thermodynamically inconsistent. Similar conclusions with the system methane-carbon dioxide-activated carbon under similar conditions of temperature, pressure, and composition were reached by Rogers.[47] The saturated volume at the normal boiling point for the pure substances was used in both coordinates of the characteristic curve developed by Rogers.

Prediction of Adsorption of Gas Mixtures from Characteristic Curve (Figure 13)

A method is presented next for the prediction of mixture gas adsorption data on activated carbon, type BPL, using the characteristic curve for pure gases represented in Figure 13.

Data Required for the Pure Substances.

1. Critical temperature and pressure, T_c and P_c
2. Normal boiling point temperature, T_{nbp}
3. Saturated liquid molar volume at the normal boiling point, $\tilde{V}_s(T_{nbp})$
4. BWR equation of state parameters.

Given the equilibrium temperature and pressure, T and P, the gas phase composition, $\{y_i\}$, the adsorption capacities for the components in the mixture are predicted from the characteristic curve in Figure 13 as follows:

Reproduced with permission of the copyright owner. Further reproduction prohibited without permission.

5. The saturation pressures for the pure components at T, $p_{si}(T)$, are evaluated with the Kirchhoff equation (see relation (90) in Appendix F)
6. The fugacities of the pure components at p_s and T, $f_{si}(p_{si},T)$, are evaluated from the BWR equation of state for the substances
7. The fugacities of the components in the gas mixture at T, P, and $\{y_i\}$, $\bar{f}_i(P,T,\{y_i\})$, are determined from the BWR equation of state for the mixture, the pure gas BWR parameters, and the mixture parameter mixing rules given by Benedict et al.[3]
8. Equations (41) and (43) are solved iteratively for all the adsorbate mole fractions, $\{x_i\}$
9. The abscissa of the characteristic curve, given by equation (44), is determined with any of the x_i's
10. $\hat{V}_{am} = n_T\tilde{V}_{am}$ is obtained graphically from the characteristic curve given in Figure 13 or analytically from equations (80) to (82) (linear least squares fit), given the abscissa determined above
11. The adsorbate mixture molar volume, $\tilde{V}_{am}$, is estimated with equations (85), (29), and (30)
12. The total amount adsorbed is evaluated as

$$n_T = (n_T\tilde{V}_{am})/\tilde{V}_{am} \tag{46}$$

and the individual components as

$$n_i = x_i n_T \tag{47}$$

Reproduced with permission of the copyright owner. Further reproduction prohibited without permission.

Correlation Method of Bering et al.[7]

The analytical method of Bering et al.[7] for binary adsorption correlation, as characterized by equations (48), (49), and (50) in Chapter IV, was tested with the experimental binary data of this study. It was found that this method of correlation does not fit these experimental data in a reasonable way; moreover, it was found that equation (50)

$$\left.\sum_{i=1}^{\text{all } i} \frac{n_i(p_i,T)}{n_{oi}(P,T)}\right|_{P = p_1+p_2 = \text{constant}} = 1.0 \qquad (50)$$

does not satisfy the well known mole fraction relation

$$\left.\sum_{i=1}^{\text{all } i} x_i\right| = 1.0 \qquad (51)$$

for the systems studied here.

Relative Volatilities

Experimental relative volatilities are shown in Tables 12-15 in Appendix G. The definition for binary systems follows equation (52) in Chapter IV

$$\alpha'_{ij} = x_j y_i / (x_i y_j) \qquad (86)$$

where component j is the more strongly adsorbed, i.e., $\alpha' > 1$. For ternary systems, relative volatilities are given only in terms of

$$\alpha'_{12} = x_2 y_1 / (x_1 y_2) \qquad (52)$$

Reproduced with permission of the copyright owner. Further reproduction prohibited without permission.

i.e., considering the methane-ethane pair. As expected, the relative volatilities or separation factors are dependent on temperature, pressure, and gas phase composition. In this experimental set of data the selectivity of the adsorbent for the more strongly adsorbed component, in methane-ethane and methane-ethylene mixtures, was found to increase both with decreasing pressure and temperature, and with decreasing concentration of that component in the gas phase at constant T and P. The same temperature and pressure dependence was found for ethane-ethylene systems. However, the relative volatility here, at constant T and P, was found to increase with increasing concentration of ethane in the gas phase. A graphical representation of the relative volatility for the methane-ethane and ethane-ethylene systems, given in Figures 25 and 26, supports these conclusions. Similar findings are reported by others.[29,47,52]

The calculation of relative volatilities for the present experimental conditions with the calculation scheme discussed above (i.e., the characteristic curve of Figure 13 and the Grant and Manes[25] method) was attempted with poor results. As the methane calculated mole fractions contain an important error the relative volatilities are affected significantly.

Method of Myers and Prausnitz[36]

An analysis of the present experimental data with the method of Myers and Prausnitz[36] was not attempted due to lack of the precise low pressure adsorption data required in the integration of equation (67).

Reproduced with permission of the copyright owner. Further reproduction prohibited without permission.

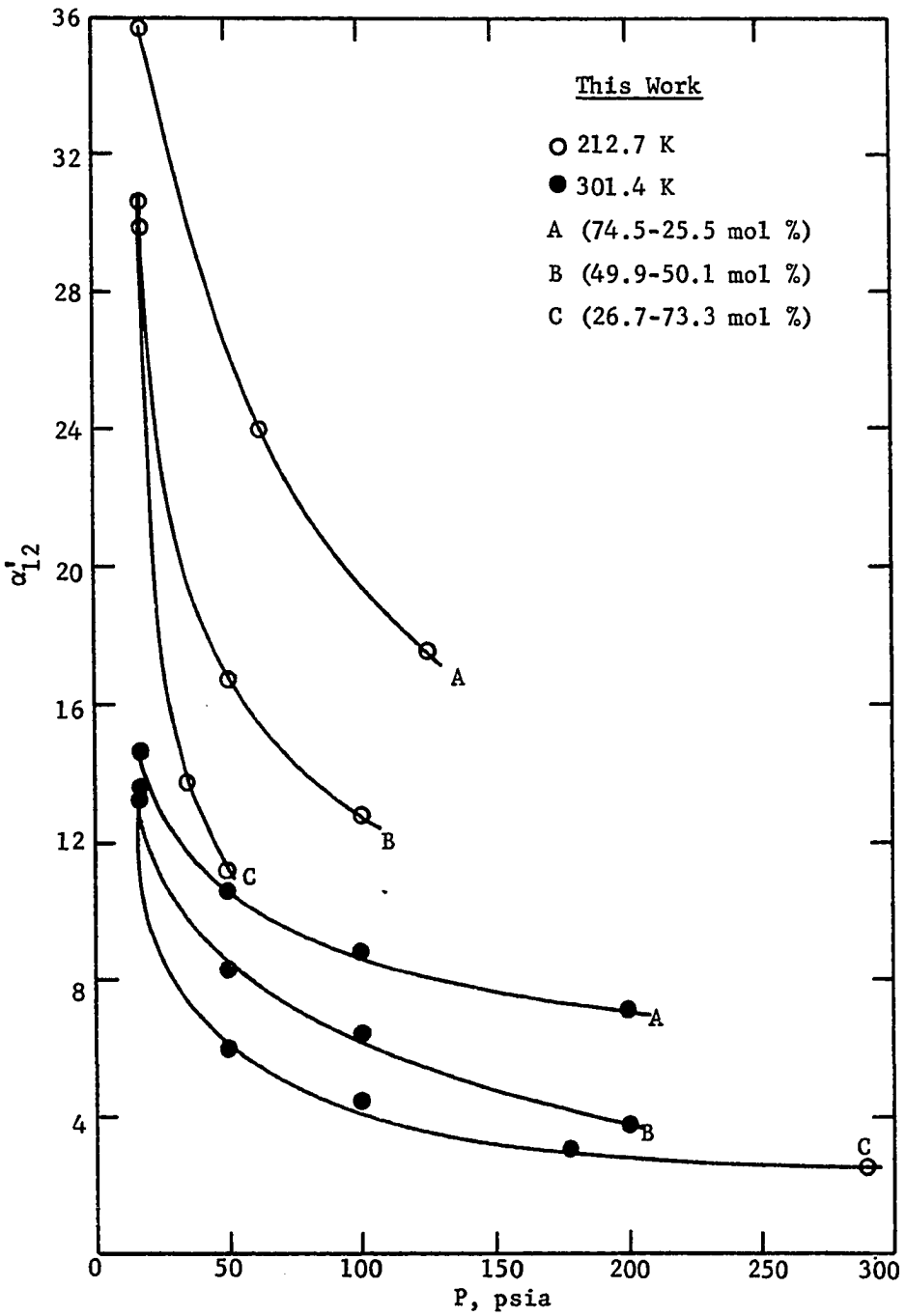

Figure 25. Relative Volatility for Methane(1)-Ethane(2) System

Reproduced with permission of the copyright owner. Further reproduction prohibited without permission.

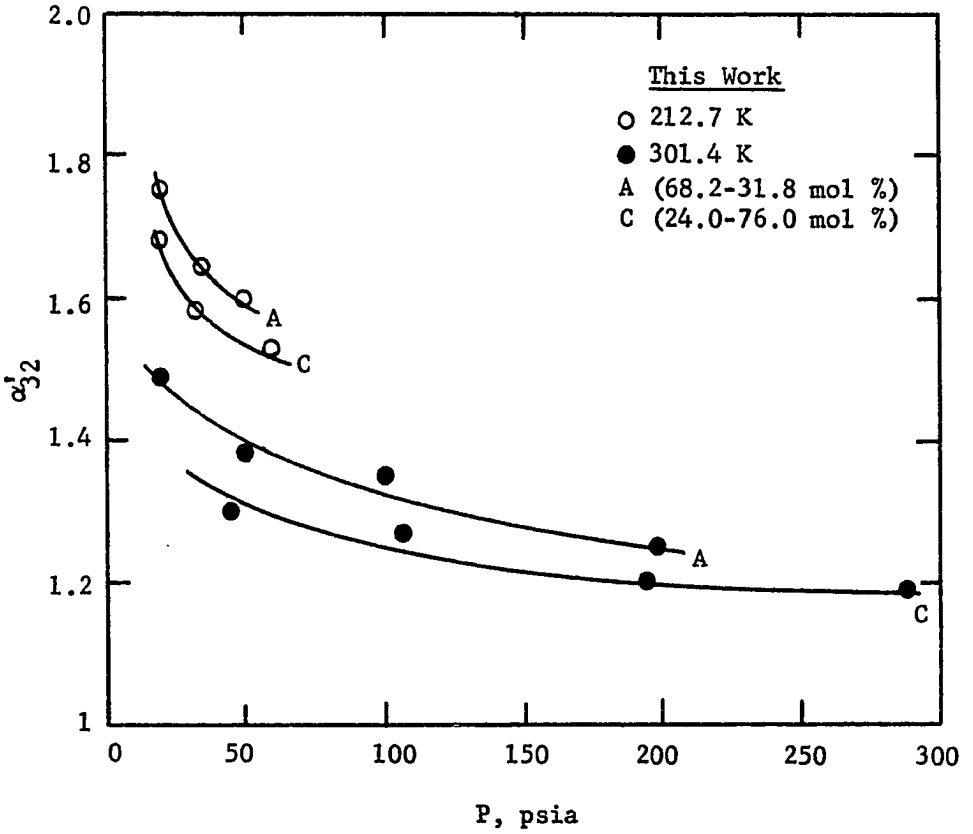

Figure 26. Relative Volatility for Ethane(2)-Ethylene(3) System

Reproduced with permission of the copyright owner. Further reproduction prohibited without permission.

CHAPTER VI

CONCLUSIONS AND RECOMMENDATIONS

Summary of Results

The work that has been completed can be summarized as follows:

1. The adsorption capacity of activated carbon, type BPL, for pure methane, ethane, ethylene, and carbon dioxide gases has been measured at 212.7 K, 260.2 K, and 301.4 K, and at equilibrium pressures ranging from 0.1 to 550 psia (0.69 to 3792 kN/m^2). The adsorption capacity for methane-ethane, methane-ethylene, and ethane-ethylene binary gas mixtures has been measured at 212.7 K, 260.2 K, and 301.4 K, at mole fractions of the first component in the gas phase of approximately 0.25, 0.50, and 0.75, and at equilibrium pressures between 19 and 300 psia (131 to 2068 kN/m^2). The adsorption capacity for methane-ethane-ethylene ternary gas mixtures has been measured at 212.7 K and 301.4 K, at mole fractions in the gas phase of approximately 0.62-0.17-0.20, 0.23-0.52-0.25, and 0.20-0.19-0.61, and at equilibrium pressures between 18 and 430 psia (124 to 2965 kN/m^2).

2. The adsorption capacity measurements for the pure gases have been used to calculate a single characteristic curve for this adsorbent-adsorbates system following the arguments of the Polanyi Potential Theory,[40] as modified by Dubinin and co-workers.[20] The ordinate of the correlation has been calculated by using absolute adsorption capacities and the Nikolaev and Dubinin scheme[37] for the adsorbate molar volume. The

Reproduced with permission of the copyright owner. Further reproduction prohibited without permission.

saturated liquid molar volume at the normal boiling point has been used as the correlating parameter in the abscissa.

3. Adsorption capacities, at the same experimental conditions as in this study, have been calculated from a least squares fit of the characteristic curve data for the pure gases following the Dubinin-Radushkevich equation[18] and a simple linear equation containing the coordinates.

4. The adsorption capacity measurements for the binary and ternary gas mixtures have been used to calculate a characteristic curve for this adsorbent-adsorbates system following the method proposed by Grant and Manes.[25] The ordinate of the correlation has been calculated by using Gibbs adsorption capacities, the Nikolaev and Dubinin scheme[37] for the adsorbate molar volume, and the additivity of the pure component adsorbate molar volumes for the adsorbate mixture volume. The saturated liquid molar volume of the pure components at the normal boiling point has been used as the correlating parameter in the abscissa.

5. Adsorption capacities of the mixtures, at the same experimental conditions as in this study, have been calculated from the linear least squares fit of the pure gas characteristic curve. A pseudo-binary method has been used for the ternary mixtures.

6. The adsorption capacity measurements for the binary gas mixtures have been used to test the correlation method of Bering et al.[7]

7. The adsorption capacity measurements for the mixtures have been used to calculate adsorption relative volatilities, according to the definition by Lewis et al.[29]

Reproduced with permission of the copyright owner. Further reproduction prohibited without permission.

Conclusions

From the experimental measurements the following conclusions are derived:

1. The adsorption isotherms for pure methane, ethane, and ethylene show a similar shape, ethane and ethylene having about equal adsorption capacities at the same pressures for all three temperature levels and methane showing much lower capacities than those two. Carbon dioxide isotherms have, in general, greater slopes and greater adsorption capacities than the other three gases. The adsorption measurements agree, in general, with measurements made by other investigators. Reproducibility of pure gas isotherms is within ± 1%, the general accuracy being estimated to be within ± 3 to 4%.

2. In general, with the exception of methane-ethane and methane-ethylene mixtures of low methane content, the estimation of component capacities is not possible solely from pure adsorption data and the partial pressures of the components at a fixed temperature. In general, component interactions are present and the different component adsorption capacities are significantly reduced with respect to their adsorption as pure gases at a total pressure equal to the partial pressure of the components in the mixture. It is apparent from the complete set of mixture data that the methane adsorption capacities are approximately temperature independent between 212.7 K and 301.4 K. Reproducibility of gas mixture adsorption measurements is within ± 2.0%. The general accuracy is estimated to be within ± 5 to 8%. No comparison with multicomponent adsorption measurements made by others is given due to lack of appropriate data in the literature.

Reproduced with permission of the copyright owner. Further reproduction prohibited without permission.

From the pure gas adsorption data correlation the following conclusions are made:

1. The adsorption capacities of methane, ethane, ethylene, and carbon dioxide on activated carbon, type BPL, in the range of temperature and pressure conditions of this study, essentially correlate in one single characteristic curve.

2. If this same correlation method is applied to the data of Szepesy and Illes[50,51] for methane, ethane, ethylene, carbon dioxide, propane, propene, and butane on a similar adsorbent and a wide range of temperature and pressure conditions, a similar characteristic curve is obtained with some branching at low pressures. This suggests that the correlation for pure gases developed in this study can be used in the prediction of adsorption capacities of several gases other than those studied.

3. The Dubinin-Radushkevich equation[18] does not represent well the data of this study over the whole range of temperature and pressure conditions, and it contains temperature dependent parameters which make its use impractical. However, it can be used satisfactorily to represent the experimental data in the low pressure region.

4. A linear least squares fit of the pure gas characteristic curve ordinates permits the calculation of adsorption capacities for the four gases, at the conditions of this study, with a maximum deviation of about 30% and an average of ± 6.1% with respect to the experimental values. It is suggested that this correlation be used for gases for which $T \leq T_c$ for best results; it should not be used at pressures less than about one atmosphere.

Reproduced with permission of the copyright owner. Further reproduction prohibited without permission.

From the mixture gas adsorption data correlation the following conclusions are made:

1. Even when the correlation method appears to be thermodynamically inconsistent,[48] the adsorption capacities of the components (methane, ethane, or ethylene) in binary and ternary systems and at the temperature and pressure conditions of this study essentially correlate in one single characteristic curve if some methane data points at 301.4 K are omitted from the correlation. This characteristic curve is superimposable on the pure gas adsorption correlation.

2. The equipotential concept does not hold at 301.4 K. However, a fair estimation of binary and ternary (methane-ethane-ethylene) gas adsorption data from the pure gas adsorption correlation is possible. Ethane and ethylene adsorption capacities in the mixtures can be predicted from the linear correlation with average deviations better than ± 15% with respect to experimental values. Methane predictions are poor with this method.

From other methods of data analysis the following conclusions are made:

1. The Bering et al.[7] correlation does not fit the experimental data of this study.

2. The relative volatility or selectivity of the adsorbent for the more strongly adsorbed component increases both with decreasing pressure and temperature and with concentration of that component in the gas phase at constant T and P.

Reproduced with permission of the copyright owner. Further reproduction prohibited without permission.

Recommendations for Future Work

1. The pure gas and gas mixture correlations developed in this study should be further tested with experimental adsorption data on other substances with higher critical temperatures than ethane and a wide range of temperatures and pressures.

2. Mixture adsorption measurements should be pursued with other components of low critical temperature replacing methane, i.e., nitrogen, nitric oxide, carbon monoxide, argon, etc., to test the equipotential concept in the Grant and Manes[25] method.

3. Further efforts should be expended to solve the thermodynamically inconsistent aspect of the Grant and Manes[25] correlation method.

Reproduced with permission of the copyright owner. Further reproduction prohibited without permission.

APPENDIX A

CONVERSION FACTORS TO SI SYSTEM

In the present work a combination of units in the Metric and English Systems has been used, mainly for practical reasons. However, an attempt has been made to place the units problem into the perspective of the Systeme International d'Unités (SI) or International System of Units. Whenever it has been possible or convenient, SI units have been added in the text or conversion factors to the SI system made available.

A summary of conversion factors to the SI system for most of the units appearing in this thesis is given below[1]:

SI Base Units

Length	m	meter
Mass	kg	kilogram
Time	s	second
Thermodynamic temperature	K	kelvin
Mole	mol	mole

Temperature

T (K)	=	t (^{o}C) + 273.15
T (K)	=	(t (^{o}F) + 459.67)/1.8

Pressure

1 atm	=	101.325 kN/m^2
1 psia	=	6.8947572 kN/m^2
1 mmHg(0^{o}C),Torr	=	133.3224 kN/m^2

Reproduced with permission of the copyright owner. Further reproduction prohibited without permission.

	Volume	
1 cm^3	=	10^{-6} m^3
1 ft^3	=	0.02831685 m^3
1 liter	=	0.001 m^3
	Density	
1 g/cm^3	=	1000 kg/m^3 = 1 kg/cm^3
1 lb/ft^3	=	16.018463 kg/m^3
	Mass	
1 lb	=	0.45359237 kg
	Energy	
1 cal, thermochemical	=	4.184 J
1 ft-lbf	=	1.3558 J

Reproduced with permission of the copyright owner. Further reproduction prohibited without permission.

APPENDIX B

SYSTEM MODIFICATIONS AND ADSORPTION CELL DETAILS

System Modifications

In the preliminary stages of the experimental work when testing and operation of the apparatus were being performed, evidence of the presence of small quantities of oil in parts of the tubing system was found. The origin of this oil was traced to one of the Bourdon gauges (P3).

It was decided to replace part of the copper tubing system. Accessory parts and instrumentation were cleaned thoroughly.

No evidence was found that the presence of the oil affected in any way the experimental results obtained by Rogers.[47]

Adsorption Cell

New Design

As mechanical problems arose in this work with a plastic Teflon gasket in the adsorption cell built by Rogers,[47] a new cell design was attempted. Its main purpose was to eliminate the gasket and so a completely sealed vessel design was selected. A description of this cell is given in Figure 27.

Adsorbent Placement

The adsorption vessel was initially cleaned and prepared without the Swagelok male connector. Glass wool was introduced and placed at the bottom of the cell. Then, 32.19 grams of activated carbon, as characterized

Reproduced with permission of the copyright owner. Further reproduction prohibited without permission.

in Appendix F, was introduced next, and covered at the top with glass wool. The Swagelok male connector was then placed in position with Teflon strip and later sealed with a 63/37 Sn-Pb solder (melting point 182^{o}C).

Reproduced with permission of the copyright owner. Further reproduction prohibited without permission.

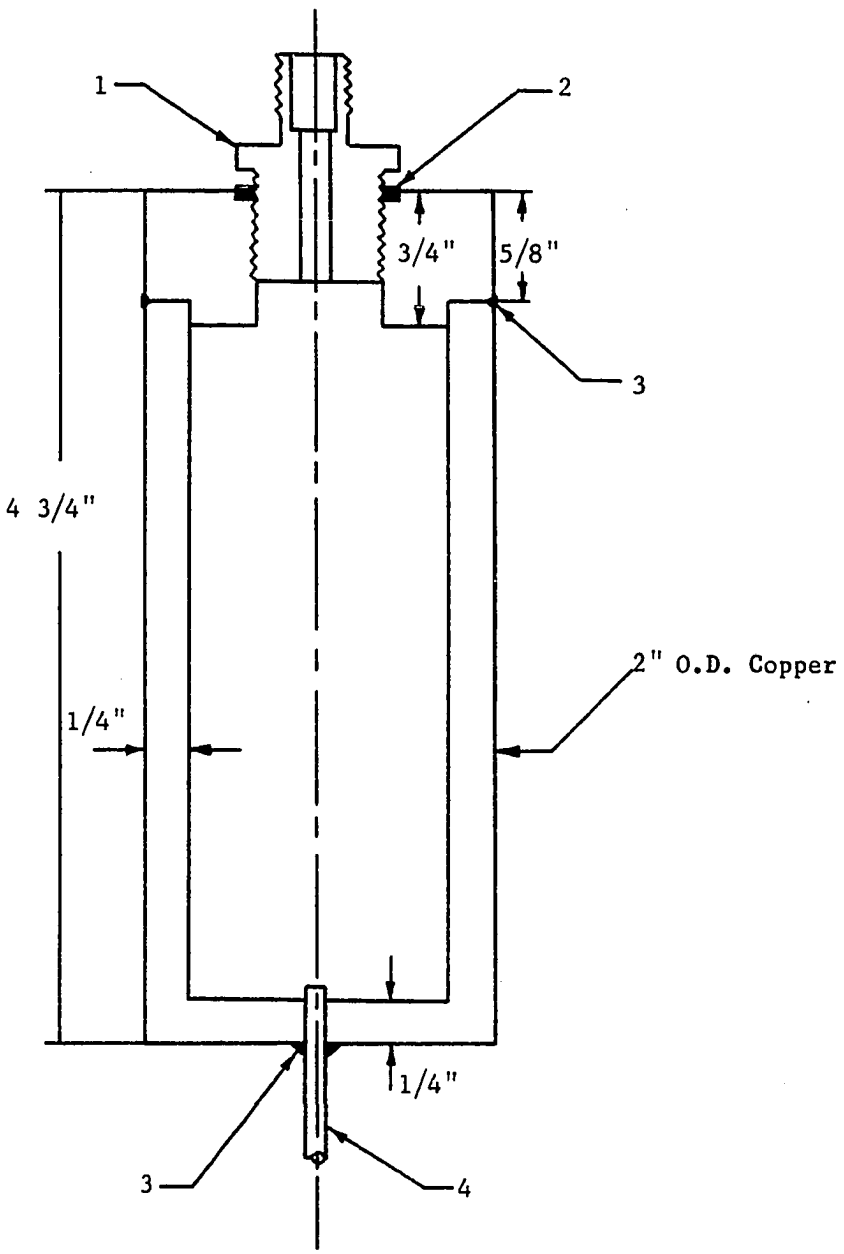

1 -- Stainless steel Swagelok male connector
1/4" tube O.D. -- 3/4" male pipe size
2 -- 63/37 Sn-Pb solder
3 -- Silver solder
4 -- 1/8" O.D. copper tubing

Figure 27. New Adsorption Cell

Reproduced with permission of the copyright owner. Further reproduction prohibited without permission.

APPENDIX C

TEMPERATURE SCALE AND CORRECTIONS FOR PRESSURE GAUGES

The temperature measurements reported in this work were obtained by using two type E, Chromel-Constantan thermocouples within the adsorption system cryostat. Details of their construction are given in Rogers's[47] thesis.

The thermocouples were calibrated using a capsule-type platinum resistance thermometer, LEEDS and NORTHRUP Serial 1583526, which had been calibrated by the U.S. National Bureau of Standards on the International Practical Temperature Scale of 1948. All temperature measurements in this work were reported on the IPTS-68 scale with an uncertainty of ± 0.1 K. The measured temperatures were converted from IPTS-48 to IPTS-68 based on the following relation given by Barber[2]:

$$T\ (\text{IPTS-68}) = 273.15 + t_{48}(^{\circ}C) + (t_{68}(^{\circ}C) - t_{48}(^{\circ}C)) \qquad (87)$$

Using an ice reference bath, the electromotive force values of the two cryostat thermocouples at 212.7 K, 260.2 K, and 301.4 K were 3.125, 0.707, and - 1.592 millivolt, respectively.

Pressure measurements in this work were obtained from mercury-in-glass manometers and Bourdon-type gauges (see Figures 1 and 2 in Chapter II), depending on the pressure level of the measurements. Manometers were used for pressures below 15 psia giving an uncertainty in the measurements

Reproduced with permission of the copyright owner. Further reproduction prohibited without permission.

of ± 0.05 psia. For the pure gas adsorption isotherm determination a Heise gauge (P3) was used for pressures between 15-250 psia ± 0.25 psia, and a Martin-Decker gauge (P2) for the range 250-550 psia ± 1.5 psia. For the mixture adsorption measurements an Ashcroft gauge (P1) was used between 15-300 psia ± 0.5 psia and gauge P2 in the range 300-450 psia ± 1.5 psia. The three gauges were calibrated by Rogers[47] against a dead weight tester. Correction plots for gauges P1 and P2 are given in Rogers's thesis. No correction was necessary for gauge P3.

Reproduced with permission of the copyright owner. Further reproduction prohibited without permission.

APPENDIX D

PURITY OF GASES AND GAS MIXTURE PREPARATION

Purity of Gases

The methane, ethane, and ethylene used in the adsorption experiments were supplied by Matheson Gas Products, the carbon dioxide by Liquid Carbonic, the quoted purity in mole percent being as follows:

Methane	99.995 mol%
Ethane	99.96 mol%
Ethylene	99.997 mol%
Carbon dioxide	99.95 mol%

The hydrogen used as the carrier gas in the gas chromatograph analyzer was supplied by Matheson Gas Products with a purity certified as 99.95 mol% minimum.

The helium gas used as a purge gas in the gas mixture isotherm measurements was supplied by Selox, Inc. The purity was quoted to be 99.995 mol%.

Gas Mixture Preparation

All binary and ternary gas mixtures used in this experimental work were prepared in a five liter ($0.005\ m^3$) evacuated commercial steel gas cylinder. Adequate mixing of the gases was accomplished by rotating the cylinder intermittently; four brass rods were placed inside the cylinder to improve mixing. The cylinder was allowed to set overnight before any

Reproduced with permission of the copyright owner. Further reproduction prohibited without permission.

gas was used. Gas chromatographic analysis performed on the different gas mixtures during the course of the adsorption experiments confirmed that good mixing was obtained.

Reproduced with permission of the copyright owner. Further reproduction prohibited without permission.

APPENDIX E

CALIBRATION OF GAS CHROMATOGRAPH

Operating Conditions

Prior to the calibration of the LOENCO, Model 2400-T1, gas chromatograph equipped with a hot wire thermal conductivity detector, the separation column, the carrier gas, and the operating conditions were selected to obtain the best component separation. The same silica gel column used by Rogers[47] was selected since it accomplished the separation of a methane, ethane, ethylene, and helium gas mixture satisfactorily under the operating conditions given in Table 2. The separating column was previously reactivated by flowing pure hydrogen carrier gas at about 200°C overnight. A PERKIN-ELMER sampling valve with a 5 cm^3 loop was used to establish the best operating conditions. Output from the analyzer was recorded on a LEEDS and NORTHRUP, Model W, potentiometer with a 2.0 millivolt span and a two inch per minute chart speed.

Calibration Procedure

It was necessary to calibrate the gas chromatograph so as to handle analyses of binary mixtures of methane, ethane, and ethylene, ternary mixtures of these binaries with helium purge gas, ternary mixtures of methane, ethane, and ethylene, and four component mixtures of these ternaries with helium gas over the full range of compositions from 0 to 100 mole percent.

This calibration was accomplished by calibrating the gas analyzer

Reproduced with permission of the copyright owner. Further reproduction prohibited without permission.

Table 2. Gas Chromatograph Operating Conditions

Column	Silica Gel, 40/80 mesh
Outside Diameter,	
inches	1/4 stainless steel
mm	6.35
Length, m	0.80
Carrier Gas	Hydrogen
Carrier Gas Inlet Pressure,	
psia	64
kN/m^2	441.3
Carrier Gas Flow Rate at Room T and P, cm^3/s	0.9
Sample Size, cm^3	5
Oven Temperature, ^oC	60
Detector Temperature, ^oC	65
Detector Filament Current, mA	135

Reproduced with permission of the copyright owner. Further reproduction prohibited without permission.

for each pure gas, i.e., methane, ethane, ethylene, or helium, as peak height response versus moles of pure gas, at different attenuation settings of the instrument. An actual sample calibration graph for the four gases at a fixed attenuation setting is given in Figure 28. The abscissas on these figures were developed by varying the amount of pure gas injected into the gas analyzer.

The number of moles of pure gas in the gas analyzer sample valve, n_{sv}, can be represented by the following relation:

$$n_{sv} = PV_{sv}/(ZRT) \tag{88}$$

where V_{sv} is the sample valve total volume (i.e., its internal volume plus the loop volume), and P, T, and Z are the gas pressure, temperature, and compressibility factor, respectively; R is the universal gas constant.

As the temperature (room conditions) was fixed, the number of moles were varied by changing the pressure of the gas and the volume of the sample valve. In practice, four pressure levels were established between 16 and 30 psia (110-207 kN/m^2) and the volume was modified by using different volume loops (5 cm^3, 1 cm^3, and 0.1 cm^3).

The practical experimental procedure to obtain a peak height versus moles of pure gas data point for a fixed instrument attenuation and sample valve volume is described next. Reference is made to the schematic diagram given in Figure 29. Initially, the sample valve was set in the position shown in Figure 29, i.e., only carrier gas flowed to the gas chromatograph, and the sample valve volume was connected to the calibration system.

Reproduced with permission of the copyright owner. Further reproduction prohibited without permission.

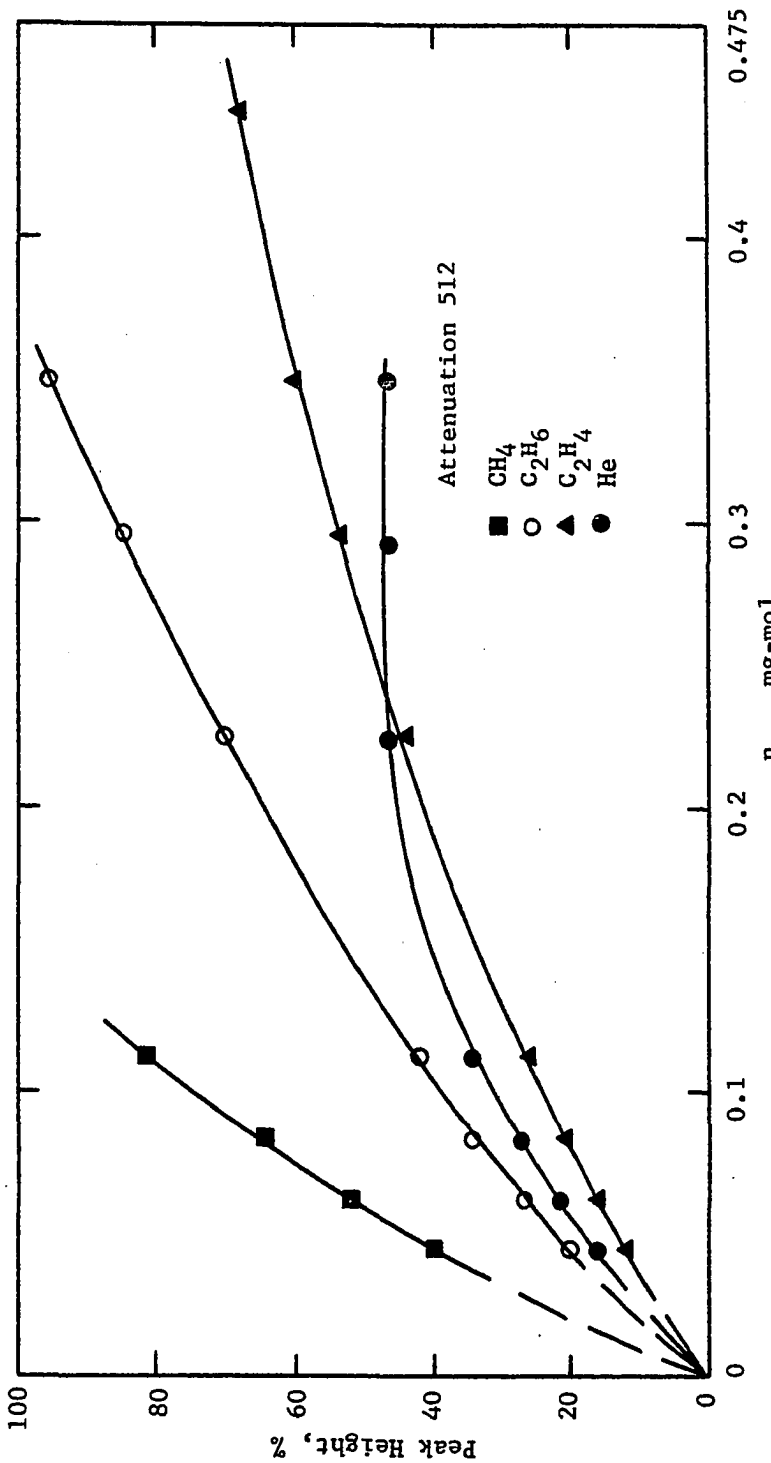

Figure 28. Gas Chromatographic Calibration Curve

Reproduced with permission of the copyright owner. Further reproduction prohibited without permission.

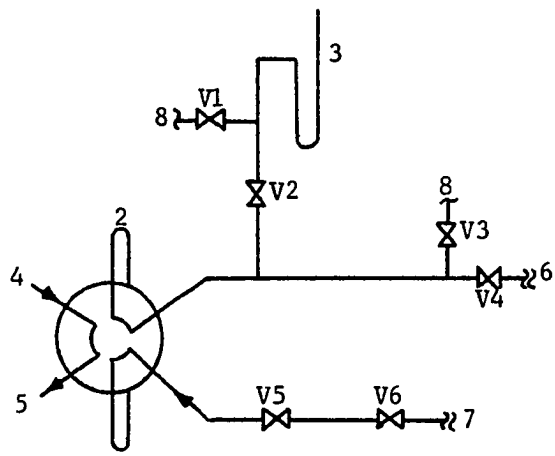

1 -- Gas chromatographic sampling valve
2 -- Variable volume loop
3 -- Mercury manometer
4 -- Carrier gas inlet stream
5 -- Stream entering gas chromatograph
6 -- To vacuum line
7 -- Calibration gas source
8 -- Venting valves

Figure 29. Schematic Diagram of Gas Chromatographic Calibration Apparatus

Reproduced with permission of the copyright owner. Further reproduction prohibited without permission.

Valves V1, V3, and V6 were closed; V2 and V5 were opened. V4 was opened to evacuate the system; then it was closed. Pure gas was allowed to flow into the system by opening V6 and monitoring manometer 3. The system was then purged with pure gas for a short period of time by opening V1 slightly. The pressure level required was attained by adjusting valves V1 and V6 and reading manometer 3. The system pressure, the room temperature, and pressure were then recorded. The analyzer sample valve was set in the position for gas sample transfer to the instrument, the peak height being evaluated from the recorder chart. Knowing the absolute pressure, temperature, and volume occupied by the gas in the sample valve, the number of moles of gas were calculated using relation (88), Z being estimated from the BWR equation of state for the gas at the same temperature and pressure.

This experimental procedure was repeated for the four gases at the three loop sample volumes and four pressure levels, producing a set of calibration curves, similar to Figure 28, which were later used in the gas mixture adsorption experimental program. The calibration curves show non-linearity at higher concentrations of the gas and are essentially linear at low concentration. In addition, the helium gas calibration curves (see Figure 28) show a tendency towards constant peak height for a number of moles in the sample valve, n_{sv}, greater than 0.23 mg-mol. However, this part of the curve was never used in evaluating analyses in this study.

These curves were checked by an independent method used in this laboratory previously. In this procedure binary gas mixtures of known composition were prepared with a sample mixing burette built by Kirk[27] and analyzed in the same gas chromatograph analyzer under the same operating conditions.

Reproduced with permission of the copyright owner. Further reproduction prohibited without permission.

The mixing burette analyses deviated from the calibration curve analyses within a maximum of 6.3% and an average deviation of ± 2.5%. These results are presented in Table 3. The accuracy of the analysis made with the mixing burette is considered to be ± 3%.[47] It is believed that the accuracy of all analyses performed during this experimental work and evaluated with the set of calibration curves described before falls within ± 5%.

To allow for day-to-day fluctuations which can affect a chromatograph calibration (i.e., atmospheric pressure, chromatograph column temperature, voltage supply, detector temperature, and recorder changes) the analyzer detector filament current was set so as to reproduce a standard pure methane peak height as measured during the calibration period. This procedure was always followed before a new set of analyses was performed. It is believed that variations of this type did not affect the mole percent analysis by more than 1%.

No chromatograph calibration was performed upon completion of the adsorption experiments. There is reason to believe that such a calibration was unnecessary because, at the end of the experimental program, a binary gas mixture used near the beginning of the binary adsorption measurements was reanalyzed; the agreement obtained was within 2%.

Reproduced with permission of the copyright owner. Further reproduction prohibited without permission.

Table 3. Comparison of Calibration Curves Analysis with Gas Mixing Burette Analysis

Gases	MB Analysis, %	CC Analysis, %	Deviation, %
Helium	66.9	67.8	-1.4
Methane	33.1	32.2	2.7
Helium	97.2	97.3	-0.1
Methane	2.8	2.7	3.6
Helium	66.7	65.4	2.0
Ethane	33.3	34.6	-3.9
Helium	97.0	97.2	-0.2
Ethane	3.0	2.8	6.3
Helium	67.0	65.8	1.8
Ethylene	33.0	34.2	-3.6
Helium	96.7	96.8	-0.1
Ethylene	3.3	3.2	3.0
Methane	2.7	2.6	3.7
Ethane	97.3	97.4	-0.1
Methane	33.1	35.0	-5.7
Ethane	66.9	65.0	2.8
Methane	66.6	64.9	2.6
Ethane	33.4	35.1	-5.1
Methane	97.4	97.3	0.1
Ethane	2.6	2.7	-3.9
Methane	3.3	3.4	-3.0
Ethylene	96.7	96.6	0.1
Methane	33.2	32.1	3.3
Ethylene	66.8	67.9	-1.7
Methane	45.8	47.7	-4.2
Ethylene	54.2	52.3	3.5
Methane	66.7	66.4	0.5
Ethylene	33.3	33.6	-0.9
Methane	96.7	96.9	-0.2
Ethylene	3.3	3.1	6.1
Ethane	66.7	66.0	1.1
Ethylene	33.3	34.0	-2.1

MB = Mixing Burette
CC = Calibration Curves
Deviation, % = (MB Analysis - CC Analysis)100/MB Analysis

Reproduced with permission of the copyright owner. Further reproduction prohibited without permission.

APPENDIX F

CHARACTERIZATION OF MATERIALS

Activated Carbon Adsorbent

The adsorbent used in this study is a microporous activated carbon with a heterogeneous surface, which has been available commercially for several years. It is described as Type BPL and manufactured by the Pittsburgh Chemical Co. This particular type of adsorbent was selected as it has been used before by others.[23-25, 28, 35, 47] Manufacturer's data for the material is reported in Table 4.

A representative sample of the 6/16 mesh size carbon batch (the same batch used by Rogers[47]), obtained by selecting about six portions of carbon at random and mixing them, was crushed and sieved to 20/65 mesh size before placing 32.19 grams of it in the adsorbent cell (see Appendix B).

As part of this study, a conventional nitrogen BET surface area determination was performed in duplicate on a portion of the carbon prepared for the sample in the adsorption cell. The results of these tests were 1000 and 975 m^2/gC, giving an average of 988 m^2/gC. This last value is between the one reported by Rogers[47] (967 m^2/gC) and that given by the manufacturer (1050-1150 m^2/gC).

Physical Property Data for Pure Components

In the different calculations involved in this thesis the following physical property data for the pure components were required:

Reproduced with permission of the copyright owner. Further reproduction prohibited without permission.

Table 4. Activated Carbon Characteristics (Manufacturer's Data)

Manufacturer: Pittsburgh Activated Carbon Division, Calgon Corp.

Type: BPL

Mesh Size: 6/16 mesh

Physical Properties:

Total Surface Area (N_2, BET method), m^2/gC	1050-1150
Apparent Density (Bulk Density, dense packing), g/cm^3	0.5
Particle Density (Hg Displacement), g/cm^3	0.8
Real Density (He Displacement), g/cm^3	2.1
Pore Volume (Within Particle), cm^3/gC	0.8
Voids in Dense Packed Column, %	40
Specific Heat at 100^oC	0.25

Pore Structure: Micropore size by water desorption isotherm shows major portion in the 18-21 Angstrom (1.8-2.1 nm) diameter range.

Reproduced with permission of the copyright owner. Further reproduction prohibited without permission.

1. Parameters for the BWR equation of state.

2. Critical constants, normal boiling point temperatures, and saturated liquid molar volumes at the normal boiling point for the condensed components.

3. Molecular weights for the components.

4. Vapor pressure data for the condensed components at 212.7 K, 260.2 K, and 301.4 K.

Benedict et al.[3] BWR parameters were selected for methane, ethane, and ethylene, and the Cullen and Kobe[14] parameters for carbon dioxide. The parameter C_o for ethane and carbon dioxide at 212.7 K was corrected for temperature dependence following the Orye[38] procedure. The parameters selected for the four gases are presented in Table 5; units are given in liter-atmosphere-Kelvin-gram-mole.

Critical constants, normal boiling point temperatures, and saturated liquid molar volumes were selected from the Canjar and Manning[10] compilation. It is believed that this source of data is reliable and appropriate for this work.

Critical temperatures and pressures for the substances are shown in Table 6. Normal boiling point temperatures for methane, ethane, and ethylene and the triple point for carbon dioxide are given in the same table. Temperatures are given in Kelvin and the pressure in atmospheres.

Saturated liquid molar volumes at the normal point are presented in Table 7. The value for carbon dioxide is taken from Rogers[47] and represents a fictitious number obtained by extrapolation of saturated liquid molar volume versus saturated pressure data at a saturation pressure of one atmosphere. Units given are in cubic centimeter per gram mole.

Reproduced with permission of the copyright owner. Further reproduction prohibited without permission.

Table 5. BWR Equation of State Parameters
(Units: liter-atm-K-gmol)

Parameters	Gas			
	Methane[3]	Ethane[3]	Ethylene[3]	Carbon Dioxide[14]
A_o	1.85500	4.15556	3.33958	2.73742
B_o	4.26000(-2)*	6.27724(-2)	5.56833(-2)	4.99101(-2)
C_o	2.25700(+4)	1.79592(+5)	1.31140(+5)	1.38567(+5)
		(1.78464(+5))**		(1.37292(+5))**
a	4.94000(-2)	3.45160(-1)	2.59000(-1)	1.36814(-1)
b	3.38004(-3)	1.11220(-2)	8.60000(-3)	7.21045(-3)
c	2.54500(+3)	3.27670(+4)	2.11200(+4)	1.49180(+4)
α	1.24359(-4)	2.43389(-4)	1.78000(-4)	8.47000(-5)
δ	6.00000(-3)	1.18000(-2)	9.23000(-3)	5.39400(-3)

*Number in parenthesis indicates power of 10

**Corrected C_o at 212.7 K

NOTE

To convert liter to m^3 multiply by 0.001

To convert atm to kN/m^2 multiply by 101.325

The unit g-mol is equivalent to mkg-mol

Reproduced with permission of the copyright owner. Further reproduction prohibited without permission.

Table 6. Critical Constants and Normal Boiling Point Temperatures for Components[10]

Gas	T_c, K	P_c, atm	T_{nbp}, K	$T_{triple\ point}$, K
Methane	190.65	45.80	111.66	
Ethane	305.38	48.30	184.34	
Ethylene	283.05	50.50	169.45	
Carbon Dioxide	304.19	72.81		183.9

NOTE
To convert from atm to kN/m^2 multiply by 101.325

Reproduced with permission of the copyright owner. Further reproduction prohibited without permission.

Table 7. Molecular Weights and Saturated Liquid Molar Volumes at Normal Boiling Point for Components

Gas	Molecular weight	$\tilde{V}_s(T_{nbp})$, $cm^3/g\text{-}mol$[10]
Methane	16.042	37.81
Ethane	30.068	55.02
Ethylene	28.054	49.35
Carbon Dioxide	44.011	(33.2*)[47]

*Fictitious value obtained by extrapolation of saturated liquid molar volume data at a saturation pressure of one atmosphere.

NOTE

The unit of $cm^3/g\text{-}mol$ is equivalent to $cm^3/mkg\text{-}mol$ in SI system

Reproduced with permission of the copyright owner. Further reproduction prohibited without permission.

Molecular weights, calculated from atomic weights based on $^{12}C = 12$, are included in the same table.

Vapor pressure data for the pure components at 212.7 K, 260.2 K, and 301.4 K were required in this work. As saturated pressures for methane at all three temperature levels and for ethylene at 301.4 K can only be considered as fictitious--they correspond to temperatures where a liquid phase cannot exist--a mathematical representation of the available data was selected. The reduced Kirchhoff vapor pressure equation[46] was used for this purpose, corresponding basically to an approximate integration of the exact thermodynamic Clausius-Clapeyron relation. The integrated relation,

$$\ln p_s = A + B/T \tag{89}$$

where A and B are constants, applied to the critical point and to the normal boiling point of the substance can be reduced to the form

$$p_s = P_c \exp(h(1 - 1/T_R)) \tag{90}$$

where

$$h = \frac{T_{nbp}}{T_c} \left(\frac{\ln P_c}{1 - \frac{T_{nbp}}{T_c}} \right) \tag{91}$$

$$T_R = T/T_c$$

Reproduced with permission of the copyright owner. Further reproduction prohibited without permission.

The Kirchhoff relation, equation (90), represented the available experimental vapor pressure data for the four substances between their normal boiling points and critical points within ± 3%, its parameters being evaluated from critical constants and normal boiling point temperatures. The same equation was used to obtain fictitious vapor pressures for methane and ethylene at temperatures above their critical points, by extrapolation.

Reproduced with permission of the copyright owner. Further reproduction prohibited without permission.

APPENDIX G

EXPERIMENTAL DATA

The experimental pure gas and mixture adsorption data obtained in this study are presented next in Tables 8 to 15, the amount adsorbed, n_o or n_i, being given in terms of the Gibbs[53] definition (see Chapter V). Thirty-two pure gas adsorption isotherms were determined over a two-month period (see Tables 8 to 11), and twenty-seven gas mixture adsorption isotherms over a subsequent three-month period (see Tables 12 to 15). A single sample of 32.19 grams of activated carbon, as characterized in Appendix F, was used over the total experimentation period.

Vapor pressures for the pure components, at the three experimental temperature levels, are given for reference below[10]:

Gas	$p_s(T)$, psia		
	301.4 K	260.2 K	212.7 K
Methane		$T > T_c$	
Ethane	651.7	280.5	54.2
Ethylene	$T > T_c$	433.2	107.3
Carbon Dioxide	1004.1	352.4	57.8

Reproduced with permission of the copyright owner. Further reproduction prohibited without permission.

Pure Gas Isotherms

In the following tables the equilibrium pressure, P, is expressed in pounds per square inch absolute and the amount of pure gas adsorbed, n_o, is given in milligram-mole per gram of adsorbent. Each isotherm data set is identified by the date of experiment in parenthesis. The entire set of pure gas adsorption measurements was determined between November 19, 1973 and January 23, 1974.

The amounts of gas adsorbed were calculated with computer program PISOTH which is briefly described in Appendix L.

The uncertainty in the pressure given in these tables is within ± 0.05 psia at pressures below 15 psia, ± 0.25 psia between 15 and 250 psia, and ± 1.5 psia between 250 and 550 psia (see Appendix C). The uncertainty in the number of moles given in the same tables is believed to be within ± 0.02-0.15 mg-mol/gC, depending on the pressure level (see Chapter III). It is recognized that the values presented in these tables are carried, in general, with more significant figures than suggested by the uncertainties given above.

NOTE

To convert from psia to kN/m^2 multiply by 6.8947572.

The unit of mg-mol is equivalent to μkg-mol in the SI system.

Reproduced with permission of the copyright owner. Further reproduction prohibited without permission.

Reproduced with permission of the copyright owner. Further reproduction prohibited without permission.

Table 8. Methane Isotherms, Gibbs Definition

P, psia	n_o, mg-mol/gC	P, psia	n_o, mg-mol/gC	P, psia	n_o, mg-mol/gC
		T = 301.4 K			
19.1	0.764	10.5	0.477	126.6	2.560
39.8	1.298	26.3	0.966	182.9	3.065
67.8	1.811	57.8	1.644	238.4	3.385
98.3	2.230	87.9	2.097	290.4	3.617
129.8	2.564	119.4	2.463	343.3	3.806
168.6	2.894	150.4	2.748	396.2	3.974
209.4	3.174	192.7	3.064	449.1	4.049
249.3	3.395 (1.9.74)	230.3	3.284 (1.10.74)	500.0	4.195
				555.4	4.250 (1.15.74)
		T = 260.2 K			
11.9	1.207	6.4	0.793	137.6	4.122
23.5	1.830	18.9	1.618	230.4	4.746
43.9	2.561	35.3	2.297	293.4	5.057
73.2	3.216	59.4	2.948	349.3	5.246
105.7	3.705	89.7	3.493	401.2	5.411
145.4	4.125	125.1	3.933	452.6	5.507
193.9	4.487	169.4	4.325	502.5	5.570
241.5	4.755 (12.18.73)	219.5	4.649 (12.19.73)	554.9	5.594 (1.17.74)
		T = 212.7 K			
3.3	1.669	1.7	1.138	100.9	5.944
10.5	2.924	7.7	2.561	212.2	6.738
19.5	3.736	16.4	3.518	284.8	7.003
38.7	4.632	34.1	4.484	343.8	7.141
68.8	5.359	64.5	5.284	395.2	7.256
102.8	5.848	94.9	5.750	500.5	7.261 (1.22.74)
143.0	6.222	140.3	6.209		
184.8	6.493	176.8	6.461 (12.5.73)		
234.2	6.715 (12.4.73)				

Table 9. Ethane Isotherms, Gibbs Definition

P, psia	n_o, mg-mol/gC	P, psia	n_o, mg-mol/gC
	T = 301.4 K		
4.5	1.620	1.8	1.013
14.0	2.749	9.4	2.388
24.7	3.329	20.6	3.176
47.3	3.965	63.4	4.226
78.6	4.417	99.2	4.598
111.4	4.708	136.1	4.839
150.5	4.925	175.6	5.014 (1.8.74)
199.1	5.100		
248.1	5.218 (1.7.74)		
	T = 260.2 K		
1.0	1.837	0.9	1.796
5.2	3.408	2.8	2.832
15.6	4.422	10.8	4.110
40.8	5.236	22.9	4.755
82.8	5.738	55.5	5.460
126.7	6.015	103.1	5.863
172.5	6.225 (12.12.73)	154.3	6.124
		198.1	6.306 (12.13.73)
	T = 212.7 K		
0.1	1.859	0.1	1.857
0.5	3.695	0.5	3.688
3.6	5.346	1.9	4.850
15.7	6.370	10.7	6.126
34.7	7.010	29.0	6.827
45.0	7.317 (11.30.73)	42.4	7.202 (12.3.73)
0.1	1.869		
0.2	2.960		
1.6	4.721		
6.9	5.844		
20.4	6.563		
43.0	7.254 (12.10.73)		

Reproduced with permission of the copyright owner. Further reproduction prohibited without permission.

Table 10. Ethylene Isotherms, Gibbs Definition

P, psia	n_o, mg-mol/gC		P, psia	n_o, mg-mol/gC	
		T = 301.4 K			
6.0	1.576		2.5	0.949	
16.9	2.570		11.9	2.227	
40.3	3.514		22.8	2.905	
74.0	4.138		63.2	3.988	
109.0	4.530		97.2	4.422	
149.2	4.822		134.8	4.732	
198.1	5.070		172.3	4.945	
246.0	5.247	(1.11.74)	205.8	5.096	(1.14.74)
		T = 260.2 K			
1.5	1.765		1.5	1.780	
6.8	3.229		4.1	2.727	
16.7	4.170		13.0	3.929	
39.6	5.046		29.6	4.782	
80.1	5.696		58.2	5.430	
124.5	6.058		102.9	5.930	
176.3	6.306		154.0	6.228	(12.17.73)
230.5	6.468	(12.14.73)			
		T = 212.7 K			
0.1	1.895		0.2	1.862	
1.0	3.727		0.6	3.010	
5.1	5.327		2.8	4.736	
15.4	6.346		10.6	5.996	
34.4	7.008		22.1	6.645	
60.7	7.488		40.2	7.102	
87.0	7.884	(12.6.73)	70.0	7.605	(12.7.73)
0.1	1.884				
0.8	3.721				
4.4	5.348				
14.3	6.437				
34.7	7.158				
61.3	7.640				
87.4	8.041	(6.26.74)			

Reproduced with permission of the copyright owner. Further reproduction prohibited without permission.

Table 11. Carbon Dioxide Isotherms, Gibbs Definition

P, psia	n_o, mg-mol/gC		P, psia	n_o, mg-mol/gC	
		T = 301.4 K			
11.3	1.190		11.6	1.210	
21.7	1.870		22.0	1.887	
40.5	2.783		36.6	2.621	
67.9	3.700		60.6	3.487	
101.3	4.468		91.4	4.272	
142.1	5.133		130.2	4.972	
183.9	5.634		173.1	5.525	(11.29.73)
230.2	6.052	(11.28.73)			
94.3	4.369				
169.9	5.514				
204.7	5.897				
247.5	6.204				
295.9	6.538				
349.3	6.778				
401.2	6.989				
452.1	7.162				
505.0	7.348				
557.0	7.379	(1.16.74)			
		T = 260.2 K			
4.2	1.608		14.6	3.453	
10.6	2.886		28.9	4.819	
17.7	3.818		66.7	6.600	
29.5	4.877		117.3	7.723	
50.0	6.002		166.4	8.290	
84.0	7.091		197.7	8.550	(1.3.74)
140.0	8.018				
219.3	8.712	(12.20.73)			
		T = 212.7 K			
0.5	1.826		0.5	1.829	
1.5	3.569		1.1	3.040	
3.4	5.219		2.6	4.736	
6.6	6.706		5.3	6.264	
11.2	7.945		9.4	7.626	(11.21.73)
27.6	9.535	(11.19.73)			
0.5	1.824		0.5	1.889	
1.3	3.266		1.7	3.698	
2.9	4.925		3.8	5.406	
5.7	6.441		7.3	6.921	
10.0	7.752	(11.26.73)	26.2	9.442	(1.23.74)

Reproduced with permission of the copyright owner. Further reproduction prohibited without permission.

Binary and Ternary Gas Mixture Isotherms

In the following tables the gas phase composition is given in parenthesis in mole percent. The equilibrium pressure, P, is expressed in pounds per square inch absolute. The amount of component i adsorbed, n_i, is expressed in milligram-mole per gram of adsorbent. The mole fractions of adsorbate i, x_i, are tabulated as defined by equation (47). The relative volatility, α', as defined for binary and ternary mixtures by equation (86), is presented in the last column. The entire set of binary and ternary adsorption measurements was determined between March 13 and June 19, 1974.

The amounts of gas adsorbed were calculated with computer program MISOTH which is briefly described in Appendix L.

The uncertainty in the pressure given in these tables is within ± 0.5 psia between 15 and 300 psia, and ± 1.5 psia between 300 and 450 psia (see Appendix C). The uncertainty in the number of moles given in the same tables is thought to be within about ± 0.003 and 0.20 mg-mol/gC, depending on the component and the pressure level (see Chapter III). It is recognized that the values presented in these tables are carried, in general, with more significant figures than suggested by the uncertainties given above.

NOTE

To convert from psia to kN/m^2 multiply by 6.8947572.

The unit of mg-mol is equivalent to μkg-mol in the SI system.

Reproduced with permission of the copyright owner. Further reproduction prohibited without permission.

Table 12. Methane-Ethane Isotherms, Gibbs Definition

P, psia	n_1	n_2 mg-mol/gC	n_T	x_1	x_2	α'_{12}
		Methane(1)-Ethane(2)/(26.7-73.3 mol%)				
		T = 301.4 K				
290.9	0.743	5.068	5.811	0.128	0.872	2.49
179.0	0.555	4.708	5.263	0.106	0.894	3.09
99.3	0.337	4.183	4.520	0.075	0.925	4.52
50.9	0.225	3.683	3.908	0.058	0.942	5.98
18.8	0.076	2.817	2.893	0.026	0.974	13.46
		T = 212.7 K				
51.2	0.229	7.011	7.240	0.032	0.968	11.14
35.4	0.174	6.563	6.737	0.026	0.974	13.75
18.9	0.077	6.356	6.433	0.012	0.988	29.91
		Methane(1)-Ethane(2)/(49.9-50.1 mol%)				
		T = 301.4 K				
200.9	1.124	4.301	5.425	0.207	0.793	3.81
100.5	0.574	3.738	4.312	0.133	0.867	6.48
49.9	0.385	3.206	3.591	0.107	0.893	8.30
19.1	0.183	2.413	2.596	0.071	0.929	13.13
		T = 212.7 K				
100.8	0.563	7.276	7.839	0.072	0.928	12.88
50.4	0.388	6.522	6.910	0.056	0.944	16.72
19.1	0.193	5.935	6.128	0.032	0.968	30.60
		Methane(1)-Ethane(2)/(74.5-25.5 mol%)				
		T = 301.4 K				
199.2	1.388	3.292	4.680	0.296	0.704	6.94
199.9	1.365	3.321	4.686	0.291	0.709	7.12
99.7	0.945	2.871	3.816	0.248	0.752	8.90
50.7	0.656	2.400	3.056	0.215	0.785	10.70
18.8	0.333	1.661	1.994	0.167	0.833	14.60
		T = 260.2 K				
136.5	1.128	4.466	5.594	0.202	0.798	11.58
59.7	0.787	3.889	4.676	0.168	0.832	14.46
18.1	0.434	3.054	3.488	0.125	0.875	20.58

Reproduced with permission of the copyright owner. Further reproduction prohibited without permission.

Table 12. (Continued)

P, psia	n_1	n_2 mg-mol/gC	n_T	x_1	x_2	α'_{12}
		T = 212.7 K				
126.9	1.032	6.198	7.230	0.143	0.857	17.57
63.3	0.723	5.943	6.666	0.109	0.891	24.05
19.1	0.430	5.256	5.686	0.076	0.924	35.75

Reproduced with permission of the copyright owner. Further reproduction prohibited without permission.

Table 13. Methane-Ethylene Isotherms, Gibbs Definition

P, psia	n_1	n_3	n_T	x_1	x_3	α'_{13}
		mg-mol/gC				
		Methane(1)-Ethylene(3)/(26.0-74.0 mol%)				
		T = 301.4 K				
290.2	0.626	5.105	5.731	0.109	0.891	2.86
177.8	0.450	4.686	5.136	0.088	0.912	3.65
99.0	0.345	4.003	4.348	0.079	0.921	4.06
50.0	0.246	3.358	3.604	0.068	0.932	4.78
19.0	0.087	2.366	2.453	0.036	0.964	9.49
		T = 212.7 K				
98.7	0.297	7.619	7.916	0.038	0.962	9.00
60.1	0.227	7.080	7.307	0.031	0.969	10.93
34.9	0.189	6.593	6.782	0.028	0.972	12.22
19.7	0.108	6.230	6.338	0.017	0.983	20.32
		Methane(1)-Ethylene(3)/(53.6-46.4 mol%)				
		T = 301.4 K				
294.6	1.331	4.060	5.391	0.247	0.753	3.53
179.9	1.002	3.776	4.778	0.210	0.790	4.36
98.1	0.686	3.248	3.934	0.174	0.826	5.48
49.9	0.488	2.689	3.177	0.154	0.846	6.37
17.7	0.217	1.836	2.053	0.106	0.894	9.79
		T = 212.7 K				
151.0	0.898	7.179	8.077	0.111	0.889	9.25
151.4	0.851	7.185	8.036	0.106	0.894	9.76
89.3	0.663	6.691	7.354	0.090	0.910	11.68
		Methane(1)-Ethylene(3)/(53.4-46.6 mol%)				
		T = 301.4 K				
75.3	0.637	3.150	3.787	0.168	0.832	5.66
		T = 212.7 K				
105.2	0.747	6.875	7.622	0.098	0.902	10.55
46.4	0.505	6.413	6.918	0.073	0.927	14.56

Reproduced with permission of the copyright owner. Further reproduction prohibited without permission.

Table 13. (Continued)

P, psia	n_1	n_3 mg-mol/gC	n_T	x_1	x_3	α'_{13}
		Methane(1)-Ethylene(3)/(76.5-23.5 mol%)				
		T = 301.4 K				
207.5	1.757	2.770	4.527	0.388	0.612	5.12
100.6	1.188	2.349	3.537	0.336	0.664	6.42
101.1	1.206	2.367	3.573	0.338	0.662	6.38
64.3	0.925	2.069	2.994	0.309	0.691	7.26
18.7	0.422	1.294	1.716	0.246	0.754	9.96
		T = 260.2 K				
204.7	1.920	4.015	5.935	0.324	0.676	6.79
99.2	1.334	3.654	4.988	0.267	0.733	8.90
99.2	1.346	3.639	4.985	0.270	0.730	8.79
50.8	1.059	3.176	4.235	0.250	0.750	9.74
21.1	0.669	2.548	3.217	0.208	0.792	12.37
		T = 212.7 K				
130.0	1.443	5.921	7.364	0.196	0.804	13.33
64.0	1.158	5.496	6.654	0.174	0.826	15.42
64.2	1.172	5.497	6.669	0.176	0.824	15.23
19.7	0.748	4.720	5.468	0.137	0.863	20.49

Reproduced with permission of the copyright owner. Further reproduction prohibited without permission.

Table 14. Ethane-Ethylene Isotherms, Gibbs Definition

P, psia	n_2	n_3	n_T	x_2	x_3	α'_{32}
		mg-mol/gC				
		Ethane(2)-Ethylene(3)/(24.0-76 mol%)				
		T = 301.4 K				
287.4	1.618	4.320	5.938	0.272	0.728	1.19
194.5	1.479	3.899	5.378	0.275	0.725	1.20
106.9	1.351	3.368	4.719	0.286	0.714	1.27
44.7	1.118	2.731	3.849	0.290	0.710	1.30
20.0	0.839	2.149	2.988	0.281	0.719	1.24
		T = 212.7 K				
58.8	2.530	5.254	7.784	0.325	0.675	1.53
32.5	2.361	4.733	7.094	0.333	0.667	1.58
20.3	2.328	4.404	6.732	0.346	0.654	1.68
		Ethane(2)-Ethylene(3)/(47.2-52.8 mol%)				
		T = 301.4 K				
164.3	2.866	2.514	5.380	0.533	0.467	1.28
79.7	2.532	2.050	4.582	0.553	0.447	1.38
31.6	2.008	1.585	3.593	0.559	0.441	1.42
		Ethane(2)-Ethylene(3)/(68.2-31.8 mol%)				
		T = 301.4 K				
198.4	4.077	1.529	5.606	0.727	0.273	1.24
100.5	3.632	1.238	4.870	0.746	0.254	1.37
50.2	3.048	1.028	4.076	0.748	0.252	1.38
20.9	2.489	0.778	3.267	0.762	0.238	1.49
		T = 212.7 K				
49.8	5.816	1.698	7.514	0.774	0.226	1.60
34.9	5.600	1.588	7.188	0.779	0.221	1.64
19.9	5.270	1.405	6.675	0.790	0.210	1.75

Reproduced with permission of the copyright owner. Further reproduction prohibited without permission.

Table 15. Methane-Ethane-Ethylene Isotherms, Gibbs Definition

P, psia	n_1	n_2 mg-mol/gC	n_3	n_T	x_1	x_2	x_3	α'_{12}
Methane(1)-Ethane(2)-Ethylene(3)/(62.4-17.4-20.2 mol%)								
			T = 301.4 K					
431.2	1.744	2.205	1.955	5.904	0.295	0.374	0.331	4.53
301.8	1.963	2.179	1.862	6.004	0.327	0.363	0.310	3.97
147.2	0.969	1.948	1.564	4.481	0.216	0.435	0.349	7.20
49.2	0.492	1.482	1.185	3.159	0.156	0.469	0.375	10.77
			T = 212.7 K					
163.0	1.038	3.970	3.014	8.022	0.129	0.495	0.376	13.69
51.4	0.566	3.752	2.467	6.785	0.083	0.553	0.364	23.74
Methane(1)-Ethane(2)-Ethylene(3)/(23.0-52.0-25.0 mol%)								
			T = 301.4 K					
302.3	0.765	3.858	1.475	6.098	0.126	0.633	0.241	2.23
177.0	0.485	3.530	1.193	5.208	0.093	0.678	0.229	3.22
100.3	0.356	3.135	1.043	4.534	0.079	0.691	0.230	3.89
49.6	0.211	2.804	0.882	3.897	0.054	0.720	0.226	5.88
19.1	0.058	2.090	0.651	2.799	0.021	0.747	0.232	15.90
			T = 212.7 K					
70.8	0.265	5.716	1.654	7.635	0.035	0.749	0.216	9.55
40.2	0.179	5.359	1.469	7.007	0.026	0.765	0.209	13.25
19.2	0.057	5.015	1.319	6.391	0.009	0.785	0.206	38.77
Methane(1)-Ethane(2)-Ethylene(3)/(20.0-19.2-60.8 mol%)								
			T = 301.4 K					
300.6	0.687	1.464	4.079	6.230	0.110	0.235	0.655	2.22
180.1	0.482	1.305	3.430	5.217	0.093	0.250	0.657	2.82
100.3	0.336	1.199	2.995	4.530	0.074	0.265	0.661	3.72
51.5	0.182	1.074	2.527	3.783	0.048	0.284	0.668	6.16
18.0	0.049	0.718	1.816	2.583	0.019	0.278	0.703	15.36
			T = 212.7 K					
71.3	0.238	2.447	4.865	7.550	0.032	0.324	0.644	10.72
40.0	0.165	2.361	4.485	7.011	0.024	0.337	0.639	14.88
18.2	0.052	2.250	4.048	6.350	0.008	0.354	0.638	45.42

Reproduced with permission of the copyright owner. Further reproduction prohibited without permission.

Table 16. Summary of Binary Reproducibility Measurements

Gas Mixture, T, and Composition	P, psia	n_i, mg-mol/gC			Deviation, %		
		CH_4	C_2H_6	C_2H_4	CH_4	C_2H_6	C_2H_4
CH_4-C_2H_4, 212.7 K	151.4	0.851	-	7.185	-5.5	-	+0.1
(53.6-46.4 mol%)	151.0	0.898	-	7.179			
CH_4-C_2H_4, 212.7 K	46.4	0.515	-	6.420	+1.9	-	+0.1
(53.4-46.6 mol%)	46.0	0.505	-	6.413			
CH_4-C_2H_4, 212.7 K	64.2	1.172	-	5.497	+1.2	-	0.0
(76.5-23.5 mol%)	64.0	1.158	-	5.496			
CH_4-C_2H_4, 260.2 K	99.2	1.334	-	3.654	-0.9	-	+0.4
(76.5-23.5 mol%)	99.2	1.346	-	3.639			
CH_4-C_2H_4, 301.4 K	101.1	1.206	-	2.367	+1.5	-	+0.8
(76.5-23.5 mol%)	100.6	1.188	-	2.349			
CH_4-C_2H_6, 301.4 K	199.9	1.365	3.321	-	-1.7	+0.9	
(74.5-25.5 mol%)	199.2	1.388	3.292	-			

NOTE

Deviations in this table are given with respect to n_i at the highest pressure.

Reproduced with permission of the copyright owner. Further reproduction prohibited without permission.

Kinetic Data

The kinetic results presented in the following figures were obtained by measuring the effluent gas composition as a function of time. Initially, the adsorption cell was maintained under vacuum condition. The gas mixture was then admitted to the adsorption space, the flow rate being established in about five minutes. The first analysis was made as soon as the flow rate became stable, which required about 2-5 minutes. The analysis of the effluent gas stream was then recorded as a function of time until equilibrium was reached, i.e., when the inlet and exit streams reached the same composition (see Chapter II). The time scale zero in these figures corresponds to the instant when the gas mixture was admitted into the adsorption system.

These kinetic data are considered to be approximate and are presented for qualitative analysis purposes only.

Reproduced with permission of the copyright owner. Further reproduction prohibited without permission.

Reproduced with permission of the copyright owner. Further reproduction prohibited without permission.

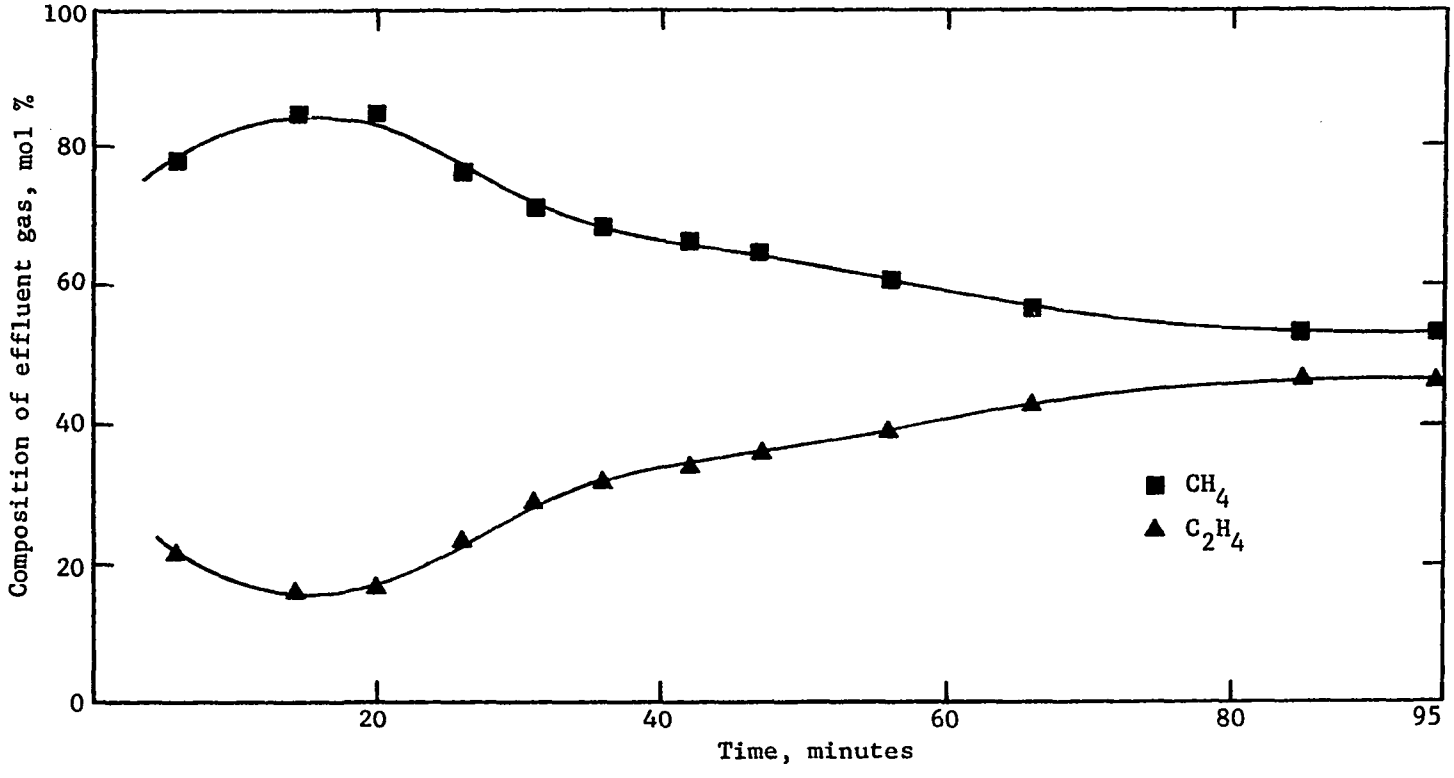

Figure 30. Kinetic Data for Methane-Ethylene (53.6-46.4 mol %) Mixture at 212.7 K and 140 psia

Reproduced with permission of the copyright owner. Further reproduction prohibited without permission.

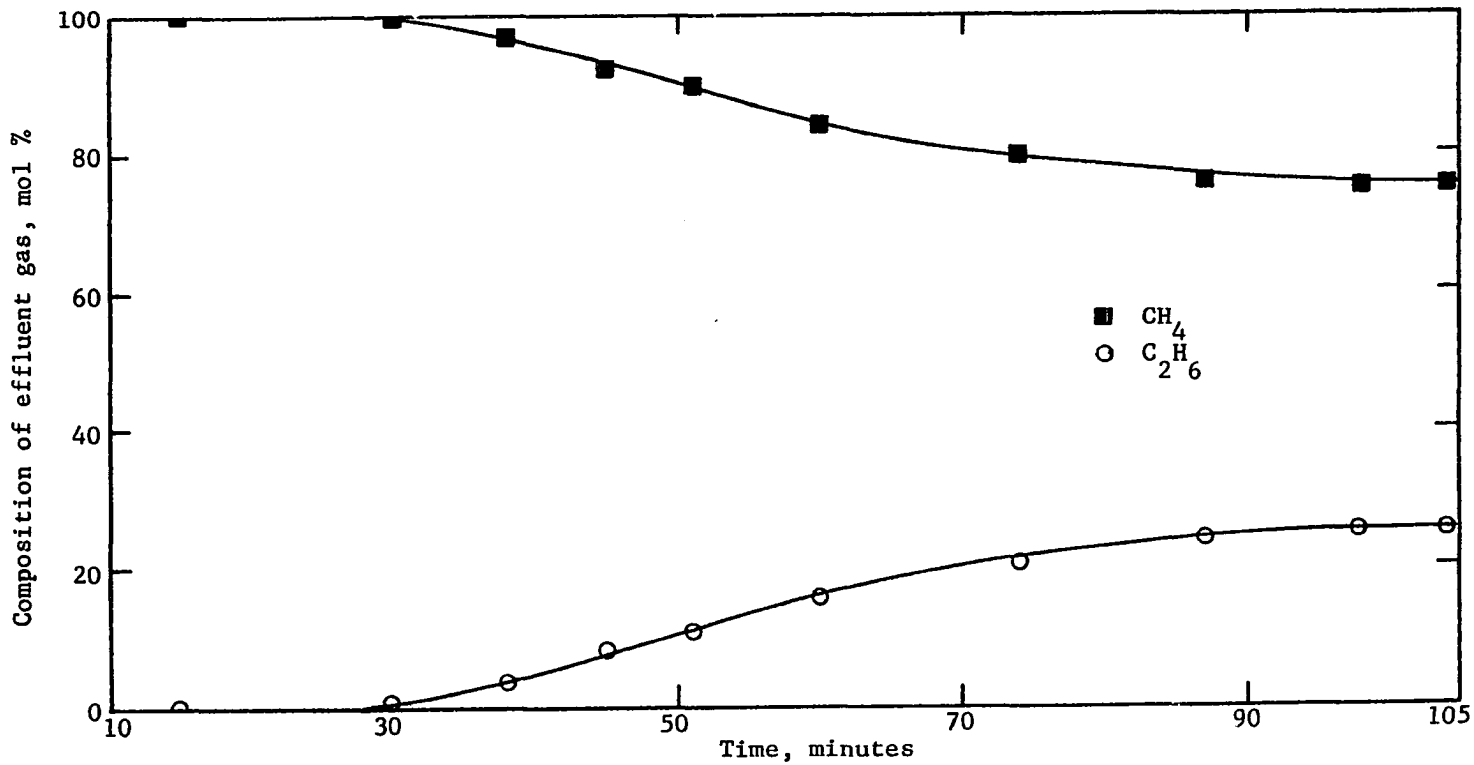

Figure 31. Kinetic Data for Methane-Ethane (74.5-25.5 mol %) Mixture at 212.7 K and 65 psia

Reproduced with permission of the copyright owner. Further reproduction prohibited without permission.

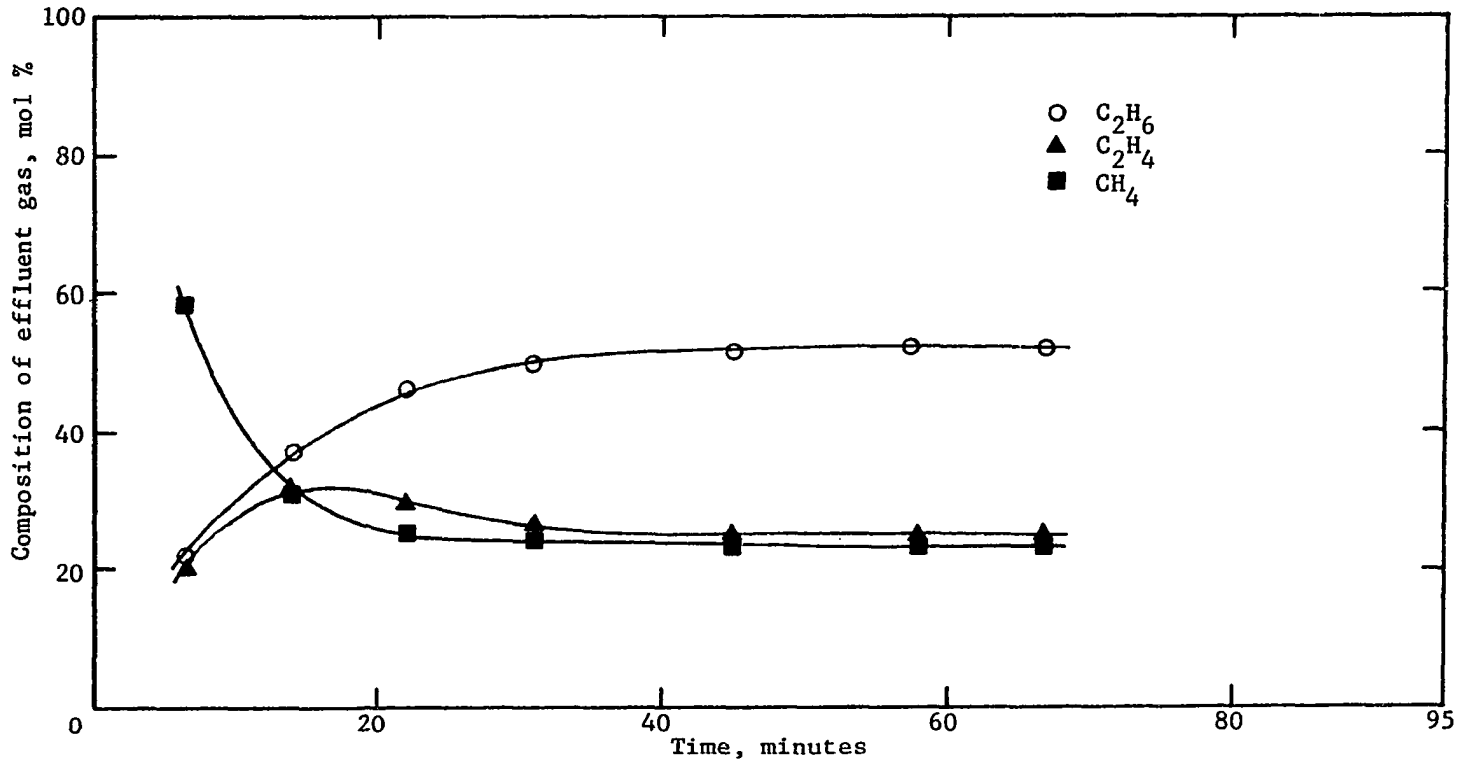

Figure 32. Kinetic Data for Methane-Ethane-Ethylene (52.0-23.0-25.0 mol %) Mixture at 212.7 K and 40 psia

APPENDIX H

ERROR ANALYSIS

Pure Gas Isotherms

Equation (1) in Chapter III describes the number of moles adsorbed by the solid adsorbent at each point on the isotherm

$$n_o' = \sum_{j=1}^{k} \left(\frac{PV}{ZRT}\right)_j^{\text{added}} - \frac{P}{R} \sum_{i=1}^{r} \left(\frac{V^o}{ZT}\right)_i \tag{92}$$

or

$$n_o' = \sum_{j=1}^{k} n_{oj}^{\text{added}} - n_o^o \tag{93}$$

where n_o^o is the number of moles in the void space represented by $\{V_i^o\}$, P, and $\{T_i\}$.

As

$$n_o = PV/(ZRT) \tag{94}$$

represents the number of moles of a pure gas in a known volume at T and P, the maximum relative error, %, anticipated in the measurement of n_o is

Reproduced with permission of the copyright owner. Further reproduction prohibited without permission.

given by

$$\frac{\Delta n_o}{n_o} 100 = \left\{\left(\frac{\partial n_o}{\partial P}\right)_{VTZ} \Delta P + \left(\frac{\partial n_o}{\partial V}\right)_{PTZ} \Delta V + \left(\frac{\partial n_o}{\partial Z}\right)_{PTV} \Delta Z + \left(\frac{\partial n_o}{\partial T}\right)_{PVZ} \Delta T\right\} \frac{100}{n_o} \tag{95}$$

Evaluating the partial derivatives by using relation (1) and taking the absolute values gives

$$\frac{\Delta n_o}{n_o} 100 = \frac{100}{n_o} \left\{\frac{\Delta P}{P} + \frac{\Delta V}{V} + \frac{\Delta Z}{Z} + \frac{\Delta T}{T}\right\} \tag{96}$$

The assignment of accuracies to each of the measurements led to the following values in equation (96):

$$\frac{\Delta P}{P} \cong 0.007 \tag{97}$$

$$\frac{\Delta V}{V} \cong 0.01$$

$$\frac{\Delta Z}{Z} \cong 0.005$$

$$\frac{\Delta T}{T} \cong 0.0002$$

If equations (96) and (97) are applied to the amount added and to the amount of gas remaining at equilibrium in the void space

$$\frac{\Delta n_{oj}^{added}}{n_{oj}^{added}} \cong 0.04 \tag{98}$$

Reproduced with permission of the copyright owner. Further reproduction prohibited without permission.

$$\frac{\Delta n_o^o}{n_o^o} \cong 0.02$$

The maximum relative error, %, anticipated in the amount adsorbed is given approximately by

$$\frac{\Delta n_o'}{n_o'} 100 = 4 \sum_{j=1}^{k} \frac{n_{oj}^{added}}{n_o'} + 2 \frac{n_o^o}{n_o'} \qquad (99)$$

The 301.4 K methane isotherm (see Table 8 in Appendix G) will be used to illustrate the magnitude of these terms. As n_o' is much larger for the other gases in this study, smaller errors can be expected in their adsorption capacities.

Table 17. Error Analysis of Methane Isotherm at 301.4 K

P, psia	n_o'	$\sum_{j=1}^{k} n_{oj}^{added}$	n_o^o	$\frac{n_o' 100}{n_o'}$
		mg-mol/gC		
19.1	24.6	30.5	5.9	5.4
39.8	41.8	54.1	12.3	5.8
67.8	58.3	79.3	21.0	6.2
98.3	71.8	102.3	30.5	6.5
129.8	82.5	122.9	40.4	6.9
168.6	93.2	146.0	52.8	7.4
209.4	102.2	168.1	65.9	7.9
249.3	109.3	188.1	78.8	8.3

Reproduced with permission of the copyright owner. Further reproduction prohibited without permission.

Thus, at 250 psia it would be possible for the data to be 8.3% in error. This is improbable, however, because for this to happen all of the terms in the summation and n_o^o in equation (93) would have to be in maximum error and all in the same direction. In all probability a cancellation of errors would greatly reduce those appearing in the table.

Mixture Gas Isotherms

The adsorbed amount for a certain component i in an adsorbate mixture, at each point of the isotherm, is given by equation (3) in Chapter III

$$n_i' = (n_i)_{system} - \frac{y_i P}{R} \sum_{j=1}^{r} \left(\frac{V^o}{Z_m T}\right)_j \tag{100}$$

or

$$n_i' = (n_i)_{system} - n_i^o \tag{101}$$

where n_i^o is the moles of i in the void space at T, P, $\{y_i\}$, and V^o.

If equation (96) is applied to

$$n_i = y_i PV^o/(ZRT) \tag{102}$$

it is possible to obtain, that

$$\frac{\Delta(n_i)_{system}}{(n_i)_{system}} \cong 0.06 \tag{103}$$

Reproduced with permission of the copyright owner. Further reproduction prohibited without permission.

$$\frac{\Delta n_i^o}{n_i^o} \cong 0.07$$

where

$$\frac{\Delta y_i}{y_i} \cong 0.05 \tag{104}$$

The maximum relative error, %, anticipated in the amount adsorbed of component i is given then by

$$\frac{\Delta n_i'}{n_i'} 100 = 6\frac{(n_i)_{system}}{n_i'} + 7\frac{n_i^o}{n_i'} \tag{105}$$

The methane-ethane (49.9-50.1 mol%) isotherm at 301.4 K (see Table 12 in Appendix G) will be used to show the magnitude of these terms.

Table 18. Error Analysis of Methane-Ethane (49.9-50.1 mol%) Isotherm at 301.4 K

P, psia	n_i'		$(n_i)_{system}$		n_i^o		$\frac{\Delta n_i'}{n_i'} 100$	
	CH_4	C_2H_6	CH_4	C_2H_6	CH_4	C_2H_6	CH_4	C_2H_6
	mg-mol/gC							
200.9	36.2	138.4	79.3	181.8	43.1	43.4	21	10
100.5	18.5	120.3	39.4	141.3	20.9	21.0	20	7.9
49.9	12.4	103.2	22.6	113.5	10.2	10.3	16	7.0
19.1	5.9	77.7	8.8	80.6	2.9	2.9	12	6.2

Reproduced with permission of the copyright owner. Further reproduction prohibited without permission.

A cancellation of errors will probably reduce significantly those appearing in the table.

Reproduced with permission of the copyright owner. Further reproduction prohibited without permission.

APPENDIX I

SUMMARY OF MODIFICATIONS TO THE POTENTIAL THEORY OF ADSORPTION APPLIED TO PURE GASES

In the following table a summary of different modifications of the Polanyi Potential Theory applied to pure gas adsorption is presented. The table is self explanatory. The reader is referred to the discussion in Chapter IV.

Reproduced with permission of the copyright owner. Further reproduction prohibited without permission.

Reproduced with permission of the copyright owner. Further reproduction prohibited without permission.

Table 19. Summary of Modifications to the Potential Theory of Adsorption Applied to Pure Gases

Author	Correlation	$\tilde{V}_a$ from	$\tilde{V}_a''$ from	p_s from	Remarks
Polanyi-Berenyi (4,5,41)	$n_o\tilde{V}_a$ vs. $RT\ln[p_s(T)/P]$	$\tilde{V}_a = \tilde{V}_s(T)$ $T \ll T_c$ $\tilde{V}_a = b^*$ $T > T_c$ as first approx.	-	$p_s = p_s(T)$ $T < T_c$ $0.14T/b$ $T > T_c$	Requires lengthy trial-error procedure
Dubinin, et al. (11,15,17, 18,21,37, 54)	$n_o\tilde{V}_a$ vs. $\frac{RT}{\tilde{V}_a''}\ln[p_s(T)/P]$	$\tilde{V}_a = \tilde{V}_s(T)$ $T \le T_{nbp}$ $\tilde{V}_a'' = \tilde{V}_a(T)$ Linear relation $\tilde{V}_a = \tilde{V}(T)$ between $\tilde{V}_a = \tilde{V}_s(T_{nbp})$ @T_{nbp} $\tilde{V}_a = b$ @T_c $\tilde{V}_a = b$ $T > T_c$		$p_s = p_s(T)$ $T \le T_c$ $p_s = T_R^2 P_c$ $T > T_c$	Not applicable at $P > T_R^2 P_c$
Lewis, et al. (30)	$n_o\tilde{V}_a$ vs. $\frac{RT}{\tilde{V}_a''}\ln\left\{\frac{f_s(p_s,T)}{f(P,T)}\right\}$	$\tilde{V}_a = \tilde{V}_s(p_s = P)$	$\tilde{V}_a'' = \tilde{V}_a$	$p_s = p_s(T)$ $T \le T_c$ extrapolation Antoine equation for $T > T_c$	Not recommended at $P < 100$ mm Hg Not applicable much above T_c or $P > P_c$
Maslan, et al. (33)	$n_o\tilde{V}_a$ vs. $\frac{RT}{\tilde{V}_a''}\ln\left\{\frac{f_s(p_s,T)}{f(P,T)}\right\}$	$\tilde{V}_a = \tilde{V}$ of compressed gas at Z, $p_s(T)$, T	$\tilde{V}_a'' = \tilde{V}_a$	$p_s = p_s(T)$ $T \le T_c$ extrapolation Antoine equation at $T > T_c$	Not applicable to liquid-like adsorbates

Reproduced with permission of the copyright owner. Further reproduction prohibited without permission.

Table 19. (Continued)

Author	Correlation	$\tilde{V}_a$ from	$\tilde{V}''_a$ from	p_s from	Remarks
Grant-Manes (23,24)	$n_o\tilde{V}_a$ vs. $\frac{RT}{\tilde{V}''_a}\ln\left\{\frac{f_s(p_s,T)}{f(P,T)}\right\}$	$\tilde{V}_a = \tilde{V}_s(p_s = P)$	$\tilde{V}''_a = \tilde{V}_s(T_{nbp})$	$p_s = p_s(T)$ $T \leq T_c$ extrapolation $\ln p_s = A + B/T$ @ $T > T_c$	Not applicable at $P > P_c$
Cook-Basmadjian (12)	$n_o^a\tilde{V}_a$ vs. $\frac{RT}{\tilde{V}''_a}\ln\left\{\frac{f_s(p_s,T)}{f(P,T)}\right\}$	$\tilde{V}_a = \tilde{V}_s(T)$ $T < T_{nbp}$ tangent to $\ln\tilde{V}_s$ vs. lnT at $T > T_{nbp}$	$\tilde{V}''_a = \tilde{V}_a$	$p_s = p_s(T)$ $T < T_{nbp}$ p_s from V_a,T,Z for $T > T_{nbp}$	Does not yield a single correlation curve
Hasz-Barrer (26)	$n_o\tilde{V}_a$ vs. $\frac{RT\phi'}{\tilde{V}''_a}\ln\left\{\frac{f_s(p_s,T)}{f(P,T)}\right\}$	same as Cook, et al.[12] $\phi' = \phi'(T)$ empirical		$p_s = p_s(T)$ $T \leq T_c$ $\ln p_s = A + B/T$ extrapolation at $T > T_c$	
Rogers (47)	$n_o\tilde{V}_a$ vs. $\frac{RT}{\tilde{V}''_a}\ln\left\{\frac{f_s(p_s,T)}{f(P,T)}\right\}$	$\tilde{V}_a = \tilde{V}_s(T_{nbp})$ all T	$\tilde{V}''_a = \tilde{V}_s(T_{nbp})$	$p_s = p_s(T)$ $T \leq T_c$ extrapolation $\ln p_s = A + B/T$ at $T > T_c$	

Reproduced with permission of the copyright owner. Further reproduction prohibited without permission.

Table 19. (Continued)

Author	Correlation	$\tilde{V}_a$ from	$\tilde{V}_a''$ from	p_s from	Remarks
Reich (This Work)	$n_o^a \tilde{V}_a$ vs. $\frac{RT}{\tilde{V}_a''} \ln\left\{\frac{f_s(p_s,T)}{f(P,T)}\right\}$	$\tilde{V}_a = \tilde{V}_s(T)$ $T \leq T_{nbp}$ Linear relation $\tilde{V}_a = \tilde{V}_a(T)$ between $\tilde{V}_a = \tilde{V}_s(T_{nbp})$ @T_{nbp} $\tilde{V}_a = b$ @T_c $\tilde{V}_a = b^*$ $T > T_c$	$\tilde{V}_a'' = \tilde{V}_s(T_{nbp})$	$p_s = p_s(T)$ from $\ln p_s = A + B/T$ at all T A,B evaluated at T_{nbp} and T_c	

*b = constant in the van der Waals equation of state = $RT_c/(8P_c)$

APPENDIX J

INCONSISTENCY IN THE USE OF THE POTENTIAL THEORY APPLIED TO MIXTURES

Sircar and Myers[48] have recently pointed out that the extension of the Polanyi-Dubinin Potential Theory to mixtures[25,29,33] is correct only when the surface potential of the pure adsorbates, as defined by Berenyi, et al.[8] and discussed in Chapter IV, are equal in the state of saturated vapor.

In the Grant and Manes[25] model for mixture adsorption prediction, a standard state is selected where the pure adsorbate is at the same volume as that of the adsorbate mixture, $\hat{V}_{am}$. This standard state may be evaluated from the potential theory characteristic curve for the pure adsorbates-adsorbent system

$$e = F(\hat{V}_a) = \frac{RT}{\tilde{V}'_a} \ln(p_s(T)/P) \tag{106}$$

(valid at low pressures) and

$$\hat{V}_a = n_o \tilde{V}_a \tag{107}$$

where

$$\tilde{V}'_a = \tilde{V}_s(T_{nbp})^{25,\text{This Work}} \tag{108}$$

$$\tilde{V}'_a = \tilde{V}_s(p_s = P)^{29,33}$$

Reproduced with permission of the copyright owner. Further reproduction prohibited without permission.

$$\tilde{V}_a = \tilde{V}_s(T)^{\text{This Work}}$$

$$\tilde{V}_a = \tilde{V}_s(p_s = P)^{25,29,33}$$

depending on the theory modification used (see Appendix I).

If $\tilde{V}_a'$ and $\tilde{V}_a$ selected in this work are used for the purpose of showing the inconsistency, then

$$\varepsilon = F(\hat{V}_a) = \frac{RT}{\tilde{V}_s(T_{nbp})} \ln(p_s(T)/P) \tag{109}$$

$$\hat{V}_a = n_o \tilde{V}_s(T) = \hat{V}_a(P,T) \tag{110}$$

Differentiating equation (109) and using equation (110)

$$d\varepsilon = -\frac{RT}{\tilde{V}_s(T_{nbp})} d\ \ln P \quad = -\frac{n_o RT\ d\ \ln P}{\frac{\hat{V}_a(P,T)}{\tilde{V}_s(T)}\ \tilde{V}_s(T_{nbp})} \tag{111}$$

$$d\varepsilon = -\frac{n_o RT\ d\ \ln P}{\hat{V}_a(P)k}\Bigg|_{T = \text{const.}}$$

where

$$k = \tilde{V}_s(T_{nbp})/\tilde{V}_s(T)$$

Consider the following four states of the adsorbate at the binary system temperature (shown graphically in Figure 33):

Reproduced with permission of the copyright owner. Further reproduction prohibited without permission.

State	x_1	x_2	P	$\hat{V}_a$	
A	1	0	P_1^*	$\hat{V}_{am}$	Standard State
B	0	1	P_2^*	$\hat{V}_{am}$	
C	0	1	P_{s2}	$\hat{V}_{s2}$	
D	1	0	P_{s1}	$\hat{V}_{s1}$	

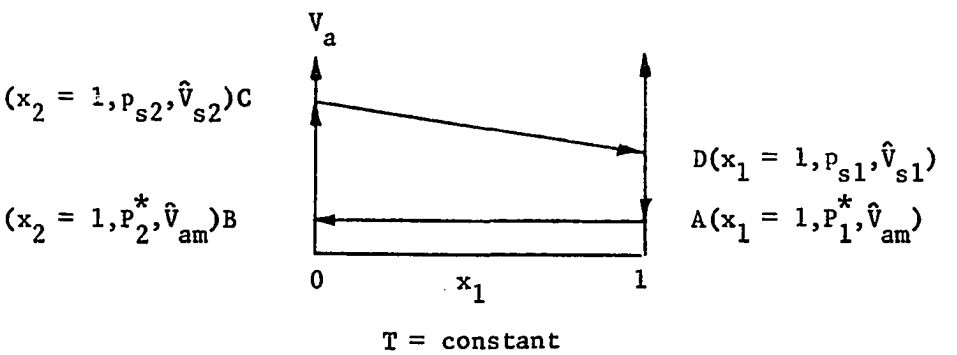

Figure 33. Schematic Representation of States. Binary System

The surface potential, $\emptyset$, may be integrated along these four states by making use of the Gibbs adsorption isotherm[48]

$$- d\emptyset = n_1 \, RT \, d\ln\bar{p}_1 + n_2 \, RT \, d\ln\bar{p}_2 \qquad (112)$$

and equation (111). The result is:

$A \rightarrow B$: As $\hat{V}_a = \hat{V}_{am} = \text{constant}$, from equation (106) $d\epsilon = 0$ and $\epsilon_A = \epsilon_B$

$$\emptyset_B - \emptyset_A = 0 \qquad (113)$$

Reproduced with permission of the copyright owner. Further reproduction prohibited without permission.

$B \rightarrow C$ (pure component 2)

$$\phi_C - \phi_B = \int_{\epsilon_B}^{0} k\hat{V}_a(P)\, d\epsilon \tag{114}$$

$C \rightarrow D$

$$\phi_D - \phi_C = \phi_{s1} - \phi_{s2} \tag{115}$$

$D \rightarrow A$ (pure component 1)

$$\phi_A - \phi_D = \int_{0}^{\epsilon_A = \epsilon_B} k\hat{V}_a(P)\, d\epsilon \tag{116}$$

If relations (113), (114), (115), and (116) are added

$$0 = \phi_{s1} - \phi_{s2} \tag{117}$$

$$\phi_{s1} = \phi_{s2}$$

As the summation of integrals is equivalent to the integration of the Gibbs isotherm around a closed path A→B→C→D→A, equation (117) represents the condition under which this thermodynamic relation is satisfied, i.e., when the surface potentials are equal at saturation. Sircar and Myers[48] have pointed out that this is an incorrect conclusion that can be true only if the composition of the adsorbed phase is equal to the composition of the bulk liquid phase.

Reproduced with permission of the copyright owner. Further reproduction prohibited without permission.

APPENDIX K

CORRELATION RESULTS

Pure Gas Isotherms

In the following table the characteristic curve ordinates, $\hat{V}_a$ and $\epsilon/\tilde{V}_s(T_{nbp})$, are presented in the last columns. The calculations were performed with computer program DUBIN1, which is briefly described in Appendix L, and follow the scheme discussed in Chapter V being represented by equations (15), (21), and (72).

The first three columns represent the experimental adsorption data in terms of absolute,[53] n_o^a, and Gibbs adsorption,[53] n_o (see Chapter V and Appendix G). The absolute adsorption capacities were calculated from Gibbs adsorption data by means of Equations (29), (30), and (76) in Chapter V. The fourth column corresponds to the adsorption capacities calculated from a linear least square fit of the characteristic curve data given in Figure 13 or Table 20. The calculations were carried out with computer program LINFIT which is briefly described in Appendix L. The deviation between columns three and four, in percentage, is given in column five. Units for all the columns are given in the table heading.

NOTE
To convert from psia to kN/m^2 multiply by 6.8947572.
To convert from cal to J multiply by 4.184.
The unit of mg-mol is equivalent to μkg-mol in the SI system.

Reproduced with permission of the copyright owner. Further reproduction prohibited without permission.

Table 20. Characteristic Curve Ordinates for Pure Gases and Calculated Capacities Using Linear Least Squares Fit

P, psia	n_o^a	n_o mg-mol/gC	n_{oc}	D, %	$\hat{V}_a \times 10^3$ cm^3/gC	$\epsilon/\tilde{V}_s(T_{nbp})$ cal/cm^3
			Methane/301.4 K			
19.1	0.765	0.764	-	-	32.7	82.7
39.8	1.304	1.298	-	-	55.7	71.1
67.8	1.825	1.811	-	-	78.0	62.7
98.3	2.256	2.230	1.720	22.9	96.4	56.9
129.8	2.604	2.564	2.285	10.9	111.3	52.5
168.6	2.953	2.894	2.807	3.0	126.2	48.4
209.4	3.256	3.174	3.231	- 1.8	139.2	45.1
249.3	3.501	3.395	3.563	- 4.9	149.6	42.4
			Methane/301.4 K			
10.5	0.478	0.477	-	-	20.4	92.1
26.3	0.969	0.966	-	-	41.4	77.6
57.8	1.655	1.644	-	-	70.7	65.2
87.9	2.120	2.097	1.490	29.0	90.6	58.6
119.4	2.499	2.463	2.116	14.1	106.8	53.8
150.4	2.799	2.748	2.581	6.1	119.6	50.2
192.7	3.137	3.064	3.069	- 0.2	134.1	46.4
230.3	3.378	3.284	3.413	- 3.9	144.4	43.6
			Methane/301.4 K			
126.6	2.600	2.560	2.235	12.7	111.1	52.9
182.9	3.133	3.065	2.969	3.1	133.9	47.2
238.4	3.485	3.385	3.479	- 2.8	149.0	43.1
290.4	3.749	3.617	3.846	- 6.3	160.2	40.0

NOTE

P = pressure, psia

n_o^a = absolute adsorption, mg-mol/gC

n_o = Gibbs adsorption, mg-mol/gC

n_{oc} = calculated Gibbs adsorption using linear fit, mg-mol/gC

$D = (n_o - n_{oc})100/n_o$ = deviation, %

$\hat{V}_a = n_o^a \tilde{V}_s(T)$ = ordinate in characteristic curve, cm^3/gC

$\epsilon/\tilde{V}_s(T_{nbp}) = \frac{RT}{\tilde{V}_s(T_{nbp})} \ln(f_s(p_s,T)/f(P,T))$ = abscissa in characteristic curve, cal/cm^3

Reproduced with permission of the copyright owner. Further reproduction prohibited without permission.

Table 20. (Continued)

P, psia	n_o^a	n_o mg-mol/gC	n_{oc}	D, %	$\hat{V}_a \times 10^3$ cm^3/gC	$\epsilon/\tilde{V}_s(T_{nbp})$ cal/cm^3
343.3	3.973	3.806	4.146	- 9.0	169.8	37.5
396.2	4.177	3.974	4.394	-10.6	178.5	35.3
449.1	4.288	4.049	4.600	-13.6	183.3	33.4
500.0	4.474	4.195	4.770	-13.7	191.2	31.8
555.4	4.569	4.250	4.927	-15.9	195.2	30.2
			Methane/260.2 K			
11.9	1.210	1.207	-	-	51.7	68.5
23.5	1.836	1.830	1.426	22.1	78.5	59.2
43.9	2.577	2.561	2.548	0.5	110.1	50.7
73.2	3.249	3.216	3.452	- 7.4	138.8	43.8
105.7	3.760	3.705	4.086	-10.3	160.7	38.8
145.4	4.211	4.125	4.620	-12.0	180.0	34.6
193.9	4.613	4.487	5.082	-13.3	197.2	30.8
241.5	4.925	4.755	5.416	-13.9	210.5	27.9
			Methane/260.2 K			
6.4	0.794	0.793	-	-	34.0	76.9
18.9	1.623	1.618	-	-	69.4	62.2
35.3	2.308	2.297	2.159	6.0	98.7	53.7
59.4	2.973	2.948	3.086	- 4.7	127.1	46.6
89.7	3.537	3.493	3.806	- 8.9	151.2	41.0
125.1	4.003	3.933	4.371	-11.1	171.1	36.6
169.4	4.430	4.325	4.868	-12.6	189.3	32.5
219.5	4.799	4.649	5.273	-13.4	205.1	29.1
			Methane/260.2 K			
137.6	4.232	4.122	4.529	- 9.9	180.9	35.3
230.4	4.907	4.746	5.346	-12.6	209.7	28.5
293.4	5.281	5.057	5.695	-12.6	225.7	25.4
349.3	5.528	5.246	5.927	-13.0	236.2	23.1
401.2	5.751	5.411	6.097	-12.7	245.8	21.4
452.6	5.906	5.507	6.231	-13.2	252.4	19.8
502.5	6.027	5.570	6.336	-13.8	257.6	18.5
554.9	6.112	5.594	6.425	-14.8	261.2	17.3
			Methane/212.7 K			
3.3	1.671	1.669	1.301	22.0	71.4	60.2
10.5	2.919	2.924	3.012	- 3.4	124.8	47.3
19.5	3.748	3.736	3.930	- 5.2	160.2	40.4
38.7	4.663	4.632	4.923	- 6.3	199.3	32.8
68.8	5.423	5.359	5.730	- 6.9	231.8	26.5
102.8	5.954	5.848	6.265	- 7.1	254.5	22.1
143.0	6.382	6.222	6.677	- 7.3	272.8	18.6
184.8	6.715	6.493	6.971	- 7.4	287.0	15.9
234.2	7.015	6.715	7.213	- 7.4	299.8	13.5

Reproduced with permission of the copyright owner. Further reproduction prohibited without permission.

Table 20. (Continued)

P, psia	n_o^a	n_o mg-mol/gC	n_{oc}	D, %	$\hat{V}_a \times 10^3$ cm^3/gC	$\epsilon/\tilde{V}_s(T_{nbp})$ cal/cm^3
			Methane/212.7 K			
1.7	1.139	1.138	-	-	48.7	67.7
7.7	2.564	2.561	2.548	0.5	109.6	50.8
16.4	3.528	3.518	3.676	- 4.5	150.8	42.3
34.1	4.510	4.484	4.742	- 5.8	192.8	34.2
64.5	5.343	5.284	5.641	- 6.8	228.3	27.2
94.9	5.846	5.750	6.161	- 7.2	249.8	23.0
140.3	6.366	6.209	6.654	- 7.2	272.1	18.8
176.8	6.671	6.461	6.922	- 7.2	285.1	16.4
			Methane/212.7 K			
100.9	6.177	5.944	6.240	- 5.0	264.0	22.3
212.2	7.008	6.738	7.116	- 5.6	299.5	14.5
284.8	7.397	7.003	7.383	- 5.4	316.1	11.5
343.8	7.647	7.141	7.514	- 5.2	326.8	9.6
395.2	7.869	7.256	7.582	- 4.5	336.3	8.3
500.5	8.110	7.261	7.622	- 5.0	346.6	6.1
			Ethane/301.4 K			
4.5	1.627	1.620	1.764	- 8.9	105.0	49.9
14.0	2.756	2.749	2.846	- 3.5	177.9	37.6
24.7	3.344	3.329	3.382	- 1.6	215.9	31.5
47.3	3.999	3.965	3.976	- 0.3	258.2	24.5
78.6	4.482	4.417	4.418	0.0	289.3	19.2
111.4	4.810	4.708	4.702	0.1	310.5	15.6
150.5	5.072	4.925	4.925	0.0	327.4	12.5
199.1	5.311	5.100	5.105	- 0.1	342.8	9.8
248.1	5.499	5.218	5.220	- 0.1	355.0	7.7
			Ethane/301.4 K			
1.8	1.015	1.013	0.888	12.4	65.5	59.9
9.4	2.392	2.388	2.468	- 3.3	154.4	41.9
20.6	3.188	3.176	3.214	- 1.2	205.8	33.4
63.4	4.276	4.226	4.234	- 0.2	276.0	21.4
99.2	4.685	4.598	4.610	- 0.3	302.4	16.8
136.1	4.969	4.839	4.853	- 0.3	320.7	13.5
175.6	5.194	5.014	5.028	- 0.3	335.3	11.0
			Ethane/260.2 K			
1.0	1.838	1.837	1.864	- 1.4	112.4	49.9
5.2	3.411	3.408	3.308	2.9	208.7	34.4
15.6	4.436	4.422	4.251	3.9	271.4	24.2
40.8	5.279	5.236	5.047	3.6	323.0	15.3
82.8	5.839	5.738	5.579	2.8	357.2	9.0
126.7	6.187	6.015	5.850	2.7	378.5	5.4
172.5	6.485	6.225	6.001	3.6	396.8	2.9

Reproduced with permission of the copyright owner. Further reproduction prohibited without permission.

Table 20. (Continued)

P, psia	n_o^a	n_o mg-mol/gC	n_{oc}	D, %	$\hat{V}_a \times 10^3$ cm^3/gC	$\epsilon/\tilde{V}_s(T_{nbp})$ cal/cm^3
			Ethane/260.2 K			
0.9	1.796	1.796	1.799	- 0.2	109.9	50.6
2.8	2.833	2.832	2.763	2.4	173.3	40.3
10.8	4.119	4.110	3.939	4.2	252.0	27.6
22.9	4.776	4.755	4.574	3.8	292.2	20.6
55.5	5.523	5.460	5.287	3.2	337.9	12.6
103.1	5.995	5.863	5.725	2.4	366.8	7.1
154.3	6.346	6.124	5.952	2.8	388.2	3.8
198.1	6.622	6.306	6.049	4.1	405.1	1.8
			Ethane/212.7 K			
0.1	1.859	1.859	1.939	- 4.3	106.5	50.4
0.5	3.696	3.695	3.500	5.3	211.8	34.8
3.6	5.350	5.346	4.947	7.5	306.5	20.2
15.7	6.393	6.370	6.044	5.1	366.3	9.0
34.7	7.068	7.010	6.596	5.9	405.0	3.1
45.0	7.397	7.317	6.763	7.6	423.8	1.3
			Ethane/212.7 K			
0.1	1.857	1.857	1.722	7.3	106.4	52.6
0.5	3.688	3.688	3.475	5.8	211.3	35.0
1.9	4.852	4.850	4.483	7.6	278.0	24.9
10.7	6.141	6.126	5.766	5.9	351.9	11.9
29.0	6.874	6.827	6.477	5.1	393.8	4.4
42.4	7.276	7.202	6.726	6.6	416.9	1.7
			Ethane/212.7 K			
0.1	1.869	1.869	2.006	- 7.3	107.1	49.8
0.2	2.960	2.960	2.830	4.4	169.6	41.5
1.6	4.722	4.721	4.358	7.7	270.6	26.1
6.9	5.853	5.844	5.435	7.0	335.3	15.2
20.4	6.594	6.563	6.232	5.1	377.8	7.0
43.0	7.330	7.254	6.735	7.2	420.0	1.6
			Ethylene/301.4 K			
6.0	1.580	1.576	1.293	18.0	90.9	56.9
16.9	2.577	2.570	2.525	1.7	148.2	44.4
40.3	3.537	3.514	3.542	- 0.8	203.5	34.0
74.0	4.188	4.138	4.230	- 2.2	240.9	26.7
109.0	4.613	4.530	4.647	- 2.6	265.4	22.2
149.2	4.946	4.822	4.964	- 2.9	284.5	18.6
198.1	5.249	5.070	5.225	- 3.1	302.0	15.4
246.0	5.484	5.247	5.403	- 3.0	315.5	13.0

Reproduced with permission of the copyright owner. Further reproduction prohibited without permission.

Table 20. (Continued)

P, psia	n_o^a	n_o mg-mol/gC	n_{oc}	D, %	$\hat{V}_a \times 10^3$ cm^3/gC	$\epsilon/\tilde{V}_s(T_{nbp})$ cal/cm^3
			Ethylene/301.4 K			
2.5	0.950	0.949	-	-	54.7	67.6
11.9	2.231	2.227	2.109	5.3	128.3	48.6
22.8	2.915	2.905	2.875	1.0	167.7	40.8
63.2	4.030	3.988	4.055	- 1.7	231.8	28.6
97.2	4.494	4.422	4.526	- 2.4	258.5	23.5
134.8	4.841	4.732	4.864	- 2.8	278.5	19.7
172.3	5.094	4.945	5.100	- 3.1	293.1	14.9
205.8	5.284	5.096	5.258	- 3.2	304.0	14.9
			Ethylene/260.2 K			
1.5	1.765	1.765	1.408	20.2	98.6	56.1
6.8	3.233	3.229	2.985	7.6	180.6	40.6
16.7	4.183	4.170	3.938	5.6	233.7	31.2
39.6	5.083	5.046	4.826	4.4	284.0	22.3
80.1	5.783	5.696	5.504	3.4	323.1	15.2
124.5	6.207	6.058	5.884	2.9	346.8	10.9
176.3	6.538	6.306	6.139	2.6	365.2	7.6
230.5	6.800	6.468	6.291	2.7	379.9	5.2
			Ethylene/260.2 K			
1.5	1.781	1.780	1.374	22.8	99.5	56.4
4.1	2.729	2.727	2.456	10.0	152.5	45.8
13.0	3.938	3.929	3.675	6.5	220.0	33.8
29.6	4.807	4.782	4.530	5.3	268.6	25.3
58.2	5.489	5.430	5.203	4.2	306.6	18.4
102.9	6.049	5.930	5.726	3.5	337.9	12.7
154.0	6.424	6.228	6.046	2.9	358.8	8.8
			Ethylene/212.7 K			
0.1	1.895	1.895	1.487	21.5	99.4	56.2
1.0	3.728	3.727	3.329	10.7	195.5	39.3
5.1	5.333	5.327	4.887	8.3	279.6	25.0
15.4	6.366	6.346	5.889	7.2	333.7	15.6
34.4	7.060	7.008	6.591	6.0	370.1	8.9
60.7	7.590	7.448	7.043	5.9	397.9	4.3
87.0	8.045	7.884	7.294	7.5	421.8	1.5
			Ethylene/212.7 K			
0.2	1.862	1.862	1.707	8.3	97.6	54.2
0.6	3.010	3.010	2.818	6.4	157.8	44.0
2.8	4.738	4.736	4.340	8.4	248.4	30.0
10.6	6.010	5.996	5.559	7.3	315.1	18.7
22.1	6.676	6.645	6.213	6.5	350.0	12.6
40.2	7.164	7.102	6.720	5.4	375.6	7.6
70.0	7.727	7.605	7.147	6.0	405.1	3.2

Reproduced with permission of the copyright owner. Further reproduction prohibited without permission.

Table 20. (Continued)

P, psia	n_o^a	n_c mg-mol/gC	n_{oc}	D, %	$\hat{V}_a \times 10^3$ cm^3/gC	$\epsilon/\tilde{V}_s(T_{nbp})$ cal/cm^3
			Ethylene/212.7 K			
0.1	1.884	1.884	1.088	42.3	98.8	59.9
0.8	3.721	3.721	3.153	15.3	195.1	40.9
4.4	5.353	5.348	4.742	11.3	280.6	26.3
14.3	6.456	6.437	5.823	9.5	338.5	16.2
34.7	7.211	7.158	6.597	7.8	378.1	8.8
61.3	7.745	7.640	7.050	7.7	406.1	4.2
87.4	8.206	8.041	7.297	9.2	430.2	1.5
			Carbon Dioxide/301.4 K			
11.3	1.192	1.190	-	-	50.8	74.5
21.7	1.875	1.870	-	-	79.9	62.8
40.5	2.796	2.783	2.436	12.5	119.2	51.6
67.9	3.730	3.700	3.642	1.6	159.1	42.5
101.3	4.523	4.468	4.554	- 1.9	192.9	35.4
142.1	5.224	5.133	5.299	- 3.2	222.8	29.6
183.9	5.767	5.634	5.844	- 3.7	245.9	25.2
230.2	6.235	6.052	6.294	- 4.0	265.9	21.4
			Carbon Dioxide/301.4 K			
11.6	1.213	1.210	-	-	51.7	74.1
22.0	1.892	1.887	-	-	80.7	62.5
36.6	2.633	2.621	2.197	16.2	112.3	53.4
60.6	3.513	3.487	3.379	3.1	149.8	44.5
91.4	4.319	4.272	4.322	- 1.2	184.2	37.2
130.2	5.053	4.972	5.109	- 2.8	215.5	31.1
173.1	5.647	5.525	5.718	- 3.5	240.8	26.2
			Carbon Dioxide/301.4 K			
94.3	4.448	4.369	4.397	- 0.7	189.7	36.7
169.9	5.633	5.514	5.684	- 3.1	240.2	26.5
204.7	6.053	5.897	6.067	- 2.9	258.1	23.4
247.5	6.407	6.204	6.438	- 3.8	273.2	20.2
295.9	6.802	6.538	6.767	- 3.5	290.0	17.3
349.3	7.110	6.778	7.049	- 4.0	303.2	14.6
401.2	7.396	6.989	7.262	- 3.9	315.4	12.5
452.1	7.647	7.162	7.426	- 3.7	326.1	10.6
505.0	7.923	7.348	7.557	- 2.8	337.9	9.0
557.0	8.040	7.379	7.654	- 3.7	342.9	7.6

Reproduced with permission of the copyright owner. Further reproduction prohibited without permission.

Table 20. (Continued)

P, psia	n_o^a	n_o mg-mol/gC	n_{oc}	D, %	$\hat{V}_a \times 10^3$ cm^3/gC	$\epsilon/\tilde{V}_s(T_{nbp})$ cal/cm^3
		Carbon Dioxide/260.2 K				
4.2	1.609	1.608	-	-	63.3	65.8
10.6	2.890	2.886	2.692	6.7	113.7	51.3
17.7	3.826	3.818	3.828	- 0.3	150.5	43.5
29.5	4.895	4.877	4.957	- 1.7	192.5	35.6
50.0	6.041	6.002	6.102	- 1.7	237.6	27.6
84.0	7.170	7.091	7.190	- 1.4	282.0	19.8
140.0	8.174	8.018	8.192	- 2.2	321.5	12.3
219.3	8.997	8.712	8.965	- 2.9	353.9	6.1
		Carbon Dioxide/260.2 K				
14.6	3.453	3.453	3.399	1.6	135.8	46.4
28.9	4.837	4.819	4.912	- 1.9	190.2	35.9
66.7	6.658	6.600	6.713	- 1.7	261.9	23.2
117.3	7.847	7.723	7.856	- 1.7	308.6	14.9
166.4	8.487	8.290	8.506	- 2.6	333.8	9.9
197.7	8.798	8.550	8.800	- 2.9	346.0	7.5
		Carbon Dioxide/212.7 K				
0.5	1.826	1.826	-	-	64.9	62.2
1.5	3.570	3.569	3.757	- 5.3	126.8	46.5
3.4	5.222	5.219	5.376	- 3.0	185.5	36.4
6.6	6.713	6.706	6.705	0.0	238.4	28.1
11.2	7.957	7.945	7.787	2.0	282.6	21.4
27.6	9.573	9.535	9.567	- 0.3	340.0	10.1
		Carbon Dioxide/212.7 K				
0.5	1.829	1.829	-	-	64.9	61.1
1.1	3.040	3.040	3.092	- 1.7	108.0	50.7
2.6	4.737	4.736	4.853	- 2.5	168.2	39.7
5.3	6.269	6.264	6.260	0.1	222.6	30.9
9.4	7.636	7.626	7.425	2.6	271.2	23.6
		Carbon Dioxide/212.7 K				
0.5	1.825	1.824	-	-	64.8	61.9
1.3	3.267	3.266	3.370	- 3.2	116.0	48.9
2.9	4.927	4.925	5.059	- 2.7	175.0	38.4
5.7	6.446	6.441	6.418	0.4	228.9	29.9
10.0	7.763	7.752	7.547	2.7	275.7	22.9
		Carbon Dioxide/212.7 K				
0.5	1.889	1.889	-	-	65.7	55.1
1.7	3.699	3.698	3.967	- 7.3	128.7	40.1
3.8	5.408	5.406	5.612	- 3.8	188.2	29.7
7.3	6.928	6.921	6.950	- 0.4	241.1	21.3
26.2	9.477	9.442	9.563	- 1.3	329.8	5.3

Reproduced with permission of the copyright owner. Further reproduction prohibited without permission.

Gas Mixture Isotherms

In the following table the characteristic curve ordinates for gas mixtures, $\hat{V}_{am}$ and $\epsilon/\tilde{V}_s(T_{nbp})$, are presented. The calculations were performed with computer program GRANTB, which is briefly described in Appendix L, and follow the scheme discussed in Chapter V being represented by Equations (41), (84), and (85).

NOTE To convert from psia to kN/m^2 multiply by 6.8947572.
To convert from cal to J multiply by 4.184.

Reproduced with permission of the copyright owner. Further reproduction prohibited without permission.

Table 21. Characteristic Curve Ordinates for Gas Mixtures

P, psia	$\hat{V}_{am} \times 10^3$ cm^3/gC	$\epsilon/\tilde{V}_s(T_{nbp})$, cal/cm^3 (1)	(2)	(3)
	Methane(1)-Ethane(2)/(26.7-73.3 mol%)			
	301.4 K			
290.9	358.7	27.9	8.1	-
179.0	327.5	32.5	13.0	-
99.3	284.3	36.3	19.3	-
51.0	247.2	42.7	26.5	-
18.8	185.0	46.2	37.5	-
	212.7 K			
51.2	411.7	5.7	2.5	-
35.4	383.7	7.5	5.2	-
19.0	367.7	6.0	9.9	-
	Methane(1)-Ethane(2)/(49.9-50.1 mol%)			
	301.4 K			
200.9	325.5	31.6	14.6	-
100.5	265.8	35.5	22.6	-
49.9	223.3	43.1	30.2	-
19.1	163.6	51.6	41.0	-
	212.7 K			
100.8	441.1	0.5	0.5	-
50.4	390.4	5.4	5.3	-
19.1	348.4	9.7	12.6	-
	Methane(1)-Ethane(2)/(74.5-25.5 mol%)			
	301.4 K			
199.2	271.6	31.2	20.6	-
199.9	272.6	30.8	20.7	-
99.7	225.6	39.1	28.4	-
50.7	182.9	47.5	36.0	-
18.8	121.4	59.2	47.3	-
	260.2 K			
136.5	321.4	17.5	15.3	-
59.7	271.5	26.2	23.0	-
18.1	205.4	38.3	34.4	-
	212.7 K			
126.9	399.3	1.4	3.4	-
63.3	371.5	5.8	8.4	-
19.1	319.7	15.0	17.4	-

Reproduced with permission of the copyright owner. Further reproduction prohibited without permission.

Table 21. (Continued)

P, psia	$\hat{V}_{am} \times 10^3$ cm^3/gC	$\epsilon/\tilde{V}_s(T_{nbp})$, cal/cm^3 (1)	(2)	(3)
	Methane(1)-Ethylene(3)/(26.0-74.0 mol%)			
	301.4 K			
290.2	320.3	26.1	-	13.4
177.8	288.6	30.2	-	19.1
99.0	244.9	37.9	-	25.9
50.0	203.6	46.3	-	34.2
19.0	139.7	51.3	-	46.2
	212.7 K			
98.7	412.3	0.7	-	2.8
60.1	381.0	4.1	-	6.7
34.9	353.9	8.9	-	11.1
19.7	331.4	9.7	-	16.0
	Methane(1)-Ethylene(3)/(53.6-46.4 mol%)			
	301.4 K			
294.6	290.3	27.4	-	16.8
179.9	259.9	32.5	-	22.9
98.1	216.0	39.0	-	30.4
49.9	175.4	47.7	-	38.7
17.7	114.8	58.1	-	51.8
	212.7 K			
151.0	414.9	0.3	-	3.0
151.4	413.2	- 0.3	-	3.0
89.3	379.3	3.6	-	7.1
	Methane(1)-Ethylene(3)/(53.4-46.6 mol%)			
	301.4 K			
75.3	208.3	42.7	-	33.5
	212.7 K			
105.2	392.5	2.8	-	5.7
46.4	357.9	8.5	-	12.4
	Methane(1)-Ethylene(3)/(76.5-23.5 mol%)			
	301.4 K			
207.5	234.3	34.4	-	26.3
100.6	185.8	43.4	-	35.6
101.1	187.6	43.4	-	35.6
64.3	158.5	49.1	-	41.4
18.7	92.4	65.0	-	57.3

Reproduced with permission of the copyright owner. Further reproduction prohibited without permission.

Table 21. (Continued)

P, psia	$\hat{V}_{am} \times 10^3$ cm^3/gC	$\epsilon/\tilde{V}_s(T_{nbp})$, cal/cm^3 (1)	(2)	(3)
	Methane(1)-Ethylene(3)/(76.5-23.5 mol%)			
	260.2 K			
204.7	306.2	18.3	-	17.1
99.2	261.1	25.3	-	24.9
99.2	260.7	25.4	-	24.9
50.8	222.6	33.4	-	31.9
21.1	170.9	42.8	-	41.5
	212.7 K			
130.0	372.2	4.4	-	8.9
64.0	337.7	10.7	-	14.6
64.2	338.4	10.8	-	14.5
19.7	279.5	21.0	-	24.6
	Ethane(2)-Ethylene(3)/(24.0-76.0 mol%)			
	301.4 K			
287.4	352.8	-	7.7	10.7
194.5	319.6	-	11.5	15.0
106.9	280.8	-	17.9	21.6
44.7	229.2	-	27.2	31.9
20.0	177.7	-	35.5	41.6
	212.7 K			
58.8	420.6	-	1.8	3.6
32.5	383.6	-	6.2	8.3
20.3	364.4	-	9.9	12.0
	Ethane(2)-Ethylene(3)/(47.2-52.8 mol%)			
	301.4 K			
164.3	329.5	-	13.0	16.0
79.7	281.2	-	20.8	23.8
31.6	220.7	-	30.7	34.7
	Ethane(2)-Ethylene(3)/(68.2-31.8 mol%)			
	301.4 K			
198.4	351.0	-	10.5	13.5
100.5	305.6	-	17.6	20.4
50.2	255.8	-	24.9	28.5
20.9	205.3	-	34.5	38.3
	212.7 K			
49.8	422.4	-	1.6	3.0
34.9	404.3	-	4.2	5.7
19.9	375.8	-	8.4	10.0

Reproduced with permission of the copyright owner. Further reproduction prohibited without permission.

Table 21. (Continued)

P, psia	$\hat{V}_{am} \times 10^3$ cm^3/gC	$\epsilon/\tilde{V}_s(T_{nbp})$, cal/cm^3 (1)	(2)	(3)
Methane(1)-Ethane(2)-Ethylene(3)/(62.4-17.4-20.2 mol%)				
	301.4 K			
431.2	329.1	22.0	10.7	12.9
301.8	331.5	29.1	13.6	15.9
147.2	257.0	33.7	22.6	25.3
49.2	184.8	45.7	34.9	39.1
	212.7 K			
163.0	430.0	- 0.5	0.7	2.2
51.4	368.6	7.1	9.1	10.7
Methane(1)-Ethane(2)-Ethylene(3)/(23.0-52.0-25.0 mol%)				
	301.4 K			
302.3	366.4	29.4	7.9	10.4
177.0	317.1	33.1	13.8	15.6
100.3	277.5	39.4	19.7	22.2
49.6	240.6	44.6	27.6	30.3
19.1	174.8	44.5	38.2	42.1
	212.7 K			
70.8	425.7	4.8	0.9	1.9
40.2	391.9	7.7	5.1	6.2
19.2	359.1	4.2	10.7	12.2
Methane(1)-Ethane(2)-Ethylene(3)/(20.0-19.2-60.8 mol%)				
	301.4 K			
300.6	358.3	29.7	8.1	11.7
180.1	302.0	35.0	13.6	17.4
100.3	263.9	40.7	20.2	24.2
51.5	222.3	44.4	27.9	32.2
18.0	152.8	46.2	38.9	45.4
	212.7 K			
71.3	405.6	5.3	2.1	3.6
40.0	377.6	8.5	6.5	8.1
18.2	343.5	5.3	12.6	14.6

Reproduced with permission of the copyright owner. Further reproduction prohibited without permission.

APPENDIX L

FORTRAN PROGRAMS

All the computer programs mentioned in this work were programmed in FORTRAN IV language and were run on a UNIVAC 1108 computer.

Basically, each program consisted of a driver program and two or more subroutines, common to all programs, which are described next.

Common Subroutines

MIXPAR

General Description. This subroutine calculates the mixture parameters in the BWR equation of state for a gas mixture (maximum three components) given the pure gas BWR parameters and using the Benedict et al.[3] mixing rules.

BWRFUG

General Description. This subroutine calculates the molar volume, density, and compressibility factor of a gas mixture (maximum three components) and the fugacities of the components, given the BWR mixture and pure gas parameters and the gas mixture temperature and pressure. The molar volume is solved from the BWR equation of state by iteration with a Newton-Raphson technique.

SYSTEM$*MATHSTAT

General Description. This is a standard library file prepared by the Georgia Institute of Technology Computer Center containing a set of mathematical subroutines with numerical analysis methods. This file was

Reproduced with permission of the copyright owner. Further reproduction prohibited without permission.

used in this thesis in programs where curve fitting by least squares was required.

Programs

PISOTH

General Description. This program, consisting of a driver program and subroutines MIXPAR and BWRFUG, calculates the adsorbed amount of a pure gas at fixed conditions of temperature and pressure, given a set of experimentally measured data.

Input. The input required is given below in appropriate order:

1. Run number and date; gas name
2. BWR pure gas parameters
3. Water thermostat, cryostat, and room temperatures, and barometric pressure
4. Number of equilibrium points
5. Type of pressure device and pressure readings

Units are explained with comment cards in the main driver program.

Output. The program gives the pure gas isotherms, i.e., step or point in the isotherm, equilibrium pressure, amount adsorbed, cumulative adsorption, and cumulative adsorption per gram of adsorbent.

MISOTH

General Description. This program, containing a main driver program and subroutines MIXPAR and BWRFUG, calculates the adsorbed amounts of different components in a gas mixture (maximum three components) at fixed temperature and pressure, given a set of experimentally measured data.

Input. The input required is given below:

1. Number of components

Reproduced with permission of the copyright owner. Further reproduction prohibited without permission.

2. BWR parameters for pure components

3. Cryostat temperature

4. Gas phase composition

5. Water thermostat and room temperatures, and barometric pressure

6. Run number and date

7. Equilibrium pressure

8. Number of transfers to sample reservoir

9. Sample reservoir composition and pressure for all transfers

Units are explained with comment cards in the main program.

Output. The program gives the gas mixture isotherm, i.e., run and date, equilibrium pressure, adsorbed amount per gram of adsorbent for each component, and total amount adsorbed.

DUBIN1

General Description. This program, containing a main driver program and subroutines MIXPAR and BWRFUG, calculates the pure gas characteristic curve ordinates, according to the scheme discussed in Chapter V, given a set of its experimental adsorption capacities.

Input. The input required is given below:

1. Gas name and BWR pure gas parameters

2. Critical temperature and pressure, normal boiling point temperature, and saturated liquid molar volume at T_{nbp} for the substance.

3. Temperature

4. Number of data points

5. Gibbs adsorption and pressure

Output. The program provides input information, Gibbs and absolute adsorption capacities, and the ordinates of the characteristic curve.

Reproduced with permission of the copyright owner. Further reproduction prohibited without permission.

LINFIT

General Description. This program, consisting of a driver program and subroutines MIXPAR, BWRFUG, and SYSTEM$*MATHSTAT, computes a linear least squares analysis of the pure gas characteristic curve ordinates given in Table 20 in Appendix K, according to equations (80) and (81) in Chapter V.

Input. It operates with the same input as program DUBIN1.

Output. The program gives the least squares fit constants, calculated values of the adsorption capacities and a comparison with respect to the experimental adsorption data.

GRANTB

General Description. This program, consisting of a driver program and subroutines MIXPAR and BWRFUG, calculates the gas mixture characteristic curve ordinates, according to the scheme discussed in Chapter V, given a set of its experimental adsorption capacities.

Input. The input required is given below:

1. BWR parameters for the pure components
2. Critical temperature and pressure, normal boiling point temperature and saturated liquid molar volume at T_{nbp} for the pure substances
3. Gas phase composition and temperature
4. Number of data points
5. Pressure and adsorption capacities for the components in the adsorbate mixture

Output. The program provides input information, run number and date, pressure, total amount adsorbed, adsorbate mole fractions, and characteristic curve ordinates.

Reproduced with permission of the copyright owner. Further reproduction prohibited without permission.

GRANTF

General Description. This program, consisting of a driver program and subroutines MIXPAR and BWRFUG, calculates mixture adsorption data from a linear least squares fit of the pure gas characteristic curve given in Table 20 in Appendix K, using the Grant and Manes method[25] discussed in Chapter V. Equations (41) and (43) are solved iteratively by a Newton-Raphson technique.

Input. Similar to program GRANTB.

Output. The program provides input information, run number and date, pressure, experimental and calculated adsorption capacities, and a comparison between the last two quantities.

Reproduced with permission of the copyright owner. Further reproduction prohibited without permission.

BIBLIOGRAPHY

1. American Society for Testing and Materials, Standard Metric Practice Guide (A Guide to the Use of SI--the International System of Units), ASTM Designation: E 380-70 (1970).

2. Barber, C. R., "The International Practical Temperature Scale of 1968," Metrologia 5, No. 2, 35-44 (1969).

3. Benedict, M., Webb, G. B., and Rubin, L. C., "An Empirical Equation for Thermodynamic Properties of Light Hydrocarbon and Their Mixtures," Chemical Engineering Progress 47, No. 8, 419-422 (1951).

4. Berenyi, L., "Prüfung der Polanyischen Theorie der Adsorption," Zeitschrift für Physikalische Chemie 94, 628-642 (1920).

5. Berenyi, L., "Neuere Adsorptionsberechnung," Zeitschrift für Physikalische Chemie 105, 55-72 (1923).

6. Bering, B. P., Serpinskii, V. V., and Surinova, S. I., "Calculation of Adsorptional Equilibrium Parameters for Adsorbent-Binary Gas Mixture Systems," Akademiia Nauk SSSR. Doklady. Physical Chemistry. Proceedings of the Academy of Sciences of the USSR 153, No. 1, 949-952 (1963).

7. Bering, B. P., Serpinskii, V. V., and Surinova, S. I., "Joint Adsorption of a Binary Mixture of Vapors on Activated Carbon," Akademiia Nauk SSSR. Bulletin. Division Chemical Science, No. 5, 753-758 (1965).

8. Bering, B. P., Myers, A. L., and Serpinskii, V. V., "The Inertness of Adsorbents," Akademiia Nauk SSR. Doklady. Physical Chemistry 193, No. 1, 494-497 (1969).

9. Bülow, M., Grossmann, A., and Schirmer, W., "Zur Adsorption von Binären Gasgemischen an Festen Oberflächen," Zeitschrift für Chemie 12, No. 5, 161-169 (1972).

10. Canjar, L. N., and Manning, F. S., Thermodynamic Properties and Reduced Correlations for Gases, Gulf Publishing Company, Houston, Texas (1967).

11. Cerofolini, G. F., "Multilayer Adsorption on Heterogeneous Surfaces," Journal of Low Temperature Physics 6, No. 5/6, 473-486 (1972).

Reproduced with permission of the copyright owner. Further reproduction prohibited without permission.

BIBLIOGRAPHY (Continued)

12. Cook, W. H., and Basmadjian, D., "Correlation of Adsorption Equilibria of Pure Gases on Activated Carbon," The Canadian Journal of Chemical Engineering 42, 146-151 (1964).

13. Cook, W. H., and Basmadjian, D., "The Prediction of Binary Adsorption Equilibria from Pure Component Isotherms," The Canadian Journal of Chemical Engineering 43, 78-83 (1965).

14. Cullen, E. J., and Kobe, K. A., "Benedict Equation of State: Application to Vapor-Liquid Equilibria," American Institute of Chemical Engineers Journal 1, No. 4, 452-455 (1955).

15. Dovaston, N. G., McEnaney, B., and Weedon, C. J., "On the Application of the Potential Theory to the Adsorption of Carbon Dioxide in Microporous Polymer Carbons," Carbon 10, No. 3, 277-284 (1972).

16. Dubinin, M. M., and Timofeyev, D. P., "Adsorption of Vapours on Active Charcoals in Relation to the Properties of the Adsorbate," Akademiia Nauk SSSR. Comptes Rendus (Doklady) de l'Academie des Sciences de l'URSS 54, No. 8, 701-704 (1946).

17. Dubinin, M. M., and Timofeyev, D. P., "Adsorption of Vapours on Active Charcoals in Relation to the Physical Properties of the Adsorbate," Akademiia Nauk SSSR. Comptes Rendus (Doklady) de l'Academie des Sciences de l'URSS 55, No. 2, 137-139 (1947).

18. Dubinin, M. M., and Radushkevich, L. V., "On the Characteristic Curve Equation for Active Charcoals," Akademiia Nauk SSSR. Comptes Rendus (Doklady) de l'Academie des Sciences de l'URSS 55, No. 4, 327-329 (1947).

19. Dubinin, M. M., and Zhukovskaia, E. G., "Adsorption Properties of Active Carbons with Respect to Benzene and Nitrogen Vapors," Akademiia Nauk SSSR. Bulletin Division Chemical Sciences, No. 5, 519-528 (1958).

20. Dubinin, M. M., "Modern State of the Theory of Gas and Vapour Adsorption by Microporous Adsorbents," Journal of Pure and Applied Chemistry 10, 309-321 (1965).

21. Dubinin, M. M., and Polstyanov, E. F., "Investigation of the Equilibrium Adsorption of Vapors within a Broad Range of Temperatures on Activated Charcoals with Various Microporous Structures," Akademiia Nauk SSSR. Bulletin. Division Chemical Sciences, No. 4, 583-589 (1966).

Reproduced with permission of the copyright owner. Further reproduction prohibited without permission.

BIBLIOGRAPHY (Continued)

22. Goldmann, F., and Polanyi, M., "Adsorption von Dämpfen an Kohle und die Wärmeausdehnung der Benetzungsschicht," Zeitschrift für Physikalische Chemie 132, 320-370 (1928).

23. Grant, R. J., Manes, M., and Smith, S. B., "Adsorption of Normal Paraffins and Sulfur Compounds on Activated Carbon," American Institute of Chemical Engineers Journal 8, No. 3, 403-406 (1962).

24. Grant, R. J., and Manes, M., "Correlation of Some Adsorption Data Extending to Low Pressures and Supercritical Temperatures," Industrial and Engineering Chemistry Fundamentals 3, No. 3, 221-224 (1964).

25. Grant, R. J., and Manes, M., "Adsorption of Binary Hydrocarbon Gas Mixtures on Activated Carbon," Industrial and Engineering Chemistry Fundamentals 5, No. 4, 490-498 (1966).

26. Hasz, J. W., and Barrere, C. A., Jr., "Prediction of Equilibrium Adsorption Capacity and Heats of Adsorption by the Polanyi Potential Theory," Chemical Engineering Progress Symposium Series 96 65, 48-60 (1969).

27. Kirk, B. S., Predicted and Experimental Gas Phase Compositions in Pressurized Binary Systems Containing an Essentially Pure Condensed Phase. Phase Equilibrium Data for the Methane-Hydrogen System from 66.88 to 116.53°K and Up to 125 Atmospheres, Ph. D. Thesis, Georgia Institute of Technology, Atlanta, Georgia (1964).

28. Laukhuf, W. L., and Plank, C. A., "Adsorption of Carbon Dioxide, Acetylene, Ethane, and Propylene on Charcoal at Near Room Temperature," Journal of Chemical Engineering Data 14, No. 1, 48-51 (1969).

29. Lewis, W. K., Gilliland, E. R., Chertow, B., and Cadogan, W. P., "Adsorption Equilibria. Hydrocarbon Gas Mixtures," Industrial and Engineering Chemistry 42, No. 7, 1319-1326 (1950).

30. Lewis, W. K., Gilliland, E. R., Chertow, B., and Cadogan, W. P., "Pure Gas Isotherms (Adsorption Equilibria)," Industrial and Engineering Chemistry 42, No. 7, 1326-1332 (1950).

31. London, F., "Uber Einige Eigenschaften und Anwendungen der Molecularkräfte," Zeitschrift für Physikalische Chemie 11, 222-251 (1931).

32. Lowry, H. H., and Olmstead, P. S., "The Adsorption of Gases by Solids with Special Reference to the Adsorption of Carbon Dioxide by Charcoal," Journal of Physical Chemistry 31, 1601-1626 (1927).

Reproduced with permission of the copyright owner. Further reproduction prohibited without permission.

BIBLIOGRAPHY (Continued)

33. Maslan, F. D., Altman, M., and Alberth, E. R., "Prediction of Gas-Adsorbent Equilibrium," Journal of Physical Chemistry 57, 106-109 (1953).

34. Menon, P. G., "Adsorption at High Pressures," Chemical Revue 68, 277-294 (1968).

35. Meredith, J. M., and Plank, C. A., "Adsorption of Carbon Dioxide and Nitrogen on Charcoal at 30° to 50°C," Journal of Chemical and Engineering Data 12, 259-261 (1967).

36. Myers, A. L., and Prausnitz, J. M., "Thermodynamics of Mixed-Gas Adsorption," American Institute of Chemical Engineers Journal 11, No. 1, 121-127 (1965).

37. Nikolaev, K. M., and Dubinin, M. M., "A Study of Adsorption Isotherms of Gases and Vapors on Active Carbons Over a Wide Interval of Temperatures, Including the Critical Region," Akademiia Nauk SSSR. Bulletin. Division of Chemical Sciences, No. 10, 1124-1133 (1958).

38. Orye, R. V., "Prediction and Correlation of Phase Equilibria and Thermal Properties with the BWR Equation of State," Industrial and Engineering Chemistry Process Design and Development 8, No. 4, 579-588 (1969).

39. Pierotti, R. P., and Thomas, H. E., Physical Adsorption: The Interaction of Gases with Solids, School of Chemistry, Georgia Institute of Technology, Atlanta, Georgia (1971).

40. Polanyi, M., "Uber die Adsorption vom Standpunkt des Dritten Wärmesatzes," Verhandlung der Deutschen Physikalische Gesellschaft 16, 1012-1016 (1914).

41. Polanyi, M., "Adsorption von Gasen (Dämpfen) durch ein Festes Nichtflüchtiges Adsorbens," Verhandlung der Deutschen Physikalische Gesellschaft 18, 55-80 (1916).

42. Polanyi, M., "Neuares über Adsorption und Ursache der Adsorptionskräfte," Zeitschrift für Elekrochemie 26, 370-374 (1920).

43. Polanyi, M., "Theories of the Adsorption of Gases. A General Survey and Some Additional Remarks," Transactions of the Faraday Society 28, 316-333 (1932).

44. Polanyi, M., "The Potential Theory of Adsorption," Science 141, 1010-1012 (1963).

Reproduced with permission of the copyright owner. Further reproduction prohibited without permission.

BIBLIOGRAPHY (Continued)

45. Ray, G. C., and Box, E. O., Jr., "Adsorption of Gases on Activated Charcoal," Industrial and Engineering Chemistry 42, No. 7, 1315-1318 (1950).

46. Reid, R. C., and Sherwood, T. K., The Properties of Gases and Liquids, McGraw-Hill Book Co., 2nd ed., New York (1966).

47. Rogers, K. A., Adsorption on Activated Carbon of Hydrogen, Methane and Carbon Dioxide Gases and Their Mixtures at 212 K to 301 K and Up to Thirty-Five Atmospheres, Ph. D. Thesis, Georgia Institute of Technology, Atlanta, Georgia (1973).

48. Sircar, S., and Myers, A. L., "Surface Potential Theory of Multilayer Adsorption from Gas Mixtures," Journal of Engineering Science 28, 489-499 (1973).

49. Steele, W. A., in Flood, E. A., Ed., The Solid-Gas Interface, Vol. I, Dekker, New York (1967).

50. Szepesy, L., and Illes, V., "Measurement of the Adsorption Isotherms of Gases on Active Carbon Up to Pressures of 1000 Torr," Acta Chimica Hungarica 35, 37-50 (1963).

51. Sezpesy, L., and Illes, V., "Measurement of the Adsorption Isotherms of Gases on Active Carbon Under Pressures of 1 to 7 Atm.," Acta Chimica Hungarica 35, 53-59 (1963).

52. Szepesy, L., and Illes, V., "Investigation of the Adsorption Equilibria of Binary Gas Mixtures," Acta Chimica Hungarica 35, 245-253 (1963).

53. Young, D. M., and Crowell, A. D., Physical Adsorption of Gases, Butterworths, 293, Washington (1962).

54. Zukal, A., Dubinin, M. M., and Lezin, Yu. S., "Theoretical Analysis of the Experimental Data on the Equilibrium Adsorption of Benzene within a Broad Range of Temperatures, Including the Supercritical Region," Akademiia Nauk SSSR. Bulletin. Division of Chemical Sciences, No. 7, 1362-1368 (1968).

Reproduced with permission of the copyright owner. Further reproduction prohibited without permission.

VITA

Ricardo Reich was born January 8, 1942, in Santiago, Chile to Eliana Albertz and Herbert Reich. He graduated from German High School in Santiago in 1959. He attended the University of Concepción in Concepción, Chile, where he received the Engineering degree in Chemical Engineering in 1965. Upon graduation, he worked as an Instructor at the School of Chemical Engineering, University of Concepción, and left this position to enroll as a graduate student in the School of Chemical Engineering at the Georgia Institute of Technology in Atlanta. He received the Master of Science degree in Chemical Engineering in 1968. He was then employed as an Assistant Professor in the School of Chemical Engineering at the University of Concepción. He was readmitted as a graduate student in the School of Chemical Engineering of the Georgia Institute of Technology in 1971. He was employed in this school as a graduate teaching assistant, and as an instructor during the 1972-73 academic school year. At present, he holds a teaching position as a Professor in the School of Chemical Engineering at the University of Concepción. He is a member of the Chile Institute of Engineers, an associate member of the American Institute of Chemical Engineers, and an associate member of the Society of the Sigma Xi.

In 1970 he married María Cecilia Morales of Concepción, Chile.

Reproduced with permission of the copyright owner. Further reproduction prohibited without permission.